Distribution Agreement

In presenting this thesis or dissertation as a partial fulfillment of the requirements for an advanced degree from Emory University, I hereby grant to Emory University and its agents the non-exclusive license to archive, make accessible, and display my thesis or dissertation in whole or in part in all forms of media, now or hereafter known, including display on the world wide web. I understand that I may select some access restrictions as part of the online submission of this thesis or dissertation. I retain all ownership rights to the copyright of the thesis or dissertation. I also retain the right to use in future works (such as articles or books) all or part of this thesis or dissertation.

Signature:

_____ _____

Dylan Holder Date

Approval Page

Arabidopsis thaliana Transcriptome and Chromatin Dynamics during a Phosphate Starvation Response Reveal New Insights Into H3K27me3 and H2A.Z mediated gene regulation

By
Dylan Holder
B.S. Auburn University, 2017

_____
Roger Deal, Ph.D.
Advisor

_____
William Kelly, Ph.D.
Committee Member

_____
Anita Corbett, Ph.D.
Committee Member

_____
Jeremy Boss, Ph.D.
Committee Member

_____
Kenneth Moberg, Ph.D.
Committee Member

Accepted:

_____
Kimberly Jacob Arriola, Ph.D, MPH
Dean of the James T. Laney School of Graduate Studies Date

_____
Date

Arabidopsis thaliana Transcriptome and Chromatin Dynamics during a Phosphate Starvation Response Reveal New Insights Into H3K27me3 and H2A.Z mediated gene regulation

By

Dylan H. Holder,

B.S., Auburn University, 2017

Advisor: Roger B. Deal, Ph. D

An abstract of a dissertation submitted to the Faculty of the James T. Laney School of Graduate Studies of Emory University in partial fulfillment of the requirements for the degree of Doctor of Philosophy in the Graduate Division of Biological and Biomedical Science Genetics and Molecular Biology

2024

Abstract

Modifications to and variants of canonical nucleosome components give each nucleosome a unique identity thought to create a chromatin state that alters the propensity for a given locus to be subject to activation or silencing. In order for plants to mount an effective transcriptional response to nutrient stress, transcription machinery must overcome the established chromatin state at responsive genes. How transcription machinery rapidly overcomes the supposed repressive chromatin landscape at quiescent genes in response to activating signals and then effectively re-silence these genes once those signals are removed is not understood. We performed time-resolved and cell type specific profiling to understand how plants alter their transcriptome and chromatin landscape to achieve effective gene activation during phosphate starvation and then rapid silencing upon phosphate resupply. To our surprise, we found that activation of phosphate starvation response genes can occur without removal of gene body H2A.Z or H3K27me3, two features of chromatin thought to contribute to gene silencing. This finding coupled with recent observations from our lab suggesting that H2A.Z lost from induced genes is continuously replenished, highlighting the need to decouple the established roles these nucleosome modifications play in developmental gene regulation from their role in responsive gene regulation. The results presented here not only provide a cell-type and time-resolved resource for studying the chromatin dynamics of a systemic nutrient stress and recovery, but also suggest that our understanding of the dynamic chromatin landscape in responsive gene activation and repression is incomplete.

Arabidopsis thaliana Transcriptome and Chromatin Dynamics during a Phosphate Starvation Response Reveal New Insights Into H3K27me3 and H2A.Z mediated gene regulation

By

Dylan H. Holder,

B.S., Auburn University, 2017

Advisor: Roger B. Deal, Ph. D

A dissertation submitted to the Faculty of the James T. Laney School of Graduate Studies of Emory University in partial fulfillment of the requirements for the degree of Doctor of Philosophy in the Graduate Division of Biological and Biomedical Science

Genetics and Molecular Biology

2024

Acknowledgements

I thank every member of the Deal lab. Paja, Kelsey, Marko, Ellen, Courtney, Maryam, and Bri, you each contributed your time, expertise, and friendship to me. When my project hit roadblocks I always knew my labmates would take time out of their day to help in any way they could. I know I was part of a special group and I consider you my friends. I am lucky to have worked alongside each of you. You're doing a great job.

Thank you Roger. Never once on my journey did question my decision to join your lab. Your unwavering positivity and determination help me get through several challenges. You always made me feel like we were in this project together and I never felt like I was struggling alone. You have a special way of never making anyone feel bad for making a mistake or not knowing something. You showed me what the best version of a mentor looks like and I only hope I can emulate what you did for me with my future mentees.

I want to thank my undergraduate mentors from Auburn University Dr. Christopher Easley and Dr. Jessica Schilling. Dr. Easley invited me into his lab and showed me for the first time what a fulfilling career and life in science looks like. Working with Dr. Jessica Schilling I learned how to deal with setbacks and unexpected findings in a healthy way. She also trusted me with experiments and analyses as a young and inexperienced researcher and this instilled a confidence in me that helped me overcome later challenges. I also thank my mentors from my time at HudsonAlpha, Dr. Richard Myers and Dr. Krysta Engel. Dr. Engel gave me projects that tested my abilities but never made me feel alone with them. I also admire the professionalism she showed both to me and to her colleagues.

I want to thank my committee members Dr. William Kelly, Dr. Anita Corbett, Dr. Jeremy Boss, and Dr. Ken Moberg. You all did a good job of calming my nerves and reassuring me that I was on the right track despite several setbacks. I would also like to thank the Biology Department staff for always being accessible and making the department a fun and welcoming place to work.

Thank you to my parents. I measure every decision I make for my family by the ones you made for me. If I can give my children even a small semblance of the life you gave me I know I will have done it right. Thank you Caleb for always calling me to talk about anything. Finally, thank you Jamie. Life with you has brought me more happiness than I could have ever found alone. I am in awe of what you do for me and our children every day. I love you more than words can tell. Thank you.

Table of Contents

Figures and Tables

Chapter 1:

Chapter 2:

Chapter 1:

Histone Variants in the Specialization of Plant Chromatin

Recreated with permission from

Dylan H. Holder[1,2*], Maryam Foroozani[1*], and Roger B. Deal[1]

Histone Variants in the Specialization of Plant Chromatin, *Annual Review of Plant Biology,* 2022. 73: 149-72

https://doi.org/10.1146/annurev-arplant-070221-050044

[1]Department of Biology, Emory University, Atlanta, Georgia, USA

[2]Graduate Program in Genetics and Molecular Biology, Emory University, Atlanta, Georgia, USA

[*]Equal contributors

Abstract

The basic unit of chromatin, the nucleosome, is an octamer of four core histone proteins (H2A, H2B, H3, and H4) and serves as a fundamental regulatory unit in all DNA-templated processes. The majority of nucleosome assembly occurs during DNA replication when these core histones are produced *en masse* to accommodate the nascent genome. In addition, there are a number of non-allelic sequence variants of H2A and H3 in particular, known as histone variants, that can be incorporated into nucleosomes in a targeted and replication-independent manner. By virtue of their sequence divergence from the replication-coupled histones, these histone variants can impart unique properties onto the nucleosomes they occupy and thereby influence transcription and epigenetic states, DNA repair, chromosome segregation, and other nuclear processes in ways that profoundly affect plant biology. In this review we discuss the evolutionary origins of these variants in plants, their known roles in chromatin, and their impacts on plant development and stress responses. We focus on the individual and combined roles of histone variants in transcriptional regulation within euchromatic and heterochromatic genome regions. Finally, we highlight gaps in our understanding of plant variants at the molecular, cellular, and organismal level, and we propose new directions for study in the field of plant histone variants.

Introduction

Throughout eons of evolution, the nucleosome has remained a defining characteristic of eukaryotes. As the fundamental unit of chromatin, the nucleosome acts as a barrier between DNA and interacting proteins, making it an integral regulatory component in virtually every DNA-templated process. The nucleosome consists of ~147 bp of DNA wrapped around a histone octamer containing a core $(H3\text{-}H4)_2$ tetramer flanked by two H2A-H2B dimers. Histone-histone and histone-DNA interactions contribute to nucleosome stability, while the tails of each histone provide a substrate for posttranslational modifications and protein binding. During replication, DNA content doubles and so does the demand for nucleosomes. To accommodate this demand, canonical histone genes evolved into often intronless multigene families whose expression is tightly linked to the cell cycle with highest expression during S phase. In contrast, histone variants have introns and often show replication-independent expression and deposition. The naming conventions for histone variants generally consist of a prefix indicating the histone protein family (e.g. H2A) to which they belong, followed by a period and a number or letter indicating a specific variant type (e.g. H2A.Z) [1].

Some histone variants such as H2A.Z are conserved throughout eukaryotes while others are lineage-specific, such as the flowering plant-specific H2A.W variant. By changing nucleosome composition, histone variants can change the internal stability of a nucleosome, DNA-histone interactions, internucleosomal interactions, accessibility to chromatin binding proteins, as well as potential posttranslational modifications. All of these changes alter the chromatin landscape and influence key nuclear processes.

Therefore, histone variants represent a wealth of currently untapped information that will contribute to answering several of the outstanding questions of eukaryotic epigenetics.

In this review, we assess the current understanding of plant variant histones with a focus on the roles they play in transcriptional control. The eukaryotic genome can be partitioned into transcriptionally permissive euchromatic regions and transcriptionally repressive heterochromatic regions of both facultative and constitutive types. Histone variants H3.3, H2A.Z and H2A.X are found in euchromatic regions. Recent reviews of H3.3, H2A.Z, and H2A.X can be found in Borg et al. and Lei and Berger [2,3]. Here, we discuss how H3.3 is implicated in promoting chromatin accessibility in ways potentially unique to plants. H2A.Z has a more complex relationship with gene expression and we discuss evidence that implicates the variant as both a transcriptional activator and repressor. While H2A.X is known primarily for its role in DNA damage response, we focus on recent evidence pointing toward a role for H2A.X in transcriptional control. Other histone variants contribute to heterochromatin function and we highlight H2A.W and H1, which have also been recently reviewed in Lei and Berger, Kotlinski et al., and Probst et al. [2,4,5]. H2A.W serves as the heterochromatic counterpart to H2A.X with respect to the DNA damage response, and its structure is thought to promote chromatin condensation. Finally, we call attention to the oft overlooked linker histone H1 and analyze how chromatin structure is dependent on H1 in both heterochromatin and euchromatin (See Figure 1).

Euchromatin-Associated Histone Variants

H3.3

In plants, histone H3 proteins are categorized into 4 groups: canonical histone H3.1, H3.3 variants, centromeric H3 variants, and H3-like histones. Centromeric H3 defines the centromere and is essential for kinetochore assembly and proper cell division, while the function of H3-like variants is largely unknown [6]. Plant H3.3 contains many features typical of histone variants including introns, replication-independent deposition into chromatin, and expression in terminally differentiated tissue [7–9]. Despite these differences, H3.3 differs from H3.1 at only 4 amino acids (written H3.1→H3.3): A31T, F41Y, S87H and A90L (Figure 1B). The *Arabidopsis* genome possesses three H3.3 genes encoding identical proteins (Table 1) [1]. Evolutionary analysis of H3 proteins shows that H3.3 evolved independently in plants and animals [10,11]. Despite their independent origins, H3.3 differs from H3.1 at three of the same amino acids in both plants and animals, with H3.1 in flowering plants having an additional amino acid substitution at residue 41 [11]. This evidence of convergent evolution strongly points toward the importance of H3.3 to the function of the eukaryotic genome.

Few studies have investigated exactly how H3.3 is deposited into plant chromatin. In mammals, H3.3 variants are incorporated into genic regions by the HIRA (Histone Transcriptional Regulator A) and in nongenic regions such as pericentromeric repeats and telomeres by ATRX/DAXX (Alpha Thalassemia-mental Retardation X-linked syndrome/Death-domain Associated protein) (Table 1) [12,13]. *Arabidopsis* ATRX mutants do indeed have altered global H3.3 levels [14,15]. While *atrx* mutants are

viable, *hira atrx* double mutants result in partial lethality and show strong developmental defects in the surviving plants, indicating a potential cooperation between ATRX and HIRA. [14]. Interestingly, *atrx* mutants display loss of H3.3 in genic regions while H3.3 enrichment at transposable elements (TEs) and pericentromeric regions is unchanged [14]. This is counter to observations in mammals where ATRX deposits H3.3 at non-genic regions, suggesting a functional divergence of ATRX-dependent H3.3 localization between plants and mammals [14].

H3.3 localization and relationship with gene expression

While the H3.3 genomic distribution pattern is different from H3.1 in both plants and animals, their respective distribution patterns are highly similar across species [9]. In *Arabidopsi*s, immunofluorescence and ChIP-seq experiments show that H3.1 is generally enriched at transposable elements, pericentromeric heterochromatin, and heterochromatin domains in the arms, while H3.3 is associated with euchromatic and nucleosome-depleted regions (NDR) [9,16–18]. Recent evidence indicates that this distinction in H3.1 and H3.3 distribution is caused in part by sequence variation at amino acid 41: Phe in H3.1 and Tyr in H3.3. Alignment analysis of monocot, dicot and ancient plant histone H3 reveals that the Phe41 residue first appeared in fern H3.1 and established in land plants [19]. Lu et al. showed that while Tyr41 is not important for the genomic distribution of H3.3, a Phe41Tyr point mutation in H3.1 causes the protein to lose its heterochromatin-specific localization and spread into active regions [19]. This is especially surprising considering that animal H3.1 and H3.3 both have Tyrosine at position 41, and are still able to maintain distinct localization patterns. Tyrosine differs

from Phenylalanine in its ability to be phosphorylated. In human cells, H3 is known to be phosphorylated at Tyr41 and this is thought to help prevent heterochromatic proteins from binding active regions [20]. Therefore, one hypothesis drawn from these results is that Phe41 evolved to differentiate H3.1 from H3.3 in plants where phosphorylation at Tyr41 has not yet been reported. Alternatively, these results could indicate that H3.1 Phe41 evolved to achieve an additional degree of chromatin targeting unique to vascular plants.

Highly expressed genes have enrichment of H3.3 over the transcribed region, or gene body, with a bias toward the 3' end [9,17,18]. However there is no correlation between H3.3 occupancy and transcriptional changes in *h3.3* knockdown (*h3.3kd*) plants, and H3.3 appears to be dispensable for general transcription. This is particularly surprising considering that complete loss of H3.3 is lethal [21]. However, a reduction in H3.3 in some stress-responsive genes was associated with reduced transcript levels in *h3.3kd* mutants. Thus, H3.3 likely plays a specific role in the activation of groups of genes that are involved in environmental responses, while not impacting transcription globally [21]. Also, a recent study demonstrated that H3.3 inhibits flowering by increasing H3K4me3 and H3K36me3 levels at the *FLOWERING LOCUS C* (FLC) gene [22]. The authors found that an interaction between FRIGIDA (FRI) and the HIRA chaperones results in the deposition of H3.3 at the 3' end of *FLC*. Consequently, increased H3.3 at the 3' of *FLC* aids in formation of a gene loop, increasing the interaction between the 5' and 3' end, thereby promoting transcriptional activation [22].

While H3.1 overlaps with several repressive chromatin modifications including DNA methylation, H3K9me2, and H3K27me1/3, H3.3 overlaps with several active chromatin marks like H3K4me3, H3K36me3, H3K9me3, H2B ubiquitylation, and RNA Pol II

occupancy [9,18]. Despite these correlations, genome-wide patterns of H3K4me3 and H3K36me3 are relatively unchanged between *h3.3kd* mutants and wild type *Arabidopsis* [21]. However, H3.3 was shown to promote H3K4me3 at a subset of genes with shorter length (<1 kb) [22]. Interestingly, loss of H3.3, specifically over gene bodies, is associated with a decrease in DNA methylation and an increase in H1 occupancy (Figure 2A) [21]. Additionally, chromatin accessibility assays showed that H3.3-containing nucleosomes are more sensitive to DNase I activity [17]. Since H1 has been shown to prevent binding of DNA methyltransferases in pericentromeric heterochromatin, H3.3 may serve as a foil to H1 in euchromatic regions, with gene body H3.3 increasing chromatin accessibility to DNA methyltransferases by preventing H1 deposition [21,23]. Crystal structures of H3 methyltransferases ATXR5/6 reveal their ability to methylate lysine 27 of H3.1 but not H3.3. Therefore, H3.3 could also attenuate the Polycomb pathway of gene repression, of which H3K27 methylation is a key element [24]. This difference also suggests that H3.3 can not only stimulate relaxed chromatin but can also perpetuate this chromatin state across cell divisions by preventing the establishment of heterochromatic marks.

H3.1 replacement by H3.3 is also a marker for cell fate transitions. Cells undergoing their last cell cycle before differentiation have a lower H3.1/H3.3 ratio and a higher rate of H3.1 eviction compared to dividing cells. This ratio is thought to change in the cells exiting the root meristem because H3.1 replacement with H3.3 occurs during the G2 phase, a phase that is longer in this last cell cycle than in earlier cycles, allowing more time for H3.1 eviction [25]. This phenomenon is found in several plant developmental processes, including the stomatal and hypocotyl cell lineages, suggesting H3.1 eviction is a general feature in cell proliferation and organogenesis [25,26].

H2A.Z

H2A.Z can be traced to a single evolutionary origin and its maintenance through nearly all branches of Eukarya underscore its vital role in multicellular development [27]. Since the discovery of H2A.Z, it has been linked with numerous biological processes like plant immunity, germline development, and stress response as well as cellular processes including genome stability, DNA repair, as well as both transcriptional activation and repression (Table 1) [28–34]. H2A.Z composes on average 15% of total H2A cellular content and loss of H2A.Z is lethal in most multicellular and some unicellular eukaryotes including *Tetrahymena*, *Drosophila*, mice and humans [28,35–38]. This surprisingly is not the case for plants, where loss of H2A.Z in *Arabidopsis* is not lethal but does lead to a severe and pleiotropic phenotype including stunted growth, early flowering, and reduced fertility [30,39–41]. This tolerance of H2A.Z loss makes plants an exciting model to probe the mechanisms of this histone variant in transcriptional regulation.

H2A.Z is deposited into the post-replicated nucleosome as an H2A.Z/H2B dimer by the SWI2/SNF2-related 1 complex (SWR1), a member of the INO80 subfamily of chromatin remodelers (Table 1) [42–44]. At the level of primary structure, H2A.Z varies from H2A in three prominent ways; the docking domain, the L1 loop and the acidic patch (Figure 1B). The implications of these differences with respect to chromatin binding and gene regulation have been reviewed by Bönisch and Hake [45]. Briefly, the extended acidic patch of H2A.Z is speculated to increase the opportunity for interactions between adjacent nucleosomes as well as secondary protein binding [46–48]. Taken

individually, the changes to the docking domain and the L1 loop appear to have opposing effects on nucleosome stability. The docking domain of H2A.Z exhibits less hydrogen bonding with H3, suggesting nucleosome destabilization, while the 4 amino acid substitutions found in the L1 loop have been shown to increase histone octamer stability [45,49,50]. Additionally, amino acid substitutions in the H2A.Z C-terminus reduce binding of linker histone H1 to the core nucleosome particle [51].

While all plants appear to have H2A.Z, they do differ in the number of H2A.Z paralogs, and in some cases distinct splice variants exist within organisms [52,53]. The *Arabidopsis* genome encodes three expressed H2A.Z proteins; HTA8, HTA9, and HTA11 (Table 1). Although mutant analysis in plants indicates substantial redundancy between isoforms, they do exhibit distinct expression levels and patterns [54]. As sub functionalization has been shown in some animals, future investigations will reveal any unique roles between paralogs in plants [55,56]. Interestingly, we found that the expression pattern across tissue types of the various *Arabidopsis* H2A.Z paralogs is synchronized with corresponding somatic H2B isoforms, with HTA11 and HTB2 having matched expression profiles, as do HTA9 and HTB4. This suggests that H2A.Z isoforms have preferred dimerization partners when deposited in the nucleosome [54].

H2A.Z localization and relationship with gene expression

There is a wealth of evidence that implicates H2A.Z as an essential player in transcriptional responses. However, understanding the exact mechanisms dictating H2A.Z-dependent transcriptional regulation are complicated by the fact that H2A.Z has reported roles as both a transcriptional activator and a repressor. In this section, we

discuss how analyses of H2A.Z mutants, structural features, and localization patterns support a role for H2A.Z as a transcriptional activator. H2A.Z's role as a repressor is discussed in a later section.

In *Arabidopsis*, most genes contain a prominent H2A.Z peak at the +1 nucleosome beyond the TSS. With respect to this enrichment pattern in plants, no gene has been studied more than *FLOWERING LOCUS C* (*FLC*). The most prominent and unifying phenotype of all H2A.Z and SWR1 mutants is the accelerated transition from vegatative to reproductive growth. Expression analysis reveals that these mutants display decreased transcript levels of the floral repressor *FLC* which leads to early flowering [30,39,54,57–62]. H2A.Z-containing nucleosomes at this locus follow the pattern expected for expressed genes with a characteristic peak of enrichment directly downstream of the TSS (Figure 1D). ChIP analysis revealed that SWR1 subunits PIE1 and ARP6 are required for deposition of H2A.Z at *FLC* as well as *FLC* paralogs *MAF4* and *MAF5* [59]. This finding, coupled with the observation that loss of HTA9 and HTA11 also result in decreased expression of these genes indicates that H2A.Z itself is required for their proper activation [30].

Recently, several protein interaction assays from independent groups have provided new insight into the composition of the plant SWR1 complex and H2A.Z interactors [41,54,63,64]. Understanding how these new subunits influence SWR1 activity will help in deconvoluting the various and sometimes contradictory functions of H2A.Z in plant transcription. Of several newfound subunits, the most studied in relation to H2A.Z deposition has been Methyl-CpG Binding Domain 9 (MBD9). ChIP-seq analysis of H2A.Z enrichment in *Arabidopsis* seedlings shows that about 20% of H2A.Z enriched sites become depleted in *mbd9* mutants [54]. Comparison of FLAG-tagged

MBD9 enrichment with corresponding ATAC-seq data indicate that MBD9 localizes primarily to areas of open chromatin and suggests that MBD9 promotes H2A.Z deposition at the 5' end of highly active genes [63]. Future experiments will be needed to determine exactly where and when during plant development this MBD9-containing SWR1 complex is performing its function, and whether specific SWR1 subtypes may be related to the activating and repressive roles of H2A.Z.

H2A.Z enrichment at the +1 nucleosome of genes in most organisms leads many to speculate that H2A.Z may help in the targeted recruitment of transcription initiation machinery. However, the presence of a second H2A.Z peak at the -1 nucleosome in some organisms suggests that H2A.Z may serve as a mere mark of transcription as opposed to a targeting factor. Bagchi et al. found that while the level of H2A.Z at the +1 nucleosome did not correlate with gene activity in yeast, it did correlate with upstream antisense transcript levels, indicating that the bimodal profile of H2A.Z at the +1 and -1 nucleosomes found in yeast is the reflection of a transcription event rather than an initiator of that event [65]. This observation is corroborated by H2A.Z enrichment patterns in other organisms. For instance in humans, where bidirectional transcription is common, H2A.Z peaks are found on both sides of the NDR [66]. Whereas in *Drosophila*, where bidirectional transcription is not frequently observed, there is a pronounced lack of H2A.Z enrichment at the -1 nucleosome [67]. Colino-Sanguino et. al reviewed recent work in mammals highlighting the contradictory results found from experiments aimed at uncovering the relationship between RNA polymerase pausing at the TSS and H2A.Z [68]. In *Arabidopsis*, GRO-seq data indicate a lack of bidirectional transcription and we again observe a lack of H2A.Z enrichment at the -1 nucleosome [69]. While H2A.Z has been implicated in gene activation across organisms, the idea

that promoter H2A.Z enrichment reflects the direction of transcription implies that H2A.Z incorporation perhaps does not facilitate targeted initiation but may help reinforce existing transcription patterns.

While H2A.Z is clearly required for high level transcription of many genes, the presence of an H2A.Z-containing nucleosome alone is likely not sufficient for transcriptional activation. For instance, recent evidence points toward acetylation of H2A.Z as a modulator of flowering time. Crevillen et al. revealed for the first time in plants the occurrence of H2A.Z acetylation and showed that this acetylation is required for proper *FLC* expression [70]. While this study marks an exciting insight into H2A.Z mediated activation, future studies are needed to determine how universal this mechanism of activation is across the plant genome. NAP1-RELATED PROTEIN 1 and 2 were recently identified as inhibitors of H2A.Z deposition [71]. Unexpectedly, *nap1;nap2* double mutants displayed an increase in H2A.Z enrichment at the TSS of *FLC* but a decrease in *FLC* expression. Wang et al. use an observed increase in nucleosome density around the TSS to explain this reduced expression and thus provide further evidence that TSS H2A.Z enrichment is likely not sufficient for activation. Additionally, *arp6* mutants also display alterations in H3K4me3 enrichment at *FLC*, but it is unclear whether this observation is a direct consequence of H2A.Z loss in the *arp6* mutant (Figure 2C) [61]. Based on current evidence it is still unclear if H2A.Z's role in active transcription is one of initiation, maintenance, or both. Indeed, various seemingly contradictory results have been reported regarding the role of H2A.Z nucleosomes as a barrier to Pol II elongation and in modulating chromatin accessibility [72–75].

H2A.X

H2A.X, the most similar histone variant to H2A, differs from canonical H2A only via a C-terminal SQL(E/D) motif in animals and a SQEF motif in plants (Figure 1B). H2A.X is present in most eukaryotes; however, unlike H2A.Z, it has evolved multiple times [53,76]. *Arabidopsis* and rice each encode two constitutively expressed and functionally redundant H2A.X genes (Table 1) [77]. The H2A.X variant is best known for its role in coordinating DNA damage responses in both animals and plants. The presence of phosphorylated H2A.X is considered a hallmark of DNA damage repair [78]. However, a number of studies suggest that phosphorylated H2A.X is also required for gene activation [79–81].

The mechanisms underlying the genome-wide distribution of H2A.X remain largely unknown in both plants and animals [82]. In humans, FACT (FAcilitates Chromatin Transcription) plays an important role in both removal and incorporation of H2A.X (Table 1) [83,84]. Studies in the mammalian system showed that H2A.X is incorporated *de novo* into damaged chromatin by FACT [82,83]. However the involvement of FACT chaperone in plant H2A.X deposition has not been investigated and we do not know if *de novo* deposition of H2A.X in response to DNA damage occurs in plants. Since the FACT chaperone is conserved among eukaryotes and domain organization of both FACT proteins, SSRP1 and SPT16, is similar between plant and mammalian, FACT may also play a role in plant H2A.X deposition [85].

H2A.X localization and relationship with gene expression

Cytologically, *Arabidopsis* H2A.X is excluded from chromocenters and primarily enriched over euchromatin [86]. Chromatin immunoprecipitation experiments reinforce this observation showing an enrichment of H2A.X over the bodies of expressed genes [87]. The relatively ubiquitous distribution of H2A.X in euchromatin is consistent with its role as a platform for DNA damage repair (DDR), as sites of DNA damage preloaded with H2A.X allow for a rapid response.

Although H2A.X is best known as a platform for DDR in plants and other eukaryotes, for the first time in plants, phosphorylated H2A.X (γH2A.X) was recently found to be required for transcriptional activation. Xiao et. al found that expression of the *ABA Insensitive 4* (*ABI4*) gene is repressed by Oxidative Stress 3 (OXS3) family proteins during seed germination. They went on to show that this repression is in fact due to an interaction between OXS3s and H2A.X that prevents H2A.X phosphorylation and subsequent ABI4 activation. Given γH2A.X's well characterized role in DNA damage response, it will be interesting to investigate whether this γH2A.X-dependent activation involves other elements of DNA damage repair. Future experiments measuring the occurrence of double-stranded breaks (DSBs) and the localization of DDR machinery around the ABI4 promoter during activation will help determine how γH2A.X-dependent activation relates to our previous understanding of γH2A.X function [81].

Although rare, there is some evidence of a non-canonical role for H2A.X in gene regulation from other eukaryotes as well. In the mammalian fibroblast cell, the *High Mobility Group AT-Hook 2* (*HMGA2*) gene also depends on γH2A.X for activation [80].

Dobersch et al. found that yH2A.X precedes DNA demethylation and transcription initiation. These results would indicate that chromatin conformation changes during activation involve DNA breakage. However, not all studies support a role for H2A.X in gene activation. Recently, Eleuteri et al. found that H2A.X curbs embryonic stem cell proliferation by repressing rRNA transcripts. They found that H2A.X, independent of H2A.X phosphorylation, at rDNA promoters is responsible for the targeted recruitment of the nucleolar remodeling complex, a complex known to establish heterochromatic features at rDNA [88].

While there is still no unifying mechanism for H2A.X/yH2A.X in transcription, evidence does suggest that H2A.X involvement in transcription is highly dependent upon cell type. Interestingly, H2A.X is maximally enriched in highly proliferative cell types compared to differentiated cell types and the enrichment patterns tend to favor transcribed genes [89,90]. Seo et al. have shown that endogenous H2A.X occupancy is positively correlated with Pol II density at a given TSS in the proliferative Jurkat cancer cell line, while they are inversely correlated in differentiated CD4-positive cells. Thus, non-canonical functions of H2A.X may arise from unique enrichment patterns present in unique cell types.

Given the apparent connection between DDR and H2A.X phosphorylation, there are surprisingly few studies profiling the mark in plants. However, profiling in mammalian cells shows yH2A.X spreads in *cis* over large domains surrounding a DSB [91]. Interestingly, the boundaries of yH2A.X domains often correspond to the native topological associated domains (TADs), suggesting yH2A.X propagation is compartmentalized by the 3D conformation of chromatin in the nucleus [92]. This will be a particularly interesting avenue to explore in plants considering the fact that

Arabidopsis has significantly fewer TAD boundaries than animal models, or even other plant species like rice [93].

Heterochromatin-associated histone variants

H2A.Z in facultative heterochromatin

Since H2A.Z incorporation at the TSS has been shown to be important for proper transcription in many organisms, it is puzzling at first to realize that the mere level of H2A.Z at this site does not reliably reflect expression level. Coupling H2A.Z ChIP-seq data with RNA-seq in *Arabidopsis* seedlings reveals that this TSS enrichment has a parabolic correlation with expression. That is, the highest and lowest expressed genes have lower levels of TSS H2A.Z enrichment than those that are moderately expressed [40,94,95]. This correlation is also found to a lesser extent in rice, where total genic H2A.Z is parabolically correlated with expression similar to promoter H2A.Z in *Arabidopsis* [95]. Looking at H2A.Z in the promoter region of genes offers a limited perspective. Recent work discussed in the following section analyzing genic H2A.Z beyond promoter enrichment help to paint a more complete picture of H2A.Z as a transcriptional regulator.

Several recent studies in plants have revealed a role for H2A.Z in gene repression. While initial experiments revealed some H2A.Z-dependent repression within specific genes or gene families, no genome-wide relationship between H2A.Z and repression had been established [96,97]. However, in 2012 Coleman-Derr and Zilberman found that H2A.Z enrichment beyond the TSS and into the gene body is anticorrelated with transcriptional output and that these lowly transcribed genes are enriched in pathways

involving environmental or developmental responses [40]. Since then, several papers have been published validating a repressive role of H2A.Z in gene transcription. Particularly, gene body H2A.Z was shown to play a repressive role in response to light, drought stress, salt stress, and heat stress response in *Arabidopsis*, as well as phosphate deficiency in rice and heat stress in Brachypodium distachyon [95,98–102]. A recent study in rice showed that reductions in both H2A.Z and H3K4me3 correlated with increased expression under phosphate starvation while decreases in H3K4me3 alone did not [103]. Additionally, loss of the INO80 chromatin remodeling complex (responsible for H2A.Z eviction from chromatin) leads to decreases in both the deposition of H3K4me3 and transcription elongation typically observed at thermomorphogenesis genes during a high temperature induction [104]. These results suggest that a coordination between H3K4me3 and H2A.Z may be required for proper activation of certain responsive genes.

Despite this recent focus on H2A.Z-mediated repression, no model has been proposed to sufficiently account for the genome-wide association between H2A.Z and repression. One idea is that gene body H2A.Z facilitates repression in a reversible manner serving as a more dynamic alternative to DNA methylation [40]. This notion is supported by findings that the SWR1 complex is required for trimethylation of H3K27 at most H2A.Z enriched sites, a key step in the Polycomb pathway of gene silencing (Figures 1D and 2B) [105]. However, several recent reports indicate that H2A.Z may use Polycomb proteins to achieve silencing outside of the accepted Polycomb pathway, raising several questions about the canonical pathway of Polycomb silencing. While SWR1 is required for H3K27me3, the small number of overlapping upregulated genes between *hta9 hta11* and PRC2 catalytic subunit CURLY LEAF (CLF) mutants suggest

that H2A.Z-mediated repression is independent of PRC2 activity [106,107]. Even more evidence that H2A.Z achieves repression via an unexplored Polycomb pathway comes from Cai et al., who found that H2A.Z enrichment is required for repression of several anthocyanin biosynthesis genes. Interestingly, while H2A.Z is required for the deposition of H3K27me3 at these genes, H3K27me3 is not necessary for their repression [108]. Recently, our group, as well as others, identified an interaction between the SWR1 complex and several ALFIN1-LIKE family proteins (AL5, AL6, and AL7) [54,63,64]. Little is known about this plant-specific family of proteins but the few studies of ALFIN1-LIKE proteins in *Arabidopsis* implicate them in Polycomb-mediated silencing. Molitor et. al. identified the same AL proteins found in SWR1 pulldowns as interactors with POLYCOMB REPRESSIVE COMPLEX 1 (PRC1) [109]. They went on to show that *al6/al7* double mutants cause a delay in the chromatin state switch from active H3K4me3 to repressive H3K27me3 in key seed developmental genes [109]. This led authors to propose that ALs bind H3K4me3 via a plant-homeodomain (PHD) and recruit PRC1 to initiate Polycomb mediated silencing. How exactly the ALs are targeted to these genes destined for repression is still unclear, and given H2A.Z's relatively newfound role in repression of responsive genes, it will be interesting to see how the interaction between SWR1 and ALs influences where silencing occurs.

Monoubiquitination of H2A.Z by the PRC1 catalytic subunit atBMI1 provides yet another connection between H2A.Z and Polycomb silencing with 68% of genes upregulated in *hta9/hta11* mutants being enriched for both H2A.Z and H2A121ub in WT [106]. H2A.Z was also found as a mark of inactive enhancers in plants, with its presence being associated with lower expression of putative target genes and increased

enrichment of H3K27me3, a finding that is in contrast to humans where enhancer H2A.Z instead colocalizes with activating marks H3K4me3 and H3K27ac [110,111].

H2A.W in constitutive heterochromatin

H2A.W variants are exclusive to the plant lineage and are defined by an extended C-terminal tail containing an SPKK motif [53,87](Figure 1B). Since green algae and non-flowering land plants lack H2A.W variants, it is proposed that H2A.W evolved from early spermatophytes [53]. Liverworts, mosses and lycophytes possess the novel H2A variant H2A.M as a potential alternative to H2A.W, with commonalities in the C-terminal tail and L1 loop [53]. In contrast to other histone variants, H2A.W has S-phase expression in *Arabidopsis*. [6]. Additionally, disruption of CAF-1, which regulates chromatin assembly after replication, results in reduced H2A.W levels, implying that its deposition is replication-dependent (Table 1) [112].

Phosphorylation dynamics of H2A.W variant HTA7 were found to play an essential role in the effective response to DNA damage in heterochromatic regions. Therefore, one proposed function of H2A.W is to serve as a functional complement to H2A.X in heterochromatin, providing a platform for phosphorylation in response to DNA damage [86]. Monocot H2A.W contains multiple copies of the SPKK motif while eudicots have a single copy [53]. This SPKK is known to promote chromatin condensation by binding to A/T rich sites on DNA generally found in the satellite repeats of constitutive heterochromatin. The presence of this motif as well as *in vitro* nucleosome assembly results indicate that H2A.W generally promotes chromatin condensation [53,87]. However, recent studies highlighted below indicate that H2A.W's role in heterochromatin is perhaps more nuanced than previously expected.

H2A.W localization and relationship with heterochromatin accessibility

H2A.W is located primarily in constitutive heterochromatin, with correlation between the variant and H3K9me2, DNA methylation, and linker histone H1 (Figure 1C) [86,87,113]. However, H2A.W deposition into heterochromatic regions does not depend on DNA methylation or H3K9me2 [87]. New H2A.W triple mutants, *h2a.w-2,* created by crossing a CRISPR generated null *hta6* allele with *hta7* and *hta12* T-DNA lines reveal a potentially unique role for H2A.W in maintaining a level of accessibility in constitutive heterochromatin [113]. Using ATAC and bisulfite sequencing analysis of *h1*, *h2a.w-2,* and *h1/h2a.w-2* double mutants, Bourguet et al. concluded that H2A.W actually antagonizes the binding of H1 to linker DNA in constitutive heterochromatin (Figure 2D). They propose the SPKK motif of H2A.W competes with the two SPKK motifs found in H1 for binding on linker DNA. Therefore, the SPKK motif of H2A.W, which was thought to promote chromatin condensation when compared to other H2A variants, may actually function to prevent even further condensation by H1. This allows regions occupied by H2A.W to maintain a heterochromatic state while still being accessible to maintenance factors like DNA methyltransferases [113].

Of course, an analysis of H2A.W alone is incomplete without considering the chromatin remodelers that act on it. Recently, Osakabe et al. identified DDM1 (DECREASE IN DNA METHYLATION 1) as a depositor of H2A.W in *Arabidopsis*. In stark contrast with *h2a.w-2*, *ddm1* mutants had significant derepression (40%) of pericentromeric TEs and no reported changes in H1 enrichment (Table 1) [114]. While H3K9me2 and DNA methylation were reduced in *ddm1*, their effects on silencing TEs

were found to be secondary to that of *ddm1*. The results of these two studies raise several exciting questions, namely; How does total H2A.W loss in *h2a.w-2* have a lesser effect on TE silencing than DDM1 loss? Is DDM1 acting independently of H2A.W to silence TEs in *h2a.w-2* mutants? Genomic profiling analysis of DDM1 enrichment in WT and *h2a.w-2* is one of many future experiments that will help answer these questions. Furthermore, deconvoluting the mechanisms behind DDM1 and H2A.W function may help to inform human disease, where Lymphocyte-Specific Helicase (LSH) and macroH2A appear to play a similar role in mammalian silencing [115].

H1

The linker histone H1 binds both the nucleosome core particle and the linker DNA to facilitate internucleosomal interactions and chromatin compaction. Interestingly, H1 and associated variants have a separate evolutionary origin from core histones, having evolved from bacterial proteins rather than archaeal ones [116]. H1 histones are also more divergent across species compared to core histones [116]. However, the general structure of a lysine rich C-terminal tail, a flexible and short N-terminus and a central globular domain are conserved across eukaryotes [51].

Due to the importance of H1 variants in chromatin dynamics, it is surprising to observe that H1 depletions in *Arabidopsis*, yeast, worms and fungi are viable while mutation of H1 variants in mouse and Drosophila are lethal [117–124]. Plant H1 variants are classified into two groups, main variants with ubiquitous and stable expression and minor variants, which accumulate in response to stress [1,4,125]. In contrast to mammals with 11 H1 variants, only three nonallelic H1 variants are found in *Arabidopsis*: two highly similar major variants H1.1 and H1.2 and the shorter

stress-induced minor variant H1.3 (Table 1) [125,126]. The key structural differences between H1.3 and H1.1/H1.2 are a decreased positive charge in H1.3, a shorter C-terminal domain, and a lack of (S/T)PXK DNA-binding motifs in both N- and C-terminal domains (Figure 1B) [127]. While H1.1/2 variants are expressed in all cell types, H1.3 is expressed constitutively in guard cells with induced expression in other cell types during stress.

H1 localization

Genome-wide analysis of H1.1/2 in *Arabidopsis* show that linker histones are found in both heterochromatic and euchromatic regions and generally associate with methylated DNA sequences, with the strongest enrichment over hypermethylated TEs and lowly expressed genes. Genic H1 enrichment however is linked with methylation status rather than expression level, with similarly expressed genes only being enriched for H1 if methylated [128]. At a closer look, gene body H1 enrichment is characterized by peaks at the 5' and 3' ends, just inside the nucleosome depleted regions. However, as genes increase in expression, total H1 occupancy falls as expected but enrichment takes on a new asymmetrical shape, with 5' ends having lower H1 levels with increasing enrichment towards the 3' ends. This asymmetry is not reported in Drosophila or mammals, and future investigations may uncover whether and how this pattern affects transcription in plants. The localization pattern of H1.3 is similar to H1.1/2 variants. However, compared to H1.1/2, H1.3 association with chromatin is far more dynamic and is more frequently associated with active chromatin marks such as H3K4me3 [129]. Additionally, increased levels of DNA methylation, which are normally observed in response to stress, were significantly decreased in *h1.3* mutants under stress conditions.

These distinctions suggest that H1.3 may outcompete H1.1/2 under stress allowing for increased accessibility to regulatory machinery like DNA methyltransferases [129].

H1-dependent silencing in euchromatin and heterochromatin

Recent evidence indicates that plant H1 contributes to the structural organization of both constitutive heterochromatin and euchromatin. Independent studies using H1 triple mutants (*3h1*) and double mutants both found chromocenter decondensation in *Arabidopsis* [128,130]. Despite this observation, H1 double and triple mutants had minimal transposable element (TE) derepression. This evidence is in conflict with the common view that chromatin compaction is required for efficient TE silencing and suggests that loss of H1 contributes to heterochromatin structure without any functional impact on silencing.

H1 variants impact the pattern of heterochromatic DNA methylation in CG, CHH and CHG contexts [127,131,132]. *h1.1 and h1.2* mutants both show increased DNA methylation in heterochromatic TEs, suggesting that H1 variants inhibit heterochromatin accessibility to DNA methyltransferases. While further investigation is still needed, considering the relationship between DNA methylation and H1 in plants as well as other eukaryotes may help to explain the surprisingly minimal impact H1 has on TE silencing. In mice, the situation is similar to plants, where *h1* mutants (mutation in both H1.1 and H1.2) show only partial TE upregulation [122]. However in *Drosophila*, where cytosine methylation is absent, H1 loss does indeed induce general TE expression [133,134]. This suggests that while H1 contributes to TE silencing, organisms with DNA methylation are able to maintain this silencing despite H1-dependent changes in

chromatin structure [128]. This theory is supported by a small number of TEs in *Arabidopsis* that were found to be derepressed more in *met1;h1* double mutants than in either single mutant alone [128]. Additionally, a recent study revealed that a family of TEs located in pericentromeric heterochromatin (where evidence suggests that silencing is achieved independently of DNA methylation) depend on H1 for their repression under heat stress. By contrast, a family of non-pericentromeric TEs affected by heat rely on DNA methylase CMT2 together with H1 for stable repression [135]. H1 overexpression in vegetative *Arabidopsis* cells also predominantly leads to the repression of pericentromeric TEs [136]. Similar to their effect on TE silencing, it was shown that loss of H1 intensifies the activation of antisense transcripts only at genes hypomethylated in *met1* [128].

As in heterochromatin, euchromatic H1 loss causes profound changes in chromatin structure with surprisingly little impact on gene expression. In WT plant cells there is a strong inverse correlation between nucleosome occupancy and transcription, with highly expressed genes having the lowest occupancy [130]. Low nucleosome occupancy is often interpreted as a requirement for increasing accessibility of a transcribed gene to transcriptional machinery and lowering the energy barrier presented by nucleosomes to RNA polymerase procession. In H1-depleted cells this correlation is almost completely lost, with all genes having similar nucleosome occupancy regardless of expression level [130]. Surprisingly, gene expression is relatively unchanged in these cells, with only about 3% of genes being misregulated. This result indicates that H1-mediated nucleosome occupancy is a consequence rather than a driver of steady state transcription. However, H1-depleted plants do have defects

in several developmental and cellular transitions including seed dormancy control, flowering time control, and lateral root initiation [130]. Collectively, these observations indicate that the massive structural alterations found in H1 mutants likely affect tight control of developmental and cellular transitions. Therefore, H1-dependent chromatin structures may have a more prominent role in transcriptional reprogramming rather than in fundamental expression. Supporting a role for H1 in transcriptional reprogramming is the observation that *3h1* mutant cells also have a dramatic reduction of nuclear H3K27me3, a hallmark of epigenetic silencing memory across plants and animals [130].

Conclusion and future directions

Most studies investigate histone variants by observing their genome-wide distributions before and after a disruption or exposure. However, it is clear that future studies will need to be performed at a higher temporal resolution to determine the exact order of events that take place during variant-mediated gene regulation. For instance, there is mounting evidence for a role of H2A.Z in regulating a majority of environmental responses but no data currently exists to explain how this repressive state comes about, or how it may change during activation. Excitingly, Willige et al. used temporally resolved H2A.Z profiling to find that gene body H2A.Z loss actually precedes activation of select red:far-red light sensitive genes, indicating that H2A.Z loss is not merely a consequence of their activation [137]. Additionally, following enrichment of H3.3 and H1 through precise time points during cell fate determinations will help explain why these histones play fundamental roles in transcriptional reprogramming during

development while being dispensable for general transcription. Similarly, conclusions in variant research have often been limited by assays profiling large cell populations. Emerging single cell data indicates that cells within these heterogeneous populations do not behave uniformly and meaningful changes in variant deposition may be masked by homogenized tissue samples. As chromatin profiling techniques advance and read depth requirements fall, single cell type profiling will uncover how these variants behave within uniform cell types and even single cells.

Modification of variants

It is reasonable to imagine that the apparent multifunctionality of H2A.Z is due in part to modifications to the histone itself. For instance, we know that H2A.Z acetylation is sufficient for gene activation at *FLC*. But what about acetylation at other genes with similar H2A.Z distribution profiles that appear inactive? Are those genes simply upstream of others in the process of activation or is there a compounding modification like methylation that is stifling activation? Future studies profiling these variant modifications genome-wide will be essential to closing the current knowledge gap between H2A.Z mediated activation and repression. Additionally, H3.3 K4 plays an essential role in mammalian embryonic stem cell differentiation, likely as a platform for methylation [138]. This essential role for H3.3K4 in the stem cell could help explain the observation in plants that H3.3 is essential for viability while being dispensable for general transcription. This residue and others known to be modified in other species are conserved in plants meaning there is great potential for the future study of plant H3.3 modifications.

Role of chromatin remodelers in regulation

Histone variant chaperones are often used as proxies for the study of histone variants. However, these chaperones often have functions outside of just histone deposition. For instance, *swr1* mutants show a global depletion of H3K27me3 while this phenotype is much less severe in *hta9 hta11* double mutants [105,106]. Similarly, *ddm1* mutants have significant TE derepression while *h2aw-2* mutants do not. Future studies are needed to decouple the functions of these chromatin remodelers from the variants themselves. Additionally, while conservation and mutant analysis implicate other chromatin remodelers as variant chaperones in plants, H2A.X and H3.3 still do not have confirmed interactions with a chromatin remodeler or chaperone.

DNA methylation and histone variants

Each histone variant discussed in this review has some relationship with DNA methylation. H2A.Z and DNA methylation are mutually exclusive in the *Arabidopsis* genome, suggesting that gene body H2A.Z may serve to protect responsive genes from the more permanent effects of DNA methylation [40,94]. However, while loss of H2A.Z does cause hypermethylation over select regions, overall methylation patterns are unaffected [40,41]. On the contrary, global reductions in DNA methylation in *met1* mutants result in an increase in H2A.Z enrichment at those sites, implying that it is DNA methylation which excludes H2A.Z rather than the inverse [94].

DNA methylation and H3.3 are both enriched over the body of active *Arabidopsis* genes [139–141]. Detailed characterization of *Arabidopsis h3.3kd* mutants revealed that

the level of DNA methylation decreases exclusively at regions where H3.3 and DNA methylation overlap on active gene bodies [21]. In the same *h3.3kd* mutants, these active gene bodies are also invaded by H1 and H2A.Z (Figure 2A). Therefore, reduced gene body methylation in *h3.3kd* might allow ectopic recruitment of H2A.Z-containing nucleosomes to gene bodies. Given H2A.Z's role in transcriptional repression, H3.3 enrichment over genes may be required to maintain suitable chromatin structure for transcription by antagonizing H1 invasion of active genes. Low H1 levels will therefore provide sufficient accessibility to DNA methyltransferases that methylate gene bodies and prevent invasion by H2A.Z. Similarly, *h2a.w-2* mutants also show an increase in H1 enrichment and a decrease in DNA methylation in constitutive heterochromatin. Therefore, H2A.W may serve as a functional complement to H3.3 with respect to maintaining the balance between H1 and DNA methylation specifically in constitutive heterochromatin.

Summary Points

- H3.3 promotes DNA accessibility in part through an antagonistic relationship with H1.
- Phe41 is an amino acid substitution unique to plant H3.1 and may impart functions on H3.1 that are plant-specific.
- H3.3 cannot be methylated at K27, implying that H3.3 can interrupt the Polycomb pathway of gene repression and potentially perpetuate the euchromatic chromatin state across cell divisions.

- Eukaryotes without bidirectional transcription have peak H2A.Z enrichment downstream of the TSS while organisms with bidirectional transcription have bimodal H2A.Z enrichment. H2A.Z is therefore a marker for transcriptional direction.
- For the first time in plants, phosphorylation of H2A.X was found to be required for transcriptional activation of *ABI4*. It will be interesting to investigate whether this yH2A.X-dependent activation involves other elements of DNA damage response and repair.
- Recent evidence shows that H2A.Z enrichment within the gene body contributes to transcriptional repression likely through a non-canonical Polycomb pathway of gene silencing.
- H2A.W is a histone variant unique to plants which may promote accessibility of constitutive heterochromatin by competing with H1 for binding to linker DNA.
- Nucleosome occupancy depends on linker histone H1 and together with DNA methylation, promotes the silencing of TEs.
- H1-dependent chromatin structures may have a more prominent role in transcriptional reprogramming than in steady state expression.

Figures

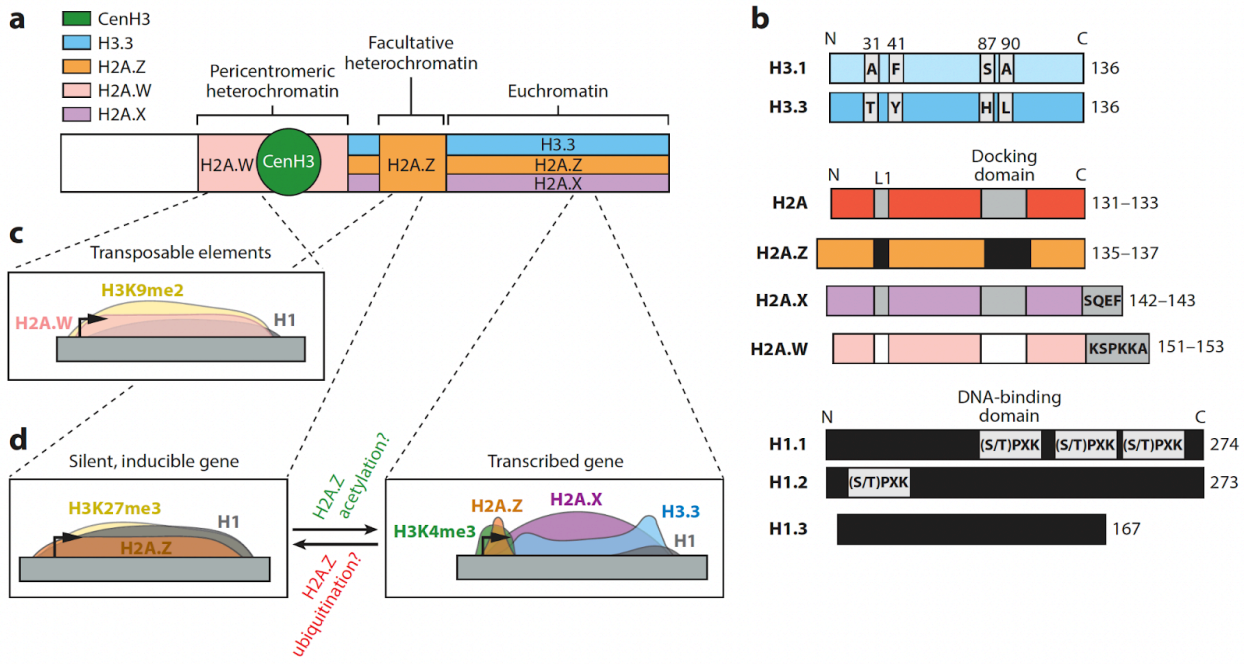

Figure 1. The nature of histone variants and their distribution in chromatin.

(A) Schematic diagram of a chromosome, showing the distribution of major chromatin types and the histone variants associated with each. (B) Diagrams comparing histone variants and their canonical counterparts. Regions of sequence differences or additions between variants and canonical types are shown as boxes. H3.1 and H3.3 differ by only four amino acid substitutions: two in the N-terminal tail and two in the histone-fold domain. H2A variants are distinguished mainly by sequence variation in the L1 loop and docking domain, while H2A.X and H2A.W have variant-specific C-terminal extensions. H1 subtypes vary in the occurrence of DNA-binding domains and their overall length. (C) Diagram showing the distribution of H2A.W on silent transposable elements and association with H1 and H3K9me2. (D) Two distinct, and perhaps interconvertible, distribution patterns of H2A.Z on silent genes in facultative heterochromatin (left) and active euchromatic genes (right). Silent genes show

ubiquitinated H2A.Z nucleosomes across the gene body and are associated with H3K27me3 and H1, while active genes show acetylated H2A.Z in the +1 nucleosome and H3.3 in the gene body.

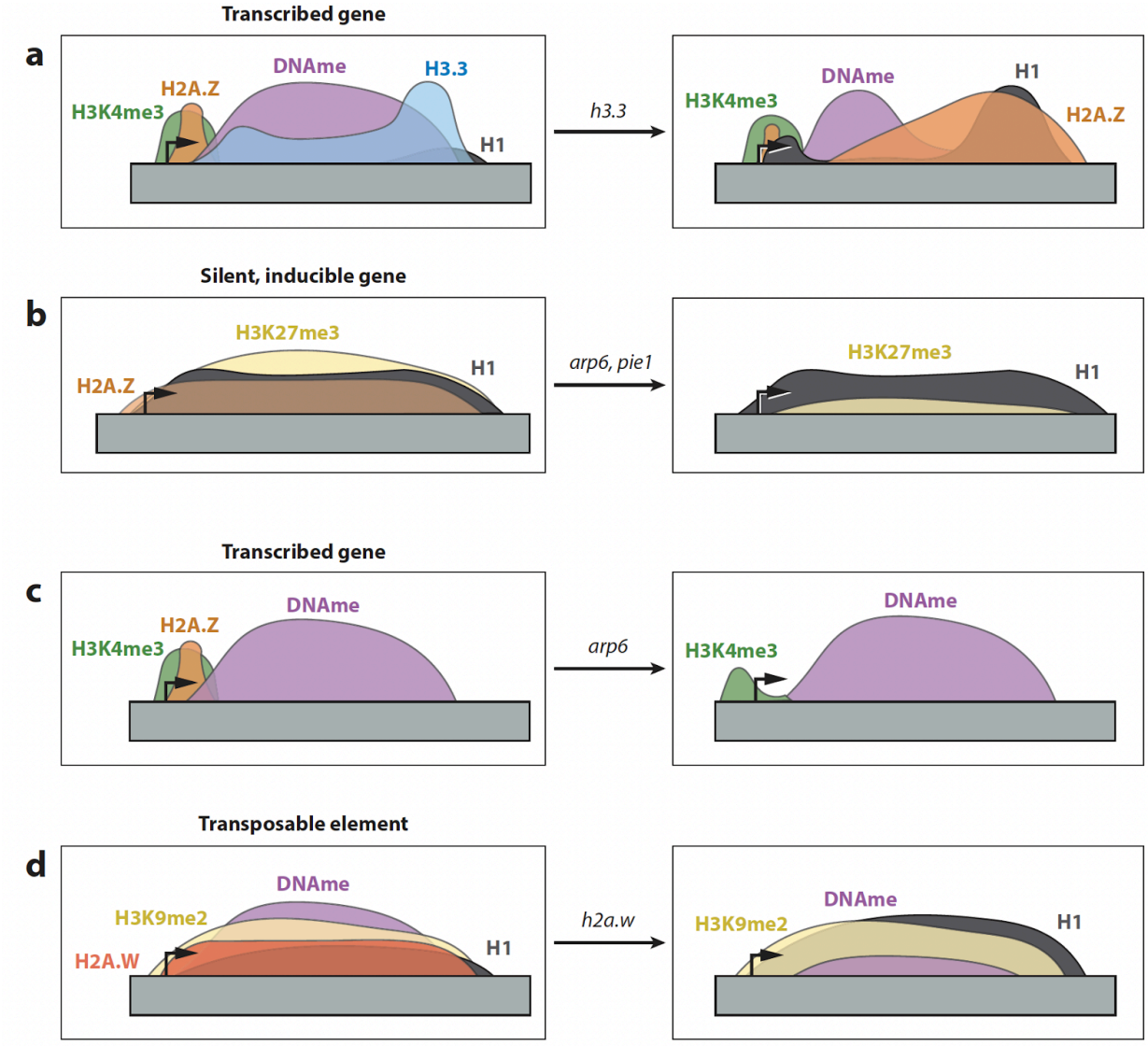

Figure 2. Chromatin landscape changes in response to histone variant depletion.

(**A**) H3.3 loss at transcribed genes results in reduced DNA methylation (DNAme) in the CG context, and increased H2A.Z and H1 in the downstream regions previously

occupied by H3.3. Active histone marks such as H3K4me3 and H4K36me3 are generally unaffected. Given that H3.3 does not seem to be methylated at K27, genes targeted for polycomb repression may be subject to silencing when H3 nucleosomes become predominant in the absence of H3.3. (**B**) H2A.Z loss from silent, inducible genes in SWR1 mutants (*arp6* and *pie1*) results in reduced H3K27me3 without affecting H1 levels. These silent genes also lose H3K27me3 and generally become active upon H2A.Z loss. (**C**) In transcribed genes, H2A.Z loss in SWR1 mutants results in a reduction of H3K4me3, particularly around the +1 nucleosome, without changes in DNA methylation. H2A.Z loss from these genes generally corresponds to decreased Pol II occupancy and transcription as well. (**D**) Loss of H2A.W at transposable elements (TEs) results in reduced DNA methylation and increased H1 occupancy, while the repressive mark H3K9me2 is generally unaffected. Interestingly, one study showed that loss of H2A.W in *h2a.w* mutants did not result in widespread expression of silent TEs (10), while another study showed that H2A.W loss resulting from mutation of DDM1 did result in increased TE expression (98). In these *ddm1* mutants, there was also a reduction in H3K9me2 without changes in H1 enrichment. These contrasting results suggest that H2A.W and the DDM1 remodeler have overlapping and distinct functions in heterochromatin.

Table 1. Histone variant genes, proteins, and functions in *Arabidopsis thaliana*

Histone variants	*Arabidopsis* genes	*Arabidopsis* loci	Proteins	Chaperones/ remodelers	Function			Knockout/knockdown *Arabidopsis* phenotype	Modification
					General	Development	Stress responses		
H3.3	HTR4 HTR5 HTR8	At4g40030 At4g40040 At5g10980	H3.3 H3.3 H3.3	HIRA (94) ATRX (34)	Transcriptional activation (120, 124, 141, 152)	Flowering time (152); male gametogenesis (53); postgermination development (5); cell proliferation and organogenesis (99)	Regulate the expression of responsive and hypervariable genes (142)	Double mutants *htr5 htr8* are phenotypically normal; triple mutants cause lethality; double mutant *htr4 htr8* plants that carry either *amiR-HTR5-1* or *amiR-HTR5-II* (*h3 3kd*) exhibit leaf serration, incomplete sterility, and growth defects (142)	H3.3K36me3 (87)
H2A.Z	HTA8 HTA9 HTA11	At2g38810 At1g52740 At3g54560	H2A.Z.8 H2A.Z.9 H2A.Z.11	SWR1 complex (42, 134)	Transcriptional activation and repression	Flowering time (16, 29, 84, 96, 121); vegetative to reproductive phase transition (42, 144); inflorescence architecture (11); germline development (153); circadian clock (130)	Temperature response (24, 65, 129); phosphate deficiency (40, 123, 148); drought stress (11, 125); immunity (6); salt stress (91)	Double/triple mutants show developmental aberrations (81, 93); triple mutants are viable but show reduced fertility (20); knockdown of all three H2A.Z genes causes early flowering (16)	H2A.Z acetylation (25); H2A.Z monoubiquitination (H2AZub) (43); H2A.Z SUMOylation and methylation?
H2A.X	HTA3 HTA5	At1g54690 At1g08880	H2A.X.3 H2A.X.5	FACT? (44)	DNA damage response (13, 66, 110); transcription activation (143)	H2A.X is unessential for *Arabidopsis* development (51)	Genotoxic stress (138)	The single/double mutants are viable, fertile, and indistinguishable from wild type (51)	Phosphorylated H2A.X (66, 110)
H2A.W	HTA6 HTA7 HTA12	At5g59870 At5g27670 At5g02560	H2A.W.6 H2A.W.7 H2A.W.12	DDM1 (98)	Chromatin condensation (147)	H2A.W is unessential for *Arabidopsis* development (10)	Not determined	H2A.W triple mutants are indistinguishable from the wild type (10)	Phosphorylated H2A.W (74, 110)
H1	HON1 HON2 HON3	At1g06760 At2g30620 At2g18050	H1.1 H1.2 H1.3	NRP1 and NRP2? (89, 100)	Chromatin condensation (14, 112)	Flowering time; seed dormancy; lateral root, stomata, and callus development (112); male and female gametogenesis (115)	Drought stress (2); combined light and water deficiency (113)	Triple mutants are viable but show extended dormancy, early flowering, increased root density and lateral root numbers, and altered stomatal pattern (112)	Phosphorylation, acetylation, mono- and dimethylation, formylation, crotonylation and propionylation (63)

Abbreviations: ATRX, Alpha thalassemia-mental retardation X-linked syndrome; DDM1, DECREASE IN DNA METHYLATION 1; FACT, Facilitates Chromatin Transcription; HIRA, Histone Transcriptional Regulator A; HON, HISTONE; HTA, HISTONE H2A; HTR, HISTONE 3 RELATED (HTR); NRP, NAP1-RELATED PROTEIN; SWR1, SWI2/SNF2-Related 1.

References

1. Talbert PB, Ahmad K, Almouzni G, Ausió J, Berger F, Bhalla PL, et al. A unified phylogeny-based nomenclature for histone variants. Epigenetics Chromatin. 2012;5: 7.

2. Lei B, Berger F. H2A Variants in Arabidopsis: Versatile Regulators of Genome Activity. Plant Communications. 2020;1: 100015.

3. Borg M, Jiang D, Berger F. Histone variants take center stage in shaping the epigenome. Curr Opin Plant Biol. 2021;61: 101991.

4. Kotliński M, Knizewski L, Muszewska A, Rutowicz K, Lirski M, Schmidt A, et al. Phylogeny-based systematization of Arabidopsis proteins with histone H1 globular domain. Plant Physiol. 2017;174: 27–34.

5. Probst AV, Desvoyes B, Gutierrez C. Similar yet critically different: the distribution, dynamics and function of histone variants. J Exp Bot. 2020;71: 5191–5204.

6. Zambrano-Mila MS, Aldaz-Villao MJ, Casas-Mollano JA. Canonical Histones and Their Variants in Plants: Evolution and Functions. Epigenetics in Plants of Agronomic Importance: Fundamentals and Applications. Springer; 2019. pp. 185–222.

7. Okada T, Endo M, Singh MB, Bhalla PL. Analysis of the histone H3 gene family in Arabidopsis and identification of the male-gamete-specific variant AtMGH3. Plant J. 2005;44: 557–568.

8. Hu Y, Lai Y. Identification and expression analysis of rice histone genes. Plant Physiol Biochem. 2015;86: 55–65.

9. Stroud H, Otero S, Desvoyes B, Ramírez-Parra E, Jacobsen SE, Gutierrez C. Genome-wide analysis of histone H3.1 and H3.3 variants in Arabidopsis thaliana. Proc Natl Acad Sci U S A. 2012;109: 5370–5375.

10. Waterborg JH, Robertson AJ. Common features of analogous replacement histone H3 genes in animals and plants. J Mol Evol. 1996;43: 194–206.

11. Waterborg JH. Evolution of histone H3: emergence of variants and conservation of post-translational modification sites. Biochem Cell Biol. 2012;90: 79–95.

12. Lewis PW, Elsaesser SJ, Noh K-M, Stadler SC, Allis CD. Daxx is an H3. 3-specific histone chaperone and cooperates with ATRX in replication-independent chromatin assembly at telomeres. Proceedings of the National Academy of Sciences. 2010;107: 14075–14080.

13. Ricketts MD, Frederick B, Hoff H, Tang Y, Schultz DC, Rai TS, et al. Ubinuclein-1 confers histone H3. 3-specific-binding by the HIRA histone chaperone complex. Nat Commun. 2015;6: 1–11.

14. Duc C, Benoit M, Détourné G, Simon L, Poulet A, Jung M, et al. Arabidopsis ATRX modulates H3. 3 occupancy and fine-tunes gene expression. Plant Cell. 2017;29: 1773–1793.

15. Nie X, Wang H, Li J, Holec S, Berger F. The HIRA complex that deposits the histone H3. 3 is conserved in Arabidopsis and facilitates transcriptional dynamics.

Biol Open. 2014;3: 794–802.

16. Shi L, Wang J, Hong F, Spector DL, Fang Y. Four amino acids guide the assembly or disassembly of Arabidopsis histone H3. 3-containing nucleosomes. Proceedings of the National Academy of Sciences. 2011;108: 10574–10578.

17. Shu H, Nakamura M, Siretskiy A, Borghi L, Moraes I, Wildhaber T, et al. Arabidopsis replacement histone variant H3. 3 occupies promoters of regulated genes. Genome Biol. 2014;15: R62.

18. Wollmann H, Holec S, Alden K, Clarke ND, Jacques P-E, Berger F. Dynamic deposition of histone variant H3. 3 accompanies developmental remodeling of the Arabidopsis transcriptome. PLoS Genet. 2012;8.

19. Lu L, Chen X, Qian S, Zhong X. The plant-specific histone residue Phe41 is important for genome-wide H3. 1 distribution. Nat Commun. 2018;9: 1–10.

20. Dawson MA, Bannister AJ, Göttgens B, Foster SD, Bartke T, Green AR, et al. JAK2 phosphorylates histone H3Y41 and excludes HP1α from chromatin. Nature. 2009;461: 819–822.

21. Wollmann H, Stroud H, Yelagandula R, Tarutani Y, Jiang D, Jing L, et al. The histone H3 variant H3.3 regulates gene body DNA methylation in Arabidopsis thaliana. Genome Biol. 2017;18: 94.

22. Zhao F, Zhang H, Zhao T, Li Z, Jiang D. The histone variant H3.3 promotes the active chromatin state to repress flowering in Arabidopsis. Plant Physiol. 2021 [cited 19 May 2021]. doi:10.1093/plphys/kiab224

23. Zemach A, Kim MY, Hsieh P-H, Coleman-Derr D, Eshed-Williams L, Thao K, et al. The Arabidopsis nucleosome remodeler DDM1 allows DNA methyltransferases to access H1-containing heterochromatin. Cell. 2013;153: 193–205.

24. Jacob Y, Bergamin E, Donoghue MTA, Mongeon V, LeBlanc C, Voigt P, et al. Selective methylation of histone H3 variant H3.1 regulates heterochromatin replication. Science. 2014;343: 1249–1253.

25. Otero S, Desvoyes B, Peiró R, Gutierrez C. Histone H3 dynamics reveal domains with distinct proliferation potential in the Arabidopsis root. Plant Cell. 2016;28: 1361–1371.

26. Hofmann NR. Last Exit to Differentiation: Histone Variants as Signposts. The Plant cell. 2016. p. 1235.

27. Malik HS, Henikoff S. Phylogenomics of the nucleosome. Nat Struct Biol. 2003;10: 882–891.

28. Jarillo JA, Piñeiro M. H2A.Z mediates different aspects of chromatin function and modulates flowering responses in Arabidopsis. Plant J. 2015;83: 96–109.

29. March-Díaz R, Reyes JC. The Beauty of Being a Variant: H2A.Z and the SWR1 Complex in Plants. Mol Plant. 2009;2: 565–577.

30. March-Díaz R, García-Domínguez M, Lozano-Juste J, León J, Florencio FJ, Reyes JC. Histone H2A.Z and homologues of components of the SWR1 complex are required to control immunity in Arabidopsis. Plant J. 2008;53: 475–487.

31. Raisner RM, Hartley PD, Meneghini MD, Bao MZ, Liu CL, Schreiber SL, et al. Histone variant H2A.Z marks the 5' ends of both active and inactive genes in euchromatin. Cell. 2005;123: 233–248.

32. Rosa M, Von Harder M, Cigliano RA, Schlögelhofer P, Mittelsten Scheid O. The Arabidopsis SWR1 chromatin-remodeling complex is important for DNA repair, somatic recombination, and meiosis. Plant Cell. 2013;25: 1990–2001.

33. Marques M, Laflamme L, Gervais AL, Gaudreau L. Reconciling the positive and negative roles of histone H2A.Z in gene transcription. Epigenetics. 2010;5: 267–272.

34. Xu Y, Ayrapetov MK, Xu C, Gursoy-Yuzugullu O, Hu Y, Price BD. Histone H2A.Z controls a critical chromatin remodeling step required for DNA double-strand break repair. Mol Cell. 2012;48: 723–733.

35. Clarkson MJ, Wells JR, Gibson F, Saint R, Tremethick DJ. Regions of variant histone His2AvD required for Drosophila development. Nature. 1999;399: 694–697.

36. Van Daal A, Elgin SCR. A Histone Variant , H2AvD , is Essential in Drosophila melanogaster. Mol Biol Cell. 1992;3: 593–602.

37. Faast R, Thonglairoam V, Schulz TC, Beall J, Wells JRE, Taylor H, et al. Histone variant H2A . Z is required for early mammalian development. Curretnt Biology. 2001;11: 1183–1187.

38. Liu X, Li B, GorovskyMA. Essential and nonessential histone H2A variants in

Tetrahymena thermophila. Mol Cell Biol. 1996;16: 4305–4311.

39. Choi K, Park C, Lee J, Oh M, Noh B, Lee I. Arabidopsis homologs of components of the SWR1 complex regulate flowering and plant development. Development. 2007;134: 1931–1941.

40. Coleman-Derr D, Zilberman D. Deposition of Histone Variant H2A.Z within Gene Bodies Regulates Responsive Genes. PLoS Genet. 2012;8. doi:10.1371/journal.pgen.1002988

41. Nie W-F, Lei M, Zhang M, Tang K, Huang H, Zhang C, et al. Histone acetylation recruits the SWR1 complex to regulate active DNA demethylation in Arabidopsis. Proc Natl Acad Sci U S A. 2019;116: 16641–16650.

42. Kobor MS, Venkatasubrahmanyam S, Meneghini MD, Gin JW, Jennings JL, Link AJ, et al. A protein complex containing the conserved Swi2/Snf2-related ATPase Swr1p deposits histone variant H2A.Z into euchromatin. PLoS Biol. 2004;2: E131.

43. Mizuguchi G, Shen X, Landry J, Wu W-H, Sen S, Wu C. ATP-driven exchange of histone H2AZ variant catalyzed by SWR1 chromatin remodeling complex. Science. 2004;303: 343–348.

44. Verbsky ML, Richards EJ. Chromatin remodeling in plants. Curr Opin Plant Biol. 2001;4: 494–500.

45. Bönisch C, Hake SB. Histone H2A variants in nucleosomes and chromatin: more or less stable? Nucleic Acids Res. 2012;40: 10719–10741.

46. Dorigo B, Schalch T, Bystricky K, Richmond TJ. Chromatin fiber folding: requirement for the histone H4 N-terminal tail. J Mol Biol. 2003;327: 85–96.

47. Fan JY, Rangasamy D, Luger K, Tremethick DJ. H2A.Z Alters the Nucleosome Surface to Promote HP1α-Mediated Chromatin Fiber Folding. Mol Cell. 2004;16: 655–661.

48. Paul S. Histone “acidic patch”: a hotspot in chromatin biology. Nucleus. 2021. doi:10.1007/s13237-021-00357-0

49. Suto RK, Clarkson MJ, Tremethick DJ, Luger K. Crystal structure of a nucleosome core particle containing the variant histone H2A.Z. Nat Struct Biol. 2000;7: 1121–1124.

50. Andrews AJ, Luger K. Nucleosome structure(s) and stability: variations on a theme. Annu Rev Biophys. 2011;40: 99–117.

51. Zhou B-R, Feng H, Kato H, Dai L, Yang Y, Zhou Y, et al. Structural insights into the histone H1-nucleosome complex. Proc Natl Acad Sci U S A. 2013;110: 19390–19395.

52. Dryhurst D, Ishibashi T, Rose KL, Eirín-López JM, McDonald D, Silva-Moreno B, et al. Characterization of the histone H2A. Z-1 and H2A. Z-2 isoforms in vertebrates. BMC Biol. 2009;7: 1–16.

53. Kawashima T, Lorković ZJ, Nishihama R, Ishizaki K, Axelsson E, Yelagandula R, et al. Diversification of histone H2A variants during plant evolution. Trends Plant Sci. 2015;20: 419–425.

54. Sijacic P, Holder DH, Bajic M, Deal RB. Methyl-CpG-binding domain 9 (MBD9) is required for H2A.Z incorporation into chromatin at a subset of H2A.Z-enriched regions in the Arabidopsis genome. PLoS Genet. 2019;15: e1008326.

55. Nishibuchi I, Suzuki H, Kinomura A, Sun J, Liu N-A, Horikoshi Y, et al. Reorganization of damaged chromatin by the exchange of histone variant H2A.Z-2. Int J Radiat Oncol Biol Phys. 2014;89: 736–744.

56. Dunn CJ, Sarkar P, Bailey ER, Farris S, Zhao M, Ward JM, et al. Histone hypervariants H2A. Z. 1 and H2A. Z. 2 play independent and context-specific roles in neuronal activity-induced transcription of Arc/Arg3. 1 and other immediate early genes. Eneuro. 2017;4. Available: https://www.ncbi.nlm.nih.gov/pmc/articles/pmc5569379/

57. Noh Y-S, Amasino RM. PIE1, an ISWI family gene, is required for FLC activation and floral repression in Arabidopsis. Plant Cell. 2003;15: 1671–1682.

58. Choi K, Kim S, Kim SY, Kim M, Hyun Y, Lee H, et al. SUPPRESSOR OF FRIGIDA3 encodes a nuclear ACTIN-RELATED PROTEIN6 required for floral repression in Arabidopsis. Plant Cell. 2005;17: 2647–2660.

59. Deal RB, Topp CN, McKinney EC, Meagher RB. Repression of flowering in Arabidopsis requires activation of FLOWERING LOCUS C expression by the histone variant H2A.Z. Plant Cell. 2007;19: 74–83.

60. Deal RB, Kandasamy MK, McKinney EC, Meagher RB. The nuclear actin-related protein ARP6 is a pleiotropic developmental regulator required for the maintenance

of FLOWERING LOCUS C expression and repression of flowering in Arabidopsis. Plant Cell. 2005;17: 2633–2646.

61. Martin-Trillo M, Lázaro A, Poethig RS, Gómez-Mena C, Piñeiro MA, Martinez-Zapater JM, et al. EARLY IN SHORT DAYS 1 (ESD1) encodes ACTIN-RELATED PROTEIN 6 (AtARP6), a putative component of chromatin remodelling complexes that positively regulates FLC accumulation in Arabidopsis. Development. 2006;133: 1241–1252.

62. Lázaro A, Gómez-Zambrano A, López-González L, Piñeiro M, Jarillo JA. Mutations in the Arabidopsis SWC6 gene, encoding a component of the SWR1 chromatin remodelling complex, accelerate flowering time and alter leaf and flower development. J Exp Bot. 2008;59: 653–666.

63. Potok ME, Wang Y, Xu L, Zhong Z, Liu W, Feng S, et al. Arabidopsis SWR1-associated protein methyl-CpG-binding domain 9 is required for histone H2A.Z deposition. Nat Commun. 2019;10: 3352.

64. Luo Y-X, Hou X-M, Zhang C-J, Tan L-M, Shao C-R, Lin R-N, et al. A plant-specific SWR1 chromatin-remodeling complex couples histone H2A. Z deposition with nucleosome sliding. EMBO J. 2020;39: e102008.

65. Bagchi DN, Battenhouse AM, Park D, Iyer VR. The histone variant H2A. Z in yeast is almost exclusively incorporated into the+ 1 nucleosome in the direction of transcription. Nucleic Acids Res. 2020;48: 157–170.

66. Trinklein ND, Aldred SF, Hartman SJ, Schroeder DI, Otillar RP, Myers RM. An

abundance of bidirectional promoters in the human genome. Genome Res. 2004;14: 62–66.

67. Core LJ, Waterfall JJ, Gilchrist DA, Fargo DC, Kwak H, Adelman K, et al. Defining the status of RNA polymerase at promoters. Cell Rep. 2012;2: 1025–1035.

68. Colino-Sanguino Y, Clark SJ, Valdes-Mora F. The H2A.Z-nuclesome code in mammals: emerging functions. Trends Genet. 2021. doi:10.1016/j.tig.2021.10.003

69. Hetzel J, Duttke SH, Benner C, Chory J. Nascent RNA sequencing reveals distinct features in plant transcription. Proc Natl Acad Sci U S A. 2016;113: 12316–12321.

70. Crevillén P, Gómez‐Zambrano Á, López JA, Vázquez J, Piñeiro M, Jarillo JA. Arabidopsis YAF9 histone readers modulate flowering time through NuA4‐complex‐dependent H4 and H2A.Z histone acetylation at FLC chromatin. New Phytol. 2019;222: 1893–1908.

71. Wang Y, Zhong Z, Zhang Y, Xu L, Feng S, Rayatpisheh S, et al. NAP1-RELATED PROTEIN1 and 2 negatively regulate H2A.Z abundance in chromatin in Arabidopsis. Nat Commun. 2020;11: 2887.

72. Weber CM, Ramachandran S, Henikoff S. Nucleosomes Are Context-Specific, H2A.Z-Modulated Barriers to RNA Polymerase. Mol Cell. 2014;53: 819–830.

73. Mylonas C, Lee C, Auld AL, Cisse II, Boyer LA. A dual role for H2A.Z.1 in modulating the dynamics of RNA polymerase II initiation and elongation. Nat Struct Mol Biol. 2021;28: 435–442.

74. Murphy KE, Meng FW, Makowski CE, Murphy PJ. Genome-wide chromatin accessibility is restricted by ANP32E. Nat Commun. 2020;11: 5063.

75. Cole L, Kurscheid S, Nekrasov M, Domaschenz R, Vera DL, Dennis JH, et al. Multiple roles of H2A.Z in regulating promoter chromatin architecture in human cells. Nat Commun. 2021;12: 1–15.

76. Talbert PB, Henikoff S. Histone variants—ancient wrap artists of the epigenome. Nat Rev Mol Cell Biol. 2010;11: 264–275.

77. Lang J, Smetana O, Sanchez‐Calderon L, Lincker F, Genestier J, Schmit A, et al. Plant γH2AX foci are required for proper DNA DSB repair responses and colocalize with E2F factors. New Phytol. 2012;194: 353–363.

78. Redon CE, Nakamura AJ, Martin OA, Parekh PR, Weyemi US, Bonner WM. Recent developments in the use of γ-H2AX as a quantitative DNA double-strand break biomarker. Aging . 2011;3: 168–174.

79. Singh I, Ozturk N, Cordero J, Mehta A, Hasan D, Cosentino C, et al. High mobility group protein-mediated transcription requires DNA damage marker γ-H2AX. Cell Res. 2015;25: 837–850.

80. Dobersch S, Rubio K, Singh I, Günther S, Graumann J, Cordero J, et al. Positioning of nucleosomes containing γ-H2AX precedes active DNA demethylation and transcription initiation. Nat Commun. 2021;12: 1–20.

81. Xiao S, Jiang L, Wang C, Ow DW. Arabidopsis OXS3 family proteins repress ABA signaling through interactions with AFP1 in the regulation of ABI4 expression. J

Exp Bot. 2021 [cited 10 Jun 2021]. doi:10.1093/jxb/erab237

82. Piquet S, Le Parc F, Bai S-K, Chevallier O, Adam S, Polo SE. The Histone Chaperone FACT Coordinates H2A.X-Dependent Signaling and Repair of DNA Damage. Mol Cell. 2018;72: 888–901.e7.

83. Heo K, Kim H, Choi SH, Choi J, Kim K, Gu J, et al. FACT-mediated exchange of histone variant H2AX regulated by phosphorylation of H2AX and ADP-ribosylation of Spt16. Mol Cell. 2008;30: 86–97.

84. Du Y-C, Gu S, Zhou J, Wang T, Cai H, MacInnes MA, et al. The dynamic alterations of H2AX complex during DNA repair detected by a proteomic approach reveal the critical roles of Ca2+/calmodulin in the ionizing radiation-induced cell cycle arrest. Mol Cell Proteomics. 2006;5: 1033–1044.

85. Grasser KD. The FACT Histone Chaperone: Tuning Gene Transcription in the Chromatin Context to Modulate Plant Growth and Development. Front Plant Sci. 2020;11: 85.

86. Lorković ZJ, Park C, Goiser M, Jiang D, Kurzbauer M-T, Schlögelhofer P, et al. Compartmentalization of DNA damage response between heterochromatin and euchromatin is mediated by distinct H2A histone variants. Curr Biol. 2017;27: 1192–1199.

87. Yelagandula R, Stroud H, Holec S, Zhou K, Feng S, Zhong X, et al. The histone variant H2A. W defines heterochromatin and promotes chromatin condensation in Arabidopsis. Cell. 2014;158: 98–109.

88. Eleuteri B, Aranda S, Ernfors P. NoRC Recruitment by H2A.X Deposition at rRNA Gene Promoter Limits Embryonic Stem Cell Proliferation. Cell Rep. 2018;23: 1853–1866.

89. Shechter D, Chitta RK, Xiao A, Shabanowitz J, Hunt DF, David Allis C. A distinct H2A.X isoform is enriched in Xenopus laevis eggs and early embryos and is phosphorylated in the absence of a checkpoint. Proc Natl Acad Sci U S A. 2009;106: 749–754.

90. Seo J, Kim SC, Lee H-S, Kim JK, Shon HJ, Salleh NLM, et al. Genome-wide profiles of H2AX and γ-H2AX differentiate endogenous and exogenous DNA damage hotspots in human cells. Nucleic Acids Res. 2012;40: 5965–5974.

91. Iacovoni JS, Caron P, Lassadi I, Nicolas E, Massip L, Trouche D, et al. High-resolution profiling of gammaH2AX around DNA double strand breaks in the mammalian genome. EMBO J. 2010;29: 1446–1457.

92. Collins PL, Purman C, Porter SI, Nganga V, Saini A, Hayer KE, et al. DNA double-strand breaks induce H2Ax phosphorylation domains in a contact-dependent manner. Nat Commun. 2020;11: 3158.

93. Liu C, Cheng Y-J, Wang J-W, Weigel D. Prominent topologically associated domains differentiate global chromatin packing in rice from Arabidopsis. Nature Plants. 2017;3: 742–748.

94. Zilberman D, Coleman-Derr D, Ballinger T, Henikoff S. Histone H2A.Z and DNA methylation are mutually antagonistic chromatin marks. Nature. 2008;456:

125–129.

95. Zahraeifard S, Foroozani M, Sepehri A, Oh D-H, Wang G, Mangu V, et al. Rice H2A.Z negatively regulates genes responsive to nutrient starvation but promotes expression of key housekeeping genes. J Exp Bot. 2018;69: 4907–4919.

96. Smith AP, Jain A, Deal RB, Nagarajan VK, Poling MD, Raghothama KG, et al. Histone H2A.Z Regulates the Expression of Several Classes of Phosphate Starvation Response Genes But Not as a Transcriptional Activator. Plant Physiol. 2010;152: 217–225.

97. Kumar SV, Wigge PA, Centre JI, Lane C, Nr N. H2A.Z-Containing Nucleosomes Mediate the Thermosensory Response in Arabidopsis. Cell. 2010;140: 136–147.

98. Cortijo S, Charoensawan V, Brestovitsky A, Buning R, Ravarani C, Rhodes D, et al. Transcriptional Regulation of the Ambient Temperature Response by H2A.Z Nucleosomes and HSF1 Transcription Factors in Arabidopsis. Mol Plant. 2017;10: 1258–1273.

99. Sura W, Kabza M, Karlowski WM, Bieluszewski T, Kus-Slowinska M, Pawełoszek Ł, et al. Dual Role of the Histone Variant H2A.Z in Transcriptional Regulation of Stress-Response Genes. Plant Cell. 2017;29. doi:10.1105/tpc.16.00573

100. Nguyen NH, Cheong J-J. H2A.Z-containing nucleosomes are evicted to activate AtMYB44 transcription in response to salt stress. Biochem Biophys Res Commun. 2018;499: 1039–1043.

101. Boden SA, Kavanová M, Finnegan EJ, Wigge PA. Thermal stress effects on grain

yield in Brachypodium distachyon occur via H2A.Z-nucleosomes. Genome Biol. 2013;14: R65.

102. Mao Z, Wei X, Li L, Xu P, Zhang J, Wang W, et al. Arabidopsis cryptochrome 1 controls photomorphogenesis through regulation of H2A.Z deposition. Plant Cell. 2021;33: 1961–1979.

103. Foroozani M, Zahraeifard S, Oh D-H, Wang G, Dassanayake M, Smith AP. Low-Phosphate Chromatin Dynamics Predict a Cell Wall Remodeling Network in Rice Shoots. Plant Physiol. 2020;182: 1494–1509.

104. Xue M, Zhang H, Zhao F, Zhao T, Li H, Jiang D. The INO80 chromatin remodeling complex promotes thermomorphogenesis by connecting H2A.Z eviction and active transcription in Arabidopsis. Mol Plant. 2021;14: 1799–1813.

105. Carter B, Bishop B, Ho KK, Huang R, Jia W, Zhang H, et al. The Chromatin Remodelers PKL and PIE1 Act in an Epigenetic Pathway that Determines H3K27me3 Homeostasis in Arabidopsis. 2018. doi:10.1105/tpc.17.00867

106. Gómez-Zambrano Á, Merini W, Calonje M. The repressive role of Arabidopsis H2A.Z in transcriptional regulation depends on AtBMI1 activity. Nat Commun. 2019;10: 2828.

107. Kralemann LEM, Liu S, Trejo-Arellano MS, Muñoz-Viana R, Köhler C, Hennig L. Removal of H2Aub1 by ubiquitin-specific proteases 12 and 13 is required for stable Polycomb-mediated gene repression in Arabidopsis. Genome Biol. 2020;21: 144.

108. Cai H, Zhang M, Chai M, He Q, Huang X, Zhao L, et al. Epigenetic regulation of

anthocyanin biosynthesis by an antagonistic interaction between H2A . Z and H3K4me3. 2019;1: 295–308.

109. Molitor AM, Bu Z, Yu Y, Shen WH. Arabidopsis AL PHD-PRC1 Complexes Promote Seed Germination through H3K4me3-to-H3K27me3 Chromatin State Switch in Repression of Seed Developmental Genes. PLoS Genet. 2014. doi:10.1371/journal.pgen.1004091

110. Dai X, Bai Y, Zhao L, Dou X, Liu Y, Wang L, et al. H2A.Z Represses Gene Expression by Modulating Promoter Nucleosome Structure and Enhancer Histone Modifications in Arabidopsis. Mol Plant. 2018;11: 635.

111. Hu G, Cui K, Northrup D, Liu C, Wang C, Tang Q, et al. H2A.Z facilitates access of active and repressive complexes to chromatin in embryonic stem cell self-renewal and differentiation. Cell Stem Cell. 2013;12: 180–192.

112. Benoit M, Simon L, Desset S, Duc C, Cotterell S, Poulet A, et al. Replication-coupled histone H3. 1 deposition determines nucleosome composition and heterochromatin dynamics during Arabidopsis seedling development. New Phytol. 2019;221: 385–398.

113. Bourguet P, Picard CL, Yelagandula R, Pélissier T, Lorković ZJ, Feng S, et al. The histone variant H2A.W and linker histone H1 co-regulate heterochromatin accessibility and DNA methylation. Nat Commun. 2021;12: 1–12.

114. Osakabe A, Jamge B, Axelsson E, Montgomery SA, Akimcheva S, Kuehn AL, et al. The chromatin remodeler DDM1 prevents transposon mobility through deposition

of histone variant H2A.W. Nat Cell Biol. 2021;23: 391–400.

115. Ni K, Ren J, Xu X, He Y, Finney R, Braun SMG, et al. LSH mediates gene repression through macroH2A deposition. Nat Commun. 2020;11: 5647.

116. Kasinsky HE, Lewis JD, Dacks JB, Ausló J. Origin of H1 linker histones. The FASEB journal. 2001;15: 34–42.

117. Shen X, Yu L, Weir JW, Gorovsky MA. Linker histories are not essential and affect chromatin condensation in vivo. Cell. 1995;82: 47–56.

118. Ushinsky SC, Bussey H, Ahmed AA, Wang Y, Friesen J, Williams BA, et al. Histone H1 in Saccharomyces cerevisiae. Yeast. 1997;13: 151–161.

119. Patterton HG, Landel CC, Landsman D, Peterson CL, Simpson RT. The biochemical and phenotypic characterization of Hho1p, the putative linker histone H1 of Saccharomyces cerevisiae. J Biol Chem. 1998;273: 7268–7276.

120. Ausió J. Are linker histones (histone H1) dispensable for survival? Bioessays. 2000;22: 873–877.

121. Jedrusik MA, Schulze E. A single histone H1 isoform (H1. 1) is essential for chromatin silencing and germline development in Caenorhabditis elegans. Development. 2001;128: 1069–1080.

122. Fan Y, Nikitina T, Zhao J, Fleury TJ, Bhattacharyya R, Bouhassira EE, et al. Histone H1 depletion in mammals alters global chromatin structure but causes specific changes in gene regulation. Cell. 2005;123: 1199–1212.

123. Lu X, Wontakal SN, Emelyanov AV, Morcillo P, Konev AY, Fyodorov DV, et al. Linker histone H1 is essential for Drosophila development, the establishment of pericentric heterochromatin, and a normal polytene chromosome structure. Genes Dev. 2009;23: 452–465.

124. She W, Grimanelli D, Rutowicz K, Whitehead MWJ, Puzio M, Kotlinski M, et al. Chromatin reprogramming during the somatic-to-reproductive cell fate transition in plants. Development. 2013;140: 4008–4019.

125. Jerzmanowski A, Przewłoka M, Grasser KD. Linker histones and HMG1 proteins of higher plants. Plant Biol. 2000;2: 586–597.

126. Ascenzi R, Gantt JS. A drought-stress-inducible histone gene in Arabidopsis thaliana is a member of a distinct class of plant linker histone variants. Plant Mol Biol. 1997;34: 629–641.

127. Rutowicz K, Puzio M, Halibart-Puzio J, Lirski M, Kotliński M, Kroteń MA, et al. A specialized histone H1 variant is required for adaptive responses to complex abiotic stress and related DNA methylation in Arabidopsis. Plant Physiol. 2015;169: 2080–2101.

128. Choi J, Lyons DB, Kim MY, Moore JD, Zilberman D. DNA Methylation and Histone H1 Jointly Repress Transposable Elements and Aberrant Intragenic Transcripts. Mol Cell. 2020;77: 310–323. e7.

129. Rutowicz K, Puzio M, Halibart-Puzio J, Lirski M, Kotliński M, Kroteń MA, et al. A Specialized Histone H1 Variant Is Required for Adaptive Responses to Complex

Abiotic Stress and Related DNA Methylation in Arabidopsis. Plant Physiol. 2015;169: 2080–2101.

130. Rutowicz K, Lirski M, Mermaz B, Teano G, Schubert J, Mestiri I, et al. Linker histones are fine-scale chromatin architects modulating developmental decisions in Arabidopsis. Genome Biol. 2019;20: 157.

131. Zemach A, Kim MY, Hsieh P-H, Coleman-Derr D, Eshed-Williams L, Thao K, et al. The Arabidopsis nucleosome remodeler DDM1 allows DNA methyltransferases to access H1-containing heterochromatin. Cell. 2013;153: 193–205.

132. Rea M, Zheng W, Chen M, Braud C, Bhangu D, Rognan TN, et al. Histone H1 affects gene imprinting and DNA methylation in Arabidopsis. Plant J. 2012;71: 776–786.

133. Lu X, Wontakal SN, Kavi H, Kim BJ, Guzzardo PM, Emelyanov AV, et al. Drosophila H1 regulates the genetic activity of heterochromatin by recruitment of Su (var) 3-9. Science. 2013;340: 78–81.

134. Iwasaki YW, Murano K, Ishizu H, Shibuya A, Iyoda Y, Siomi MC, et al. Piwi modulates chromatin accessibility by regulating multiple factors including histone H1 to repress transposons. Mol Cell. 2016;63: 408–419.

135. Liu S, de Jonge J, Trejo-Arellano MS, Santos-González J, Köhler C, Hennig L. Role of H1 and DNA methylation in selective regulation of transposable elements during heat stress. New Phytol. 2021;229: 2238–2250.

136. He S, Vickers M, Zhang J, Feng X. Natural depletion of histone H1 in sex cells

causes DNA demethylation, heterochromatin decondensation and transposon activation. Elife. 2019;8: e42530.

137. Willige BC, Zander M, Yoo CY, Phan A, Garza RM, Trigg SA, et al. PHYTOCHROME-INTERACTING FACTORs trigger environmentally responsive chromatin dynamics in plants. Nat Genet. 2021; 1–7.

138. Gehre M, Bunina D, Sidoli S, Lübke MJ, Diaz N, Trovato M, et al. Lysine 4 of histone H3.3 is required for embryonic stem cell differentiation, histone enrichment at regulatory regions and transcription accuracy. Nat Genet. 2020;52: 273–282.

139. Zhang X, Yazaki J, Sundaresan A, Cokus S, Chan SW-L, Chen H, et al. Genome-wide high-resolution mapping and functional analysis of DNA methylation in Arabidopsis. Cell. 2006;126: 1189–1201.

140. Cokus SJ, Feng S, Zhang X, Chen Z, Merriman B, Haudenschild CD, et al. Shotgun bisulphite sequencing of the Arabidopsis genome reveals DNA methylation patterning. Nature. 2008;452: 215–219.

141. Lister R, O'Malley RC, Tonti-Filippini J, Gregory BD, Berry CC, Millar AH, et al. Highly integrated single-base resolution maps of the epigenome in Arabidopsis. Cell. 2008;133: 523–536.

Chapter 2:

Temporal profiling of the phosphate starvation response in Arabidopsis root hair cells reveals that induction of polycomb target genes does not depend on removal of H3K27me3 or H2A.Z

Available on *Biorxiv*: https://doi.org/10.1101/2024.07.14.603443

Dylan H. Holder[1,2*], and Roger B. Deal[1]

[1]Department of Biology, Emory University, Atlanta, Georgia, USA

[2]Graduate Program in Genetics and Molecular Biology, Emory University, Atlanta, Georgia, USA

Abstract

Altered nutrient conditions can trigger massive transcriptional reprogramming in plants, leading to the activation and silencing of thousands of genes. To gain a deeper understanding of the phosphate starvation response and the relationships between transcriptional and epigenomic changes that occur during this reprogramming, we conducted a time-resolved analysis of transcriptome and chromatin alterations in root hair cells of Arabidopsis thaliana during phosphate (P) starvation and subsequent resupply. We found that 96 hours of P starvation causes induction or repression of thousands of transcripts, and most of these transcripts recover to pre-starvation levels within four hours of P resupply. Among the phosphate starvation-induced genes are many polycomb targets with high levels of H3K27me3 and histone variant H2A.Z. When induced, these genes often show increased H3K4me3 consistent with active transcription, but surprisingly minimal loss of H3K27me3 or H2A.Z. These results indicate that the removal of silencing marks is not a prerequisite for activation of these genes. Our data provide a cell type- and time-resolved resource for studying the dynamics of a systemic nutrient stress and recovery and suggest that our current understanding of the mechanisms for switching between silent and active transcriptional states is incomplete.

Introduction

The nucleosome is the fundamental unit of chromatin in eukaryotes and is therefore a key substrate for transcriptional regulation. Nucleosomes can be modified via posttranslational modifications such as phosphorylation, ubiquitination, acetylation, methylation, or post-replicative exchange of canonical histone subunits with histone variants [1,2]. This array of modifications gives each nucleosome a unique identity thought to create a chromatin state that alters a given locus's propensity for activation or silencing. It is known that proper organism development depends on the maintenance of these chromatin states across eukaryotes. Mutants deficient in several chromatin modification "writers", "erasers", and chromatin remodelers display pleiotropic developmental phenotypes that threaten the viability of the organism and its ability to properly respond to environmental cues [3,4]. Terminally differentiated cells require dramatic changes in transcription rate at genes in response to intrinsic and extrinsic signals without cell division. Transcription machinery must therefore overcome the established chromatin state and transform the locus to accommodate gene activation or silencing. How the transcription machinery rapidly overcomes the repressive chromatin landscape at quiescent genes in response to activating signals, and then effectively re-silence these genes once those signals are gone, is not well understood.

Deposition of histone variant H2A.Z into postreplicated nucleosomes is required for proper development in eukaryotes. In animals, H2A.Z is required for embryonic viability and cancer cell suppression [5–8]. In plants, H2A.Z deficiency leads to severe post embryonic developmental phenotypes and impaired responses to abiotic stimuli

[9–13]. Unlike H3K27me3 and H3K4me3, whose roles are characterized as repressors and activators, respectively, H2A.Z enrichment at plant genes is found to either promote or repress transcription depending on the context [1,14,15]. As a result, a unifying mechanism for H2A.Z's role in regulating transcription has yet to be identified. H2A.Z is deposited by the SWR1 chromatin remodeling complex primarily into euchromatic genes and regulatory elements [16,17]. Genes occupied by H2A.Z nucleosomes in Arabidopsis are broadly defined by either a prominent enrichment peak near the transcription start site (TSS) or enrichment spanning the entire gene body. While TSS-proximal H2A.Z enrichment has been shown to promote both gene activation or repression depending on the experimental context, gene body enrichment is negatively associated with transcription, especially among genes implicated in environmental responses [18–20].

Since the initial observation that gene body H2A.Z enrichment associates with transcriptionally repressed stress-responsive genes, studies exploring the role of H2A.Z during osmotic, heat, light, phosphate, and hypoxic stress in *Arabidopsis thaliana, Oryza sativa,* and *Brachypodium distachyon* have implicated gene body H2A.Z in functioning as a repressor of environmentally responsive genes [11,21–25]. While these studies were conducted with a variety of techniques, tissues, and exposure lengths, two observations are consistent regardless of the stressor: 1) H2A.Z enrichment at these stress response genes is reduced following induction, and 2) These genes are often ectopically induced in H2A.Z-deficient plants, implying that H2A.Z has a causal role in their repression. Gene body H2A.Z loss during activation, and overexpression in H2A.Z deficient plants, certainly suggests that H2A.Z has a causal role in gene repression.

However, no unifying mechanism has been proposed to explain how H2A.Z mediated repression is achieved across all stress responses or how H2A.Z eviction directly promotes transcription. Notably, the differences in primary structure between H2A.Z and canonical H2A have not been sufficient to explain the variant's complex relationship with gene expression [19].

A complete grasp of H2A.Z's role in gene repression is likely not possible without understanding the surrounding chromatin environment into which H2A.Z is deposited and coupled with analyzing changes during transcriptional activation or repression. One key factor to deciphering H2A.Z's role in silencing is its relationship to the Polycomb Repressive Complex 1 and 2 (PRC1 and 2). The polycomb silencing system promotes gene silencing in both plants and animals and is hallmarked by trimethylation of histone H3 on lysine 27 (H3K27me3) by PRC2 and monoubiquitination of C-terminal lysine on H2A or H2A.Z (H2Aub) by PRC1 [26]. In mammalian stem cells, H2A.Z is associated with H3K27me3 at repressed genes [27,28]. In *Arabidopsis,* H2A.Z and H3K27me3 enrichment are correlated across gene bodies and anticorrelated with transcript abundance. Furthermore, H2A.Z deficient plants have reduced H3K27me3 genome wide and PRC2 mutants have reduced H2A.Z, suggesting a mutual reinforcement of these two factors at target genes [29]. However, recent work has called into question the silencing role of H3K27me3 at these genes and highlighted the requirement for H2A.Z monoubiquitination by PRC1 in plant polycomb gene silencing (Gómez-Zambrano et al. 2019).

During a phosphate starvation response (PSR), plants undergo system-wide transcriptional reprogramming to improve inorganic phosphate uptake efficiency from the soil and internal P utilization [30]. This involves induction and repression of transcripts from a diverse set of biological processes including phosphate transport (intercellular, extracellular, and intracellular), phosphatase secretion in root, supplementing phospholipid loss in the plasma membrane, ATP conservation, and prominent reorganization of root system morphology [30]. The phosphate starvation response has been characterized at the transcriptome level in whole shoot and root [31–33]. However, how a phosphate starvation-induced (PSi) gene's chromatin state changes during this responsive activation and later re-silencing is not understood. Root hair cells are among the first cells to encounter changes in phosphate availability in the soil, as they are located on the root epidermis and project into the substrate in search of nutrients. As a terminally differentiated cell type, root hair cells possess their own unique chromatin landscape that is a history of the cell's journey through differentiation and dictates transcription events to come as the cell encounters exogenous challenges.

Numerous PSi genes are marked with H3K27me3 along with H2A.Z under normal conditions, and H2A.Z deficient plants overexpress several key PSi genes even on P-rich media [12,18,29]. Phosphate (P) is a growth limiting nutrient and plants must rapidly overcome these repressive chromatin marks to activate and then re-silence PSi genes to adapt to changing P availability in the soil. Given H2A.Z's relationship with polycomb mediated silencing and its implication in responsive gene repression, we hypothesized that H2A.Z-containing nucleosomes mediate the endogenous rate of gene activation and aid in rapid re-silencing through cooperation with polycomb, possibly

acting as a preferred substrate for polycomb machinery promoting a more flexible alternative to repression via DNA methylation. To test this hypothesis and explore the dynamics of PSi gene induction and subsequent re-silencing, we performed a cell-type and time resolved multi-omic study of transcript levels, histone modifications, and chromatin accessibility in Arabidopsis. We probed the chromatin and transcriptional landscape over a P starvation and resupply time course experiment to understand how root hairs overcome the repressive effects of H2A.Z and H3K27me3. We took rapid measurements in root hair cells following P resupply to examine the order of events that take place on chromatin to establish an H2A.Z-mediated silent state. To address the confounding factors inherent with traditional whole tissue chromatin profiling techniques, we utilized Isolation of Nuclei TAgged in a specific Cell Types (INTACT) followed by Cleavage Under Targets and Tagmentation (CUT&Tag) to capture the chromatin landscape exclusively in the root epidermal hair cell, where P sensing and uptake first occur [34,35].

To our surprise, despite robust PSi gene induction and re-silencing across the time course, changes in H2A.Z and H3K27me3 levels in PSi genes were modest, with both being maintained at high levels across gene bodies after gene induction. We went on to find that while H3K27me3 is highly enriched at PSi genes, it does not appear to be required for P-dependent gene activation or re-silencing. The data presented here provide a resource for studying *in-vivo* cell type-specific transcriptome and chromatin dynamics during a systemic transcriptional activation and re-silencing event. The results not only provide a resource for more deeply understanding the PSR, but also

indicate that transcription can occur even in the continued presence of H3K27me3 and H2A.Z across gene bodies.

Results

Transcript profiling during phosphate starvation and resupply reveals major starvation-induced changes that generally recover rapidly upon resupply

To examine transcriptional changes associated with P starvation and resupply, we utilized an Arabidopsis INTACT transgenic line in which nuclei of the root hair cell type are labeled [35]. We chose the root hair cell type due to the physical interaction of this cell type with the phosphate-containing soil environment and the pronounced morphological changes in response to P starvation. Measuring this response in a single cell type also eliminates the confounding factors inherent to probing the transcriptional landscape across the diverse population of cell types that compose the root. Seedlings were grown vertically on ½ MS plates for 10 days (0h+P), transferred to phosphate depleted media for 96 hours (96h-P), and finally moved back to P rich media and sampled at four time points following P resupply (30m, 1h, 4h+P) (**Figure 1a**). We settled on this sampling scheme given that initial RT-qPCR experiments on whole roots with higher temporal resolution showed that two hallmark PSR genes, *PHOSPHATE TRANSPORTER 1;2* and *1;9*, are induced after 96h -P and reach near-complete repression within 4 hours of P resupply (**Figure 1b**). At each of the 6 time points sampled, root segments containing fully differentiated root hair cells (~1 cm segment from above the differentiation zone and below the first lateral roots) were harvested for INTACT nuclei purification [36] followed by nuclear RNA-seq and ATAC-seq analyses.

Differentially expressed genes (DEGs) were c-means clustered into 6 groups based on common expression patterns across the time-course via TC-seq (**Fig 1c, Dataset S1**) [37]. This analysis revealed 5,674 genes were differentially expressed between any two measured timepoints, with 2,592 differentially expressed genes after 96h of P starvation (**Dataset S1**). We deemed the 915 genes in time course cluster 3 (TC3) as phosphate starvation-induced (PSi) genes due to increased transcript levels after 96 hr P starvation that fell rapidly after P resupply (TC3, **Figure 1c**). Gene ontology analysis confirmed that known PSi genes occupy this cluster (including *PHT1;2* and *PHT1;9*) with enrichment for protein families like secretory peroxidases and hypoxia response genes which have been identified in other PSR experiments (**Dataset S2**). The P1BS motif, which is known to be bound by the PSR transcription factor (TF) PHR1 and related TFs [38], was enriched in the accessible chromatin (via INTACT-ATAC-seq) overlapping with TC3 promoters when compared to the other TC clusters (**Dataset S3**, p-value = 4.15e-5, enrichment ratio 2.65). Additionally, Simple Enrichment Analysis of ATAC-accessible sites in TC3 promoters for known TF motifs revealed enrichment for several MYB family TF motifs involved in biological processes known to be linked with phosphate sensing including cell polarity, nitrate sensing, circadian clock, and PHR1-like transcription factors (**Dataset S3**).

Interestingly, we also identified several other classes of transcriptional responses during the starvation/resupply event (**Figure 1c, Figure S1**). Of note, TC5 reflects a group of phosphate starvation-repressed (PSr) genes that recover to baseline levels after 4 h of P resupply. These genes are enriched for functions involved in maintaining chromosome integrity and mitochondrial gene expression, possibly reflecting transcriptional reprioritization as ATP production falls during starvation. TC2 genes are

also silenced during P starvation but fail to recover within 4 h of resupply. These genes consist of cell cycle and cell wall organization genes, likely reflecting the cellular expansion root hair cells undergo during P starved conditions. A unique pattern of expression is observed in the TC4 genes, as these are maximally induced within 1 hour of P resupply but then return to baseline by 4 hours. These data are a rich resource to explore the biological processes involved in the PSR that do not follow the canonical path of upregulation during starvation and repression during resupply.

INTACT-CUT&Tag recapitulates ChIP-seq profiles

To examine chromatin dynamics across the time course, we next used INTACT-purified root hair cell nuclei for CUT&Tag targeting H3K4me3, H3K27me3, and H2A.Z. K-means clustering of the root-hair CUT&Tag datasets with corresponding publicly available ChIP-seq from seedling tissue at genes for each mark revealed a strong agreement across the different data types (**Figure 2a**). Peak calling using MACS2 reveals a high degree of overlap between whole seedling and root hair nuclei across H3K27me3, H2A.Z and H3K4me3 (50, 75, and 70% of root hair peaks overlap with seedling peaks respectively) (**Figure 2b**) [39]. However, root hair cells still possess a unique chromatin footprint when compared to seedling tissue with 10945, 3492, and 4807 root hair specific peaks for H3K4me3, H3K27me3, and H2A.Z, respectively (**Figure 2c**). Peaks called exclusively in ChIP samples still have enrichment in the corresponding CUT&Tag sample, likely reflecting limitations of using a peak caller designed for high background ChIP-seq data on low background CUT&Tag data. Stratifying genic chromatin profiles by their transcript levels in the root hair RNA-seq data recapitulates the previously observed relationship between each chromatin mark,

ATAC accessibility, and expression. For example, H3K27me3 is negatively correlated with transcript abundance, H3K4me3 is positively correlated with transcript abundance with enrichment downstream of the TSS, while H2A.Z enrichment shifts from the TSS to the gene body as transcript abundance falls (**Figure 2d**). The observable differences in enrichment across expression quantiles also confirm that this technique has a dynamic range comparable to other chromatin profiling techniques and will reliably measure changes in enrichment at a given site across a P starvation event.

Chromatin dynamics across the time course are mostly limited to H3K4me3 changes

Although each chromatin profile correlated with steady state transcript levels as expected, we found this profile did not hold when comparing the dynamics of these profiles across time. After 96h -P, only 51 genes were differentially enriched for H3K27me3 and only 9 genes were differentially enriched for H2A.Z (padj<.05) (**Figure 3a**). The lack of H2A.Z and H3K27me3 dynamics were also observed across all differentially expressed genes, where log2 fold changes were restricted to between +/- 1 (**Figure 3b**). H3K4me3 changed the most across the P starvation and repletion, with 1,900 genes differentially enriched for the mark after 96h -P. However, only 390 of those genes overlapped with differentially expressed genes across the same time points (**Figure 3a, Figure S2**). While accessibility changes are observed at DEGs across the time course, almost no changes were statistically significant (**Figure 3b, Figure S2**). This lack of significant ATAC changes is true both at DEG promoter regions (-200bp +100bp TSS) and at ATAC hypersensitive sites and is in contrast to a previous study that found thousands of differentially accessible regions after 10 days of phosphate

starvation in whole roots [40]. The discrepancy between this study and our findings could be explained by the experimental conditions. While Barragán-Rosillo et al. collected whole roots from 10 day old seedlings grown from germination on phosphate limited media, we collected root hair cell nuclei grown for only 96h on phosphate depleted media. Our results suggest that significant changes in chromatin accessibility may depend on longer starvation periods or even cell division. We next examined the persistence of each chromatin mark across the time course to determine the stability of the chromatin changes caused by 96h of P starvation (**Figure 3a**). For H3K4me3, 79% of the 1900 genes with differential H3K4me3 enrichment at 96h were still differentially enriched after 4h of P resupply compared to 0h. Likewise for H3K27me3, 63% of the 51 differentially enriched genes after starvation were still differentially enriched after 4h of resupply. While only 9 genes were differentially enriched for H2A.Z, 3 of those were still differentially enriched after 4h. Interestingly, the RNA landscape returns to pre-starvation levels faster than the measured chromatin marks, with 74% of the 2592 differentially expressed transcripts after starvation returning to pre-starvation levels after 4h of resupply.

To better understand how each chromatin profile changes in relation to transcript abundance we performed Spearman correlations between the Log2 fold-change (L2FC) for each mark at each gene (relative to the previous time point) and the corresponding L2FC of RNA at each gene (**Figure 3c**). We found no correlation between RNA changes and chromatin accessibility changes measured by ATAC, and weak negative correlations between changes in RNA and both H2A.Z and H3K27me3. However, changes in H2A.Z at genes were still anticorrelated with RNA dynamics across the time course, perhaps indicating that H2A.Z dynamics reflect general transcription as

opposed to influencing a specific mechanism of transcription at certain genes (**Figure 3c**). Interestingly, H3K4me3 dynamics were positively correlated with RNA level changes after 96h of P starvation, but not between any of the shorter time points after P resupply (**Figure 3c**).

Many phosphate starvation-induced genes are enriched for gene body H2A.Z and H3K27me3 but these marks are not significantly altered after 96h of P starvation

Given the presumed role of H2A.Z in repression of responsive genes, we sought to identify a chromatin signature that might distinguish the responsive gene clusters identified by TCseq (**Figure 1c**). In particular, we expected many PSi genes to be enriched for H3K27me3 and H2A.Z in the gene body (gbH2A.Z) before starvation (0h). Upon visualization using deepTools, we confirmed that the PSi genes in TC3 are in fact enriched for H3K27me3 compared to other clusters and contain gbH2A.Z (**Figure 4a**). Considering the high average of H3K27me3 and H2A.Z gene body enrichment at TC3, it was surprising to discover that genes in TC3 also have the highest average transcript abundance before P starvation, together with TC6 (**Figure 4a**).

Upon closer examination by k-means clustering, TC3 has more transcriptionally quiescent H3K27me3 and gbH2A.Z enriched genes but also has active genes with more RNA abundance than other clusters (**Figure 4b**). This result indicates that while PSi genes have a wide spectrum of steady state transcript levels, many of these genes are indeed silent under normal conditions and are enriched for H3K27me3 and gbH2A.Z. We isolated H3K27me3 enriched genes (C1 and C3) from TC3 via k-means clustering and compared them to the remaining genes in TC3 (C2 and C4). We found that

H3K27me3 enriched genes in TC3 had lower ATAC enrichment, H3K4me3 enrichment, and lower corresponding transcript abundance than genes in TC3 without H3K27me3 enrichment (**Figure 4b**).

We hypothesized that since H2A.Z at these genes is required for their repression under P rich conditions [12], we would observe an eviction of H2A.Z and H3K27me3 after 96 hr P starvation and a re-deposition of H2A.Z and H3K27me3 during their re-silencing, based on their established co-dependence [12,29]. Surprisingly, PSi genes with the highest transcriptional dynamics displayed only minor changes in H3K27me3 and H2A.Z (**Figure 4c**). This increase in PSi transcript and maintenance of the H3K27me3/gbH2A.Z chromatin state during P starvation were confirmed by RT-qPCR and ChIP-qPCR on whole root tissue (**Figure S3**).

Phosphate starvation-induced genes are highly enriched for H3K27me3, but PRC2 activity is not required for their phosphate-dependent activation or silencing

To confirm that the elevated enrichment of H3K27me3 is unique to PSi genes and not just a reflection of the expression levels of the genes at 0h, we generated a control dataset of non-differentially expressed genes with equivalent expression to each gene in TC3 at 0h -P. Comparing H3K27me3 enriched PSi genes to the control set reveals that they have significantly greater enrichment of H3K27me3 (**Figure 5a**). Interestingly, these H3K27me3 enriched PSi genes have more H3K27me3 on average than even the lowest 10% of expressed genes (**Figure 5b**).

Based on our understanding of gbH2A.Z and H3K27me3 as barriers to transcriptional activation, it was surprising to observe both relatively unchanged despite

a vast transcriptional reprogramming during phosphate starvation and resupply. While H3K27me3 does not appear to be dynamic in response to phosphate starvation or repletion, many PSi genes are highly enriched for H3K27me3 (**Figure 4b**). To assess the dependence of the PSi response on H3K27me3, we exposed PRC2 catalytic subunit *CURLY LEAF* mutant plants (*clf-28* homozygotes) to a P starvation and resupply event (**Figure S4**). Using RT-qPCR, we found no significant change in induction or silencing rates of three canonical polycomb-target PSi genes in *clf-28* mutants compared to WT (**Figure S4**). However, it is possible that the loss of CLF is compensated by expression of a paralogous SET domain PRC2 component, SWINGER. To account for this possibility, we developed an estradiol inducible artificial microRNA (amiRNA) knockdown of *FERTILIZATION INDEPENDENT ENDOSPERM* (*FIE*), a nonredundant and essential component of the PRC2 complex [41]. After confirming efficient knockdown of FIE after 10 days of amiRNA induction (**Figure 5c**), we put plants through a phosphate starvation and resupply event and measured expression of the *PHT1;2* and *PHT1;9* PSi genes by RT-qPCR in roots. Surprisingly, we observed that PSi gene induction and repression after resupply are not affected by this loss of PRC2 activity, unlike nitrogen and drought stress response genes (**Figure 5d**) [42,43]. There is a slight decrease in expression of *PHT1;9* and *PHT1;2* when comparing the *FIE* knockdown plants to controls. However, these differences are slight and the rate of induction, absolute expression, and repression are not significantly affected.

Genes induced after 30m of P resupply lose H2A.Z and H3K4me3 while genes induced after 96h of P starvation largely do not

We initially included H3K4me3 to use in combination with RNA-seq to distinguish post-transcriptional changes in RNA abundance from increases in transcription. Interestingly, we found that the relationship between RNA levels and H3K4me3 levels was positively correlated over long time scales but negatively correlated on shorter time scales (**Figure 3c**). After 96h of -P stress, the expression of genes gaining H3K4me3 increased significantly more than those without H3K4me3 changes or those losing H3K4me3 (**Figure 6a**). These results follow the expected trend and suggest that increased H3K4me3 is not absolutely necessary for activation, but may facilitate the degree of gene activation in some cases.

We next extended this analysis to time points after P resupply and noticed that the relationship between H3K4me3 and RNA dynamics is largely reversed in the 30m after P resupply (**Figure 6b**). At 96h of P starvation, only 48% (114) of differentially expressed (DE) genes that lose H3K4me3 are induced while 93% (196) of DE genes that gain H3K4me3 are induced. This is a dramatic difference compared to H3K4me3 dynamics 30m after P resupply, where 91% (181) of DE genes that lose H3K4me3 are induced while only 64% (16) of DE genes that gain H3K4me3 are induced. Interestingly, of the 29 genes that become induced and lose H2A.Z after 30m +P, 23 (79%) also lose H3K4me3 at the same time. This appears to occur without any changes to chromatin accessibility or H3K27me3, with both features barely changing from 96h -P to 30m +P (**Figure S6**).

We finally expanded our analysis to all differentially expressed genes irrespective of their chromatin changes. We compared the L2FC of H2A.Z to the L2FC of H3K4me3 at all differentially expressed genes after 96h of P starvation and again after 30m of P resupply. After 96h of P starvation, gene activation is poorly correlated with H2A.Z

changes and has a weak positive correlation with H3K4me3 changes (**Figure 6c)**. Interestingly, this relationship is flipped after 30m of +P resupply (**Figure 6d**). Here, H3K4me3 and H2A.Z are anticorrelated with increases in transcript, and the correlation is much stronger than after 96h -P, with most induced genes losing H2A.Z and H3K4me3 (R^2 = 1.69E-7 at 96h v 0h, R^2 = 0.277 at 30m v 96h). One possible explanation for these results is that the early stages of transcriptional induction (e.g. 30 min + P) are more disruptive to nucleosomes, causing losses of H2A.Z/H2B and H3/H4 dimers, which may be ameliorated after longer periods of induction (e.g. 96 h - P), allowing stabilization of H2A.Z levels and accumulation of H3K4me3.

We noticed that a small group of genes induced after 96h -P stand out by significantly losing H2A.Z and H3K4me3, similar to the majority of induced genes after 30m P resupply (**Figure 6c**, SPX1, SRG3, G3pP1, and AT5G20790). Intriguingly, these same genes were previously found to be the four highest expressed PSi genes after 30m of P starvation in whole root tissue [44]. Perhaps the mechanism of activation observed after 30m of Pi resupply is sustained in these 4 genes even after 96h of starvation. Interestingly, we found that at steady state, there is significantly less H3K27me3 at genes induced after 30m of P resupply than genes induced after 96h of P starvation, while H2A.Z and H3K4me3 levels were comparable (**Figure 6e**). Additionally, the 4 genes that do lose H2A.Z and H3K4me3 after 96h -P had H3K27me3 enrichment levels similar to the genes induced after 30m (**Figure 6e**). This raises the notion that H3K27me3 may aid in retention of nucleosomal components during transcription.

Discussion

In this study, we used INTACT cell type-specific nuclei purification followed by RNA-seq, ATAC-seq, and CUT&Tag to profile the transcriptomic and epigenomic responses of the Arabidopsis root hair cell type to a time course of phosphate starvation and subsequent resupply (**Figure 1a**). Analysis of our nuclear RNA-seq data across the time course identified 6 major patterns of transcript level changes. Time course cluster 3 (TC3) contained transcripts increased by P starvation that returned to baseline levels after four hours of P resupply (**Figure 1c**). The TC3 class represents classical phosphate starvation-induced (PSi) transcripts, whose regulatory regions were found to be enriched for binding sites of TFs known to drive the PSR (**Dataset S3**). We also identified two classes of phosphate starvation-repressed (PSr) transcripts in the TC5 and TC2 groups. The behavior of these classes of PSr transcripts differ in that TC5 transcripts return to pre-starvation levels after 4 hours of phosphate repletion, while those in the TC2 class do not. Interestingly, there are 3 classes of transcripts that respond distinctly to resupply of P after starvation. TC1 class transcripts reach a maximum level after 30 minutes of resupply and return to baseline within 4 hours. The TC4 genes show a very similar profile but are only induced after 30 minutes of resupply and reach a maximum level at 1 hour before returning to baseline at 4 hours. Finally, the TC6 class transcripts do not show significant alterations during P starvation and generally decrease progressively in the 4 hours after resupply. In total, we identified 5,674 differentially expressed genes between any two time points across the time course, indicating major reprogramming in the root hair cell transcriptome. While some of the transcript level changes are likely due to post-transcriptional control mechanisms, others are driven by changes in transcription. These data offer an opportunity to explore

a variety of questions and could be used in conjunction with other datasets, for example a previous root hair nuclear RNA secondary structure and RNA-binding profile analysis [45].

To address the relationships between transcript levels and chromatin features, we employed ATAC-seq as well as CUT&Tag to monitor histone variant H2A.Z, the transcription-associated mark H3K4me3, and polycomb silencing-associated mark H3K27me3. Comparison of our root hair CUT&Tag datasets for each mark with those generated using ChIP-seq on seedling tissue showed a strong concordance in locations and profiles of each signal (**Figure 2a-c**), giving confidence that our data are accurate. Major advantages of the CUT&Tag approach compared to ChIP-seq are the low nuclei input requirement and higher-signal to noise ratio, which allowed us to manageably generate triplicate datasets for each mark across 6 time points. Combining root hair RNA-seq data with chromatin profiles under phosphate-replete conditions, we found that transcript levels correlate well with each chromatin profile at steady state (**Figure 2d**). To our surprise, however, the chromatin changes associated with differential transcript levels during phosphate starvation and recovery were relatively minimal across the time course and were seen most prominently for H3K4me3 (**Figure 3b**). Of the chromatin changes that were significant after 96 h -P, many were retained after 4 hours of phosphate resupply, when the corresponding transcripts had returned to baseline levels (**Figure 3a**). For example, 80% of the genes significantly altered in H3K4me3 levels after 96 h -P were still differentially enriched at 4 hours after resupply. The relatively limited chromatin changes observed relative to transcript level changes is likely due in part to post-transcriptional regulation.

A major motivation for this study was to understand how polycomb-target genes marked with both H3K27me3 and gene body H2A.Z are activated and re-silenced. We thus focused on genes induced by 96 h -P (the TC3 class), as many of these PSi genes were already known targets of PRC2 and H2A.Z. Examination of the starting chromatin state of these and each of the other 5 DEG clusters confirmed that the TC3 genes were highly enriched for H3K27me3 and gbH2A.Z, although not exclusively. Roughly 30% of these TC3 genes showed very low or no expression, low chromatin accessibility, gbH2A.Z and high H3K27me3 levels (**Figure 4a and b, Figure 5a and b**). While these genes showed large gains in transcript levels during P starvation, they surprisingly showed minimal changes to H3K27me3 and H2A.Z (**Figure 4c**). This result is counter to findings in similar experiments exploring H2A.Z dynamics which showed pronounced H2A.Z loss at genes induced during drought, heat, osmotic, hypoxic, light stress, and ethylene responses [11,21–25,46].

The lack of a requirement for H2A.Z eviction during transcriptional induction was also recently observed in our lab when profiling the dynamics of H2A.Z and the SWR1 complex at gbH2A.Z/H3K27me3-enriched ABA responsive genes [47]. While many of these genes were induced following 4h of ABA treatment, H2A.Z levels and distribution across most were unperturbed or only slightly diminished. Interestingly, induction of these previously silent genes by ABA was accompanied by proportional increases in recruitment of SWR1 complex components, suggesting that SWR1 is recruited to replace H2A.Z lost during transcription. Thus, it seems likely that a similar mechanism is operating at PSi genes to maintain gbH2A.Z during transcription. The question remains open as to how these genes become permissive for transcription while retaining gbH2A.Z and H3K27me3.

Some H3K27me3/gbH2A.Z genes, such as those responsive to temperature, far-red light, and ethylene appear to depend upon H2A.Z removal by the INO80 complex for induction [46,48–50], and this may be coupled with active H3K27me3 removal by REF6 (Zander et al 2019) or perhaps passive loss due to H2A.Z eviction. In contrast, the PSi genes described here lose neither mark yet are able to support transcriptional induction. How this happens is not yet clear but could involve simple loss of ubiquitinated H2A.Z [51] from chromatin in early rounds of transcription and replacement with unmodified H2A.Z by SWR1, and/or active deubiquitination by enzymes such as UBP5 [52]. The emerging picture is one of multiple mechanisms for activation of polycomb/gbH2A.Z target genes, where in some cases H2A.Z is evicted, and others where it is actively replaced.

Given the unusually high levels of H3K27me3 at polycomb/H2A.Z target genes in TC3 (**Figure 5a and b**), we speculated that while H3K27me3 may not be dynamic across the activation/repression of these genes in response to phosphate, H3K27me3 could affect the kinetics of induction or repression, or the absolute levels of transcript produced upon induction. *CURLY LEAF* deficient plants were previously shown to have an aberrant increase in expression of *NRT1.2* during nitrogen starvation [42]. A similar phenomenon was observed in drought stress response genes, where H3K27me3 remained unchanged during drought stress at induced genes but *clf* mutants displayed higher induction of drought responsive genes under stress [43]. Counter to these findings, we saw no such ablation of the rate of induction, absolute expression, or repression of H3K27me3 enriched PSi genes *PHT1;2*, *PHT1;9,* or *ASK11* after P stress and resupply in *clf* or an estradiol inducible knockdown of the PRC2 core subunit *FIE* (**Figure 5c and d, Figure S4**). Interestingly, a recent study of cold stress in

Arabidopsis also observed limited H3K27me3 changes upon gene induction, and a lack of requirement for CLF in maintaining gene repression [53]. Taken together, the differences observed in gene regulation between environmental responses argue against a single model of H2A.Z and H3K27me3 action and invite further investigation through direct comparisons of different responses.

Another interesting and unexpected finding in this study was the shift in correlations between transcript levels and those of H2A.Z and H3K4me3 across different time points. Considering all differentially expressed genes after 96h of -P, H3K4me3 changes show a positive correlation with transcript level changes, but this relationship is reversed when comparing the 96h -P time point to the 30 min resupply time point (**Figure 3c**). This trend becomes clearer upon examination specifically of genes with differential H3K4me3 enrichment across these two different time windows (**Figure 6a and b**). Interestingly, we observed that DEGs after 96h -P tend to show an increase in enrichment of H3K4me3 when induced and a reduction of H3K4me3 when repressed, with very little change in H2A.Z regardless of the direction of change (**Figure 6c**). In contrast, genes induced in expression after 30 minutes of P resupply show a loss of both H3K4me3 and H2A.Z (**Figure 6d**). Both changes after 30 m proved to be transient, as of the 22 genes that significantly lost H2A.Z and 2764 genes that significantly lost H3K4me3 after 30m of P resupply, only 1 and 313 were still differentially enriched by 4h after P resupply, respectively. A distinguishing feature of the genes induced after 96 h -P is a higher level of H3K27me3 compared to those induced after 30 min of P resupply. The differences in chromatin dynamics observed between the gene sets could thus reflect a role for H3K27me3 in promoting the retention of nucleosome components during transcription. Given the transient loss of H2A.Z at

induced genes after 30m of resupply, and the new finding that SWR1 enrichment increases at induced genes [47], we propose that loss of H2A.Z at 30m +P induced genes is quickly replenished by SWR1. Therefore, a sample of the transcriptome at a later time (4h+P) would only capture increased transcript levels but a chromatin sample taken at the same time would not capture the corresponding H2A.Z loss. This phenomenon could explain the 4 outlier PSi genes that lose H2A.Z after 96h (**Figure 6C**). In this scenario, H2A.Z incorporation by SWR1 would not occur fast enough to account for H2A.Z lost via transcription, thus a loss of H2A.Z is observed. These results indicate that distinct relationships between transcription and chromatin dynamics can exist, and these may be time-dependent with respect to the onset and level of transcription at a given gene.

Recently, live cell imaging revealed that induction of PSi gene SPX1 occurs in bursts of transcription heterogeneously across root cells [44]. Chromatin changes at PSi genes responding in this way would be limited only to the cells in the population undergoing a burst of induction and detection of those changes would be dampened by the population of nuclei not induced at the time of sample collection. Furthermore, mature root tissues including root hair cells are often polypoid meaning chromatin levels measured at a given gene in an induced cell may represent an average of silent and active alleles. However, we do see several significant changes to H3K4me3 indicating that not all starvation induced genes obey this mechanism of activation or that changes to H3K4me3 are maintained longer than H2A.Z after a transcription burst occurs (**Figure 3b**). Hani et al. also reported that active *SPX1* alleles in polyploid root cells tend to co-localize in the nucleus. It will be interesting to investigate whether the

H3K4me3/H2A.Z loss we observed at *SPX1* depends on the spatial arrangement of active genes within the nucleus.

In conclusion, here we report several surprising findings with respect to the relationships between transcription and chromatin changes on short time scales and in the absence of cell division, which we hope will spur further work. In addition, the data generated here will serve as a useful resource for the field to explore how P starvation response and recovery are orchestrated in the root hair cell type, as well as to probe additional questions about the complex relationships between transcriptional activity and the epigenome.

Methods

Growth conditions and transformation

Seeds of Arabidopsis thaliana (Col-0 strain) were grown on half-strength Murashige and Skoog (½ MS) media agar plates supplemented with 1% sucrose. Plates were stratified in dark conditions for 3 days at 4°C followed by 10 days of vertical growth at 20°C under a 16 hour light/8 hour dark cycle. Plasmids used for plant transformation were introduced into *Agrobacterium tumefaciens* GV3101 strain by electroporation and transformed into plants using the floral dip method [54]. Transgenic plants were selected on ½ MS containing 50 mg/L Kanamycin and 100 mg/L timentin.

For phosphate starvation conditions, seedlings were transferred to ½ MS media without potassium phosphate and supplemented with 1% sucrose and potassium sulfate to balance the ionic composition with phosphate rich plates. After 96 hours of starvation, seedlings were transferred back to ½ MS containing phosphate.

Plasmid DNA constructs

To produce an INTACT construct driven by the root hair-specific *ADF8* promoter (AT4g00680) we first cloned the *AtADF8* regulatory region from - 750 bp to +427 bp relative to the TSS into the gateway-compatible pENTR-D/TOPO plasmid (Invitrogen). This fragment consisted of the promoter, first exon (one codon), first intron of ADF8, which contains a root hair-specific enhancer, as well as the first two codons of exon 2. We then subcloned this fragment into pK7WG-INTACT-At gateway destination plasmid [55] using the LR clonase II enzyme in an LR recombination reaction (Invitrogen) so that the NTF component of INTACT was driven by the *ADF8* regulatory sequences. The amiRNA construct targeting the first exon of *FIE* (GTCTTCGTTACCGCTGGTGGA) was generated with zero mismatches using the "Design" feature of the Web MicroRNA Designer (WMD3; [56] and synthesized into a Gateway entry vector by TWIST Bioscience . The construct was then recombined by Gateway cloning into pMDC7 for estradiol inducible expression and pEG100 for constitutive expression via a 35S promoter [57,58].

Real-time RT-PCR (qRT-PCR) for testing PSi genes in *clf-28* and FIE knockdowns

Total RNA was isolated from root tissue 1 cm above the root tip using the RNeasy plant mini kit (Qiagen). Extracted RNA was DNase treated and converted into cDNA with LunaScript RT SuperMix kit (New England Biolabs). cDNA was used as templates for real-time PCR on StepOnePlus real-time PCR system (Applied Biosystems) using SYBR

Green as a detection reagent. *PP2A* mRNA (AT1G13320) primers were used as the endogenous control [59]. The primer sets used can be found in **Supplemental Table 1**.

RNA-seq library preparation and analysis

Biotin tagged nuclei from ADF8 INTACT root tissue (~100 mg) were isolated from a 1 cm section of the fully differentiated root hair zone (above the differentiation zone and below the first lateral root) and captured on 25 uL of Streptavidin M280 Dynabeads according to the Isolation of Nuclei TAgged in specific Cell Types (INTACT) protocol [60]. Bead bound nuclei from each timepoint in the starvation assay were counted and nuclei were split three ways to ~100,000 nuclei per sample in NPBt for three replicates. RNA was isolated from bead bound nuclei using the RNeasy plant micro kit (Qiagen) with on column DNase treatment and quantified via Quant-it™ RiboGreen RNA Assay Kit (Thermo-Fisher). Libraries for RNA-seq were generated according to the QuantSeq 3' mRNA-Seq Library Prep Kit FWD V1 (Lexogen, cat.no. 015.24) following the manufacturer's protocol with modified steps for low input samples.

All amplified libraries were pooled and sequenced using single-end 50 nt reads on an Illumina NextSeq 2000 instrument. Reads were mapped to the *Arabidopsis thaliana* TAIR10 genome assembly, converted to the BAM file format, and sorted by coordinate using the STAR aligner with the default parameters [61]. Duplicate reads were removed using Picard markDuplicates [62]. Strand specific fragment counting on genes was performed with a TAIR10 specific GTF file using featureCounts with the following parameters: -s 1 -t exon -g gene_id [63]**.** Differentially expressed genes were clustered based on direction of response to phosphate starvation using TCseq [37].

Briefly, pairwise differential analysis was performed across all time point combinations using DBanalysis. Then results were filtered for genes with an adjusted p value >0.05 and absolute fold change > 2 using timecourseTable. Finally, the remaining differentially expressed genes were grouped into 6 c-means clusters using timeclust. Gene ontology was performed via WEBGestalt using default parameters [64]. Simple Enrichment Analysis was performed on all TC3 gene promoters overlapping with ATAC hypersensitive sites using the SEA tool in the MEME Suite with default parameters and all other accessible TC gene promoters as a control [65]. To find a control set of equally expressing genes, average RNA counts at 0h for each TC3 gene were matched to a gene with equivalent average RNA counts at 0h that was not differentially expressed.

INTACT-CUT&Tag and ATAC-seq on root hair nuclei

Biotin tagged nuclei from ~100 mg from ADF8 INTACT root tissue (same 1 cm segment as for RNA-seq) were captured on 25 uL of Streptavidin M280 Dynabeads according to the Isolation of Nuclei TAgged in specific Cell Types (INTACT) protocol [60]. Bead bound nuclei for each timepoint in the starvation assay were counted and nuclei were split three ways to ~100,000 nuclei per sample in NPBt for three replicates.

CUT&Tag was performed on these bead bound nuclei (100,000 per reaction) according to the Epicypher CUT&Tag Protocol v1.7 [66] with the following changes. All buffers were prepared without Digitonin and streptavidin bead bound nuclei were resuspended directly from NPBt into 50 uL of Antibody150 Buffer containing 0.5 ug of anti-H3K27me3 (Millipore 07-449), anti-H2A.Z [10], anti-H3K4me3 (Milipore 07-473) or anti-IgG (sigma I-5006) and incubated at 4°C overnight. Guinea pig anti-rabbit secondary (0.5 ug, Sigma SAB3700889) was incubated for 1 hr at room temperature in

50 uL Wash150 Buffer. Tagmented libraries were amplified using 17 PCR cycles. ATAC was performed in duplicate (~20k nuclei each) on the same pools of bead bound nuclei, as previously described [60].

INTACT-CUT&Tag sequencing and data analysis

All amplified libraries were pooled and sequenced using paired-end 150 nt reads on an Illumina NovaSeq 6000 instrument. Data processing was performed with guidance from Zheng et al. 2020 [67]. Reads were trimmed of adapter content using Trimgalore and mapped to the *Arabidopsis thaliana* Col-PEK genome assembly [68] using Bowtie2 with the following parameters: --local --very-sensitive --no-mixed --no-discordant --phred33 -I 10 -X 700 [68,69]. Aligned reads were converted to the BAM file format using Samtools [70]. Duplicate reads were removed using Picard markDuplicates [62]. For CUT&Tag samples, reads from fragments less than 150bp were discarded to eliminate sub-nucleosome sized fragments. Peaks were called on deduplicated BAM files using MACS2 with IgG as a control where applicable [39]. For visualization, deduplicated BAM files of each sample were RPKM normalized and subtracted from their corresponding normalized IgG BAM file using bamCompare from deepTools [71]. RNA, ATAC, and CUT&Tag average plots stratified by expression quantile were generated using SeqPlots [72]. Quantile normalized counts for each CUT&Tag result were generated using multibigwigsummary with --binSize 100 to generate a matrix of counts across samples [71]**.** The resulting matrix was quantile normalized using the R package preprocessCore. Quantile normalized scores per 100 bp bins were then averaged across single genes and again across biological replicates. Mapped fragments overlapping with the TSS (-200bp +100bp from TSS) were counted

using featureCounts for ATAC samples [63]. Mapped fragments overlapping with genes were counted using featureCounts for CUT&Tag samples. Gene counts were then analyzed for differential enrichment using DESeq2 [73]. DESeq2 results were visualized in R using ggplot2 and pheatmap packages [74].

RT-PCR and ChIP-qPCR to confirm RNA-seq and Cut&Tag results at *PHT1;2* and *PHT1;9*

Wild type seeds were germinated on ½ MS media and grown vertically for 5 days before seedlings were transferred to ½ MS without Pi. Whole root samples were taken just before transfer to -P media and 48 hours after transfer to -P media. RNA was isolated using the Qiagen RNeasy Plant Mini Kit and first strand cDNA was produced using the SuperScript III first-strand cDNA kit (Thermo). cDNAs from the +P and -P samples were used as templates for real-time PCR on the StepOnePlus real-time PCR system (Applied Biosystems) using SYBR Green as a detection reagent and the ACTIN2 transcript as an endogenous control.

Samples for ChIP-qPCR were crosslinked with formaldehyde before processing using the enhanced ChIP protocol reported previously [75], with the following modifications: per replicate, 200 mg of 7-day old root tissue was harvested, crosslinked in 1% formaldehyde, and flash frozen in liquid nitrogen. Tissue was ground in a mortar and pestle, homogenized into a slurry in 250 µl of Buffer S and moved directly to sonication. Post sonication, lysate was diluted 10x with Buffer F for use in pulldowns. 50 µl of diluted lysate was saved as input. Antibodies against H2A.Z (2 µg/mL) (described above for CUT&Tag) or αH3K27me3 (0.5 µg/mL) (Millipore 07-449) antibody was added to diluted lysates and incubated overnight at 4°C on a nutator. 20 µl of washed

Protein G Dynabeads (Invitrogen) was added to each pulldown. Antibodies against H2A.Z and H3K27me3 were the same as used for CUT&Tag. Two biological replicates were performed using the 3' UTR of the ACT2 gene as the endogenous control for both RT-qPCR and ChIP-qPCR. The primer sets used can be found in **Supplemental Table 1**.

Publically available data

Seedling ChIP-seq data for H3K27me3, H2A.Z, and H3K4me3 (Figure 2a) were obtained from the NIH Sequencing Read Archive database under the following accessions, respectively; SRR5278091, SRR5364421 and SRR5364426 [76,77]. Data was processed as above.

Data Availability

All sequencing data generated in this study have been deposited in the NCBI GEO database under accession number GSE271993.

Acknowledgements

We thank members of the Deal lab for critical comments and suggestions on the manuscript.

Funding

This work was supported by an NIH grant to RBD (R01GM134245) and DHH was also supported by an NIH training grant (T32GM008490).

Figures

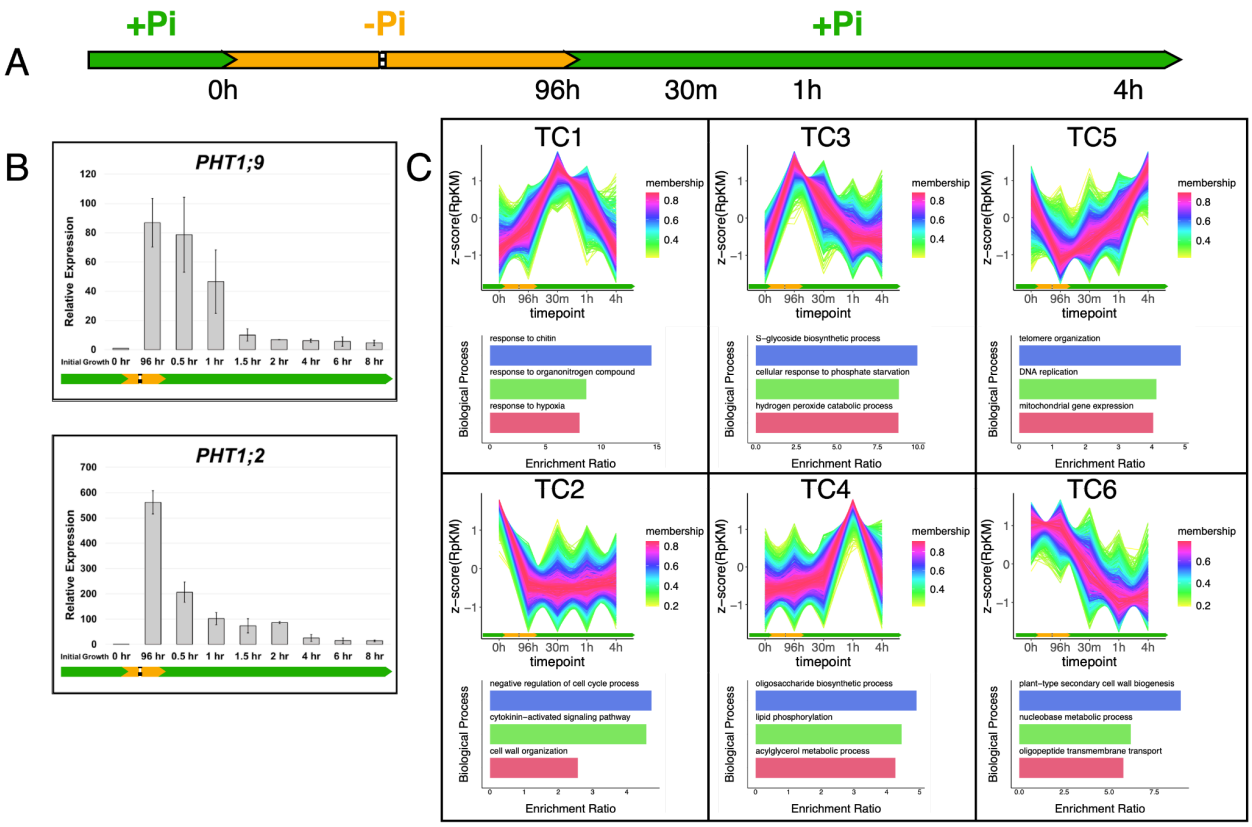

Figure 1. ***Root-hair RNA-seq during a phosphate starvation reveals several classes of phosphate starvation responses.***

(A) Schematic of the phosphate (P) starvation and resupply treatment. Each time point represents a sample taken for INTACT-RNA-seq. (B) Quantitative RT-PCR analysis of RNA from whole roots exposed to P starvation and resupply. Error bars represent standard deviation from the mean for 3 replicates. Expression is represented as amounts relative to the pre- starvation time point (0h). (C) C-means clustering analysis of INTACT-RNA-seq results via TC-seq. Each line represents a single differentially expressed gene. Line color corresponds to the degree of membership to

each c-means cluster. Below each cluster are enrichment ratios for three biological processes enriched in each cluster as identified by GO analysis via WebGestalt.

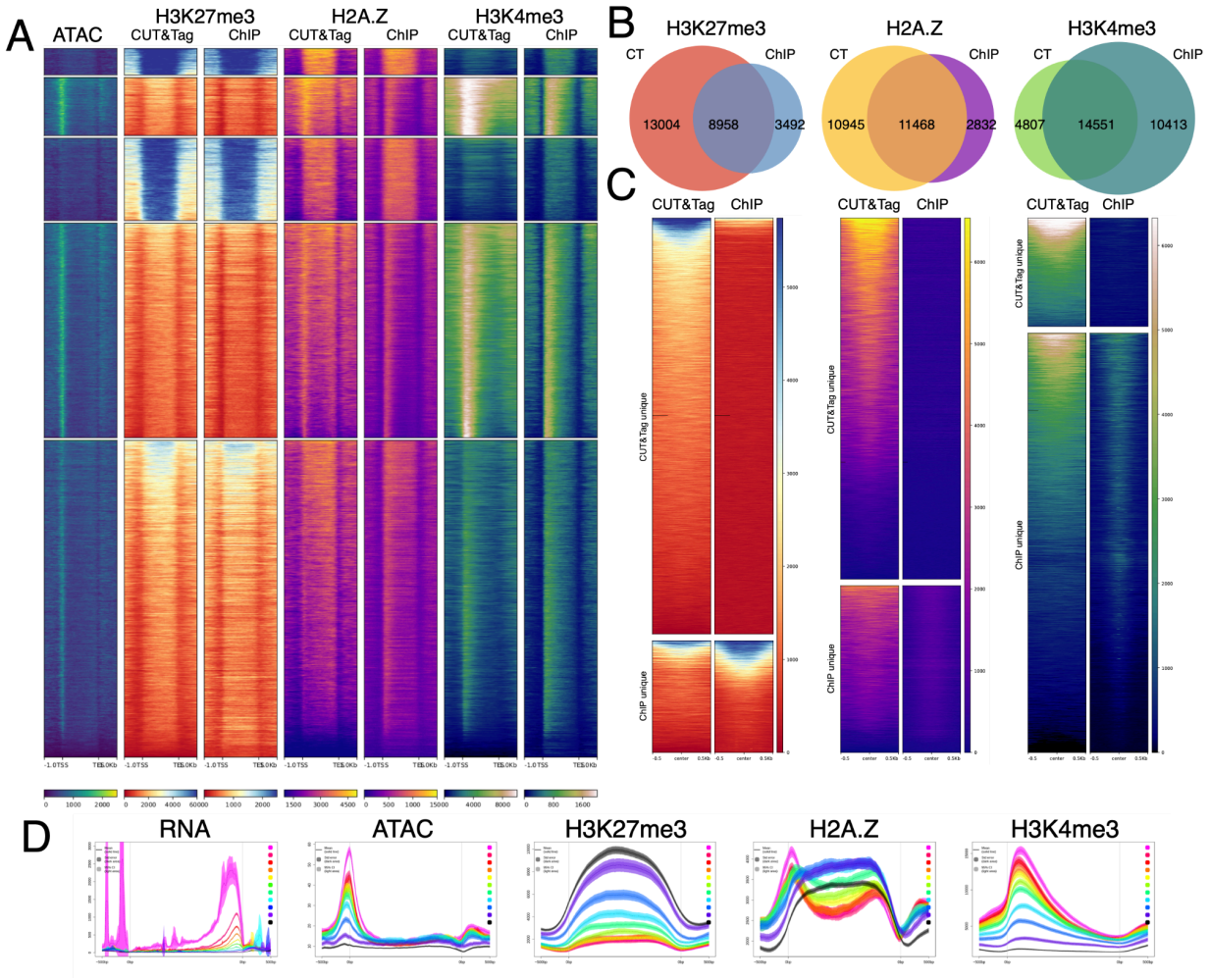

Figure 2. ***Root-hair INTACT-CUT&Tag compared to seedling ChIP-seq.***

(**A**) K-means clustered heatmaps of RPKM normalized signal at all Arabidopsis genes (TSS to TES, +/- 1 kb) comparing the enrichment of H3K27me3, H2A.Z, H3K4me3 between whole seedling ChIP-seq samples and root hair cell CUT&Tag samples. (**B**) Overlapping peaks between whole seedling ChIP-seq samples and root hair CUT&Tag samples for H3K27me3, H2A.Z, and H3K4me3. (**C**) RPKM normalized heatmaps of

seedling ChIP-seq unique peaks or root hair CUT&Tag unique peaks (+/- 0.5 kb from center). **(D)** RPKM normalized average plots for each signal stratified by RNA expression decile in root hair cells showing highest expressed (warm colors) to lowest expressed (cool colors) genes. Black represents non-expressed genes.

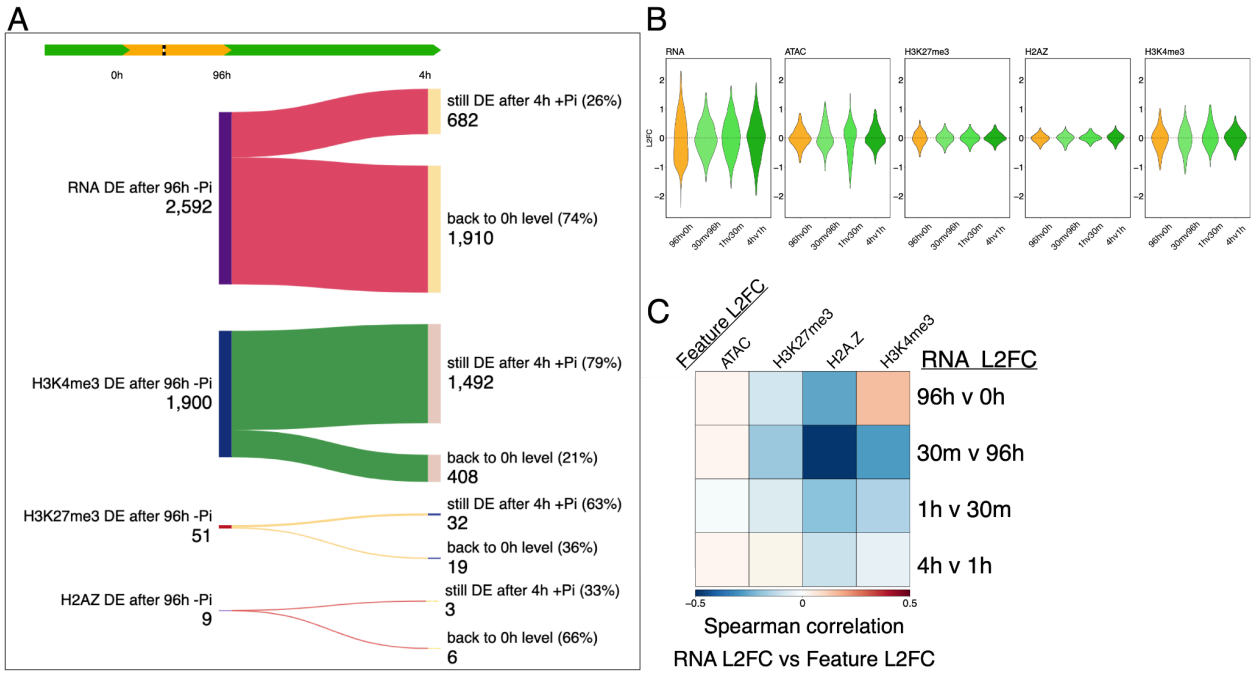

Figure 3. ***Chromatin dynamics during a phosphate starvation and recovery.***

(**A**) Flow chart of each chromatin profile tracking the trajectory of each differentially enriched (DE) gene at 96h -P to 4h of P resupply (padj < 0.05 via DESeq2). Generated using SankeyMATIC. (**B**) Log2 fold change (L2FC) violin plots of each chromatin profile across the time course. Data in the plot are limited to differentially expressed genes identified via TC-seq (n= 5,647) with outliers excluded from each plot. (**C**) L2FC

Spearman correlation between RNA and each chromatin profile across the time course. Each L2FC is measured relative to the previous time-point.

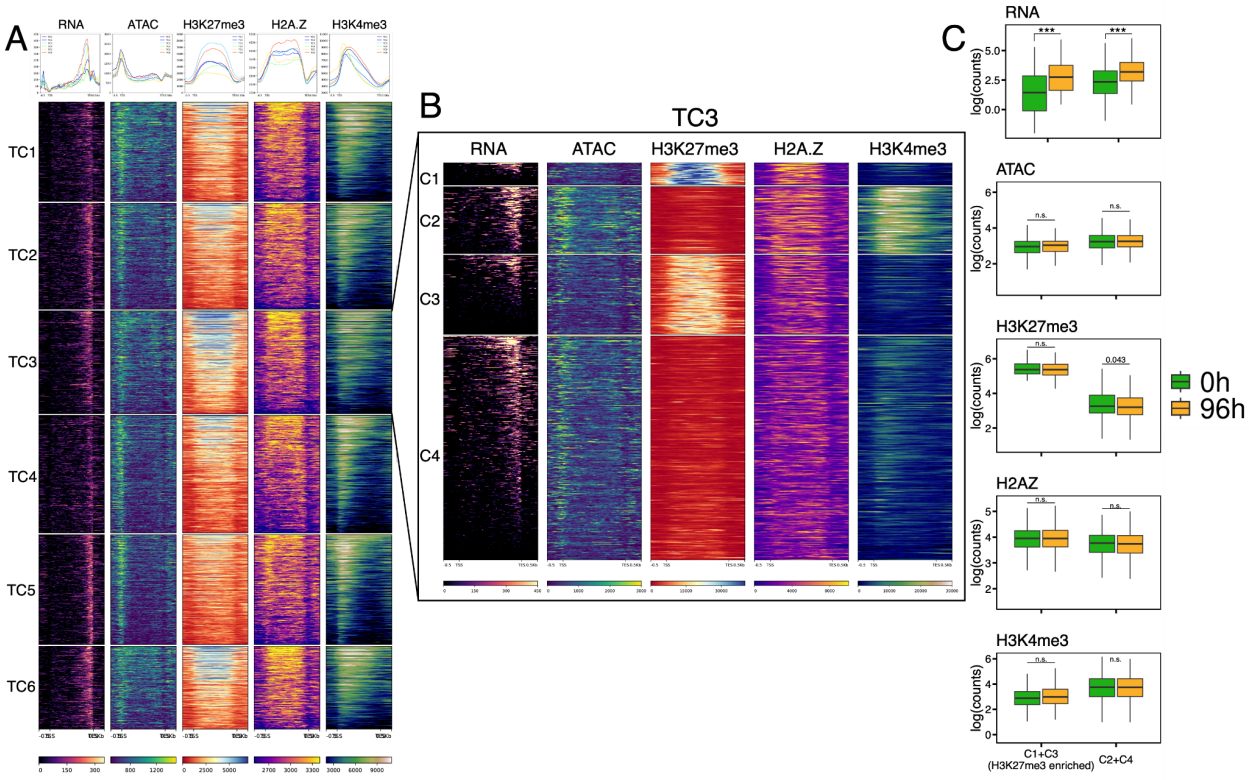

Figure 4. ***Phosphate starvation-induced (PSi) genes are enriched for H3K27me3 and gbH2A.Z but do not show significant changes in chromatin profile enrichment after P starvation.***

(**A**) RPKM normalized heatmaps of each RNA-seq TC cluster before starvation (0h), ranked by average signal across all profiles within each cluster. (**B**) K-means clustered heatmaps of chromatin profiles at all TC3 PSi genes (+/- 0.5 kb) before P starvation (0h) in root hair cells, RPKM normalized. Ranked by RNA signal. (**C**) Boxplot of log(quantile normalized counts) for each profile at H3K27me3 enriched TC3 genes (C1 and C3) and

non-H3K27me3 enriched TC3 genes (C2 and C4) at 0h and 96h. ***p<0.001 (unpaired Student's t-test).

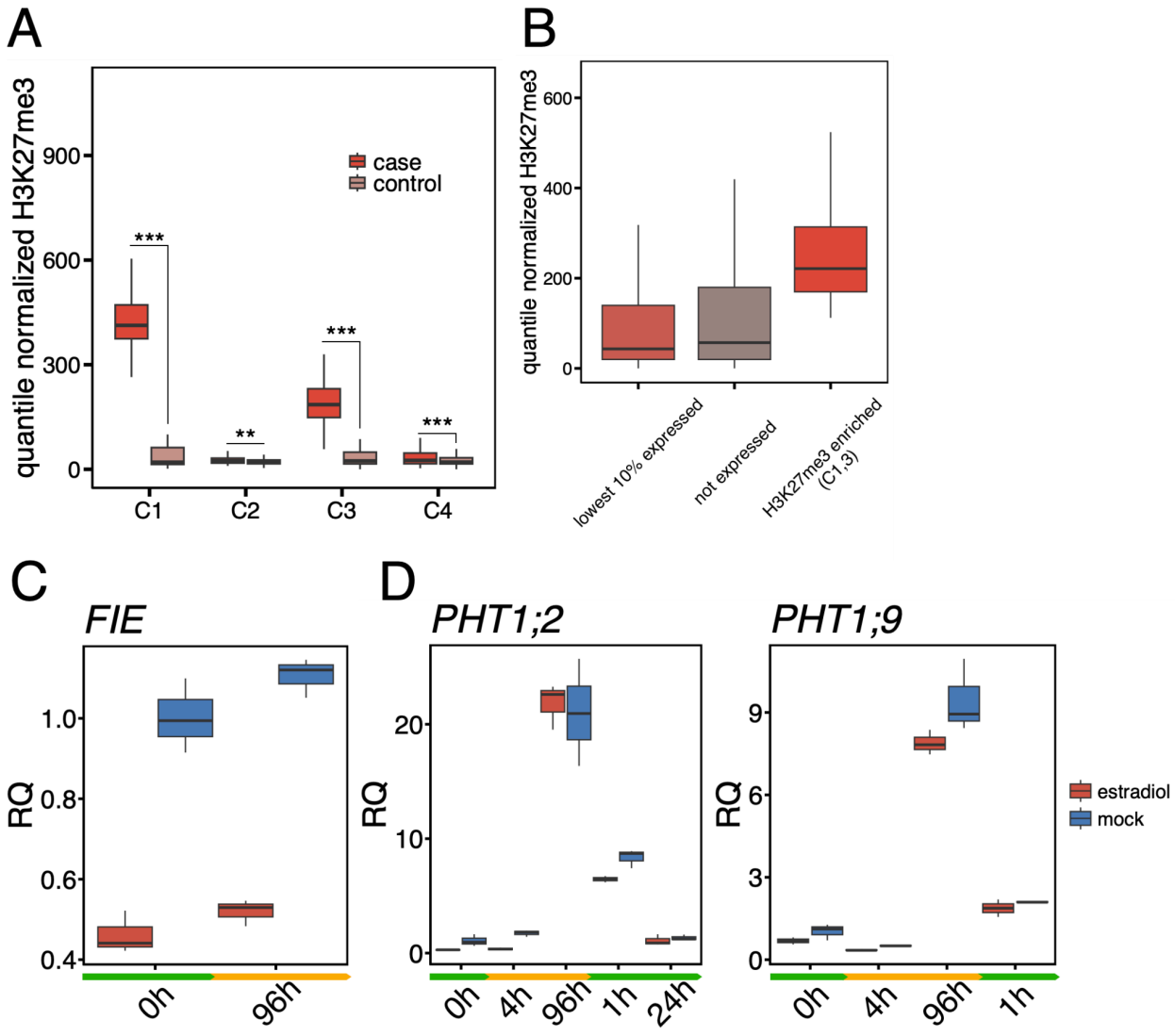

Figure 5. ***H3K27me3 enriched PSi genes do not rely on PRC2 for proper regulation***

(**A**) Boxplot of quantile normalized H3K27me3 enrichment at each k-means cluster from A compared to a set of control genes with equivalent expression at 0h. ***p<0.001 (Wilcoxon two-sided test). (**B**) Boxplot of quantile normalized H3K27me3 enrichment at the lowest 10% of expressed genes, not expressed genes and H3K27me3 enriched genes from TC3 (C1 and C3 from Figure 4b). (**C**) Relative quantity of FIE mRNA after 96h of 10 uM estradiol treatment vs mock (DMSO), normalized to 0h mock treated samples, 3 biological replicates. (**D**) Relative quantity of PHT1:2 and PHT1:9 mRNA before (0h) during (4h and 96h) and after (1h and 24h) of -P starvation. Plants were germinated and grown for 10 days on ½ MS media with 10 uM estradiol or "mock' plates (same media but with DMSO).

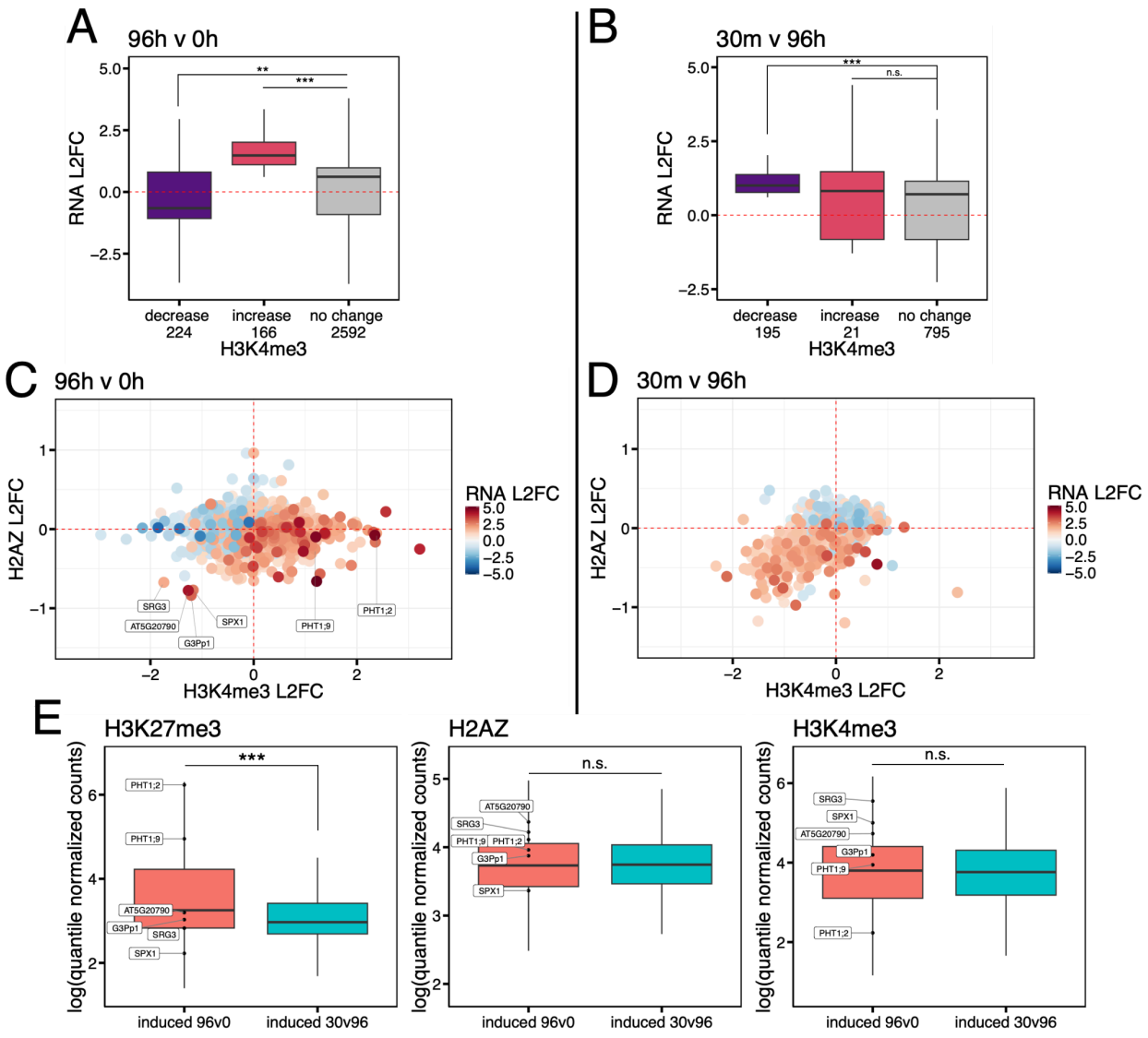

Figure 6. ***Genes induced after 30m of P resupply lose H2A.Z and H3K4me3 while genes induced after 96h of P starvation do not.***

(**A**) Boxplot of RNA L2FC of genes with increased, decreased and unchanged H3K4me3 after 96h of Pi starvation. ***p<0.001 (unpaired Student's t-test) (**B**) Same as (A) for RNA L2FC from 96h Pi starvation to 30m Pi resupply. (**C**) L2FC of H3K4me3 after 96h of P starvation vs L2FC of H2A.Z after 96h of P starvation. Color represents L2FC of RNA after 96h of starvation. Points represent all differentially expressed genes from 0h

to 96h -P (|L2FC| > 1, padj < 0.05). (**D**) Same as C for L2FC from 96h P starvation to 30m Pi resupply. (**E**) Quantile normalized counts at genes induced after 96h -P vs genes induced after 30m +P. ***p<0.001 (Wilcoxon two-sided test).

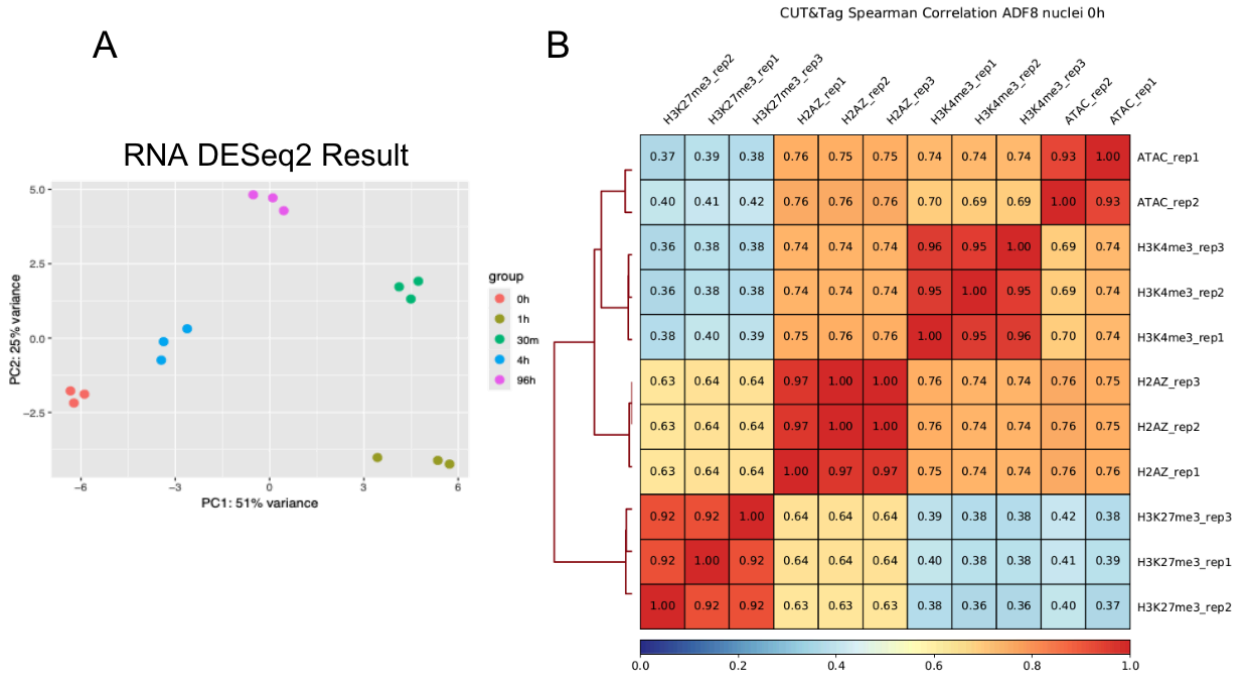

Supplemental Figure 1. Overview of RNA-seq and chromatin profiling data. (A) PCA1 vs PCA2 of RNA DESeq2 results across all timepoints (3 biological replicates per time point). (**B**) 1000 bp bin genome wide hierarchical clustered Spearman correlation across every CUT&Tag and ATAC-seq replicate at 0h.

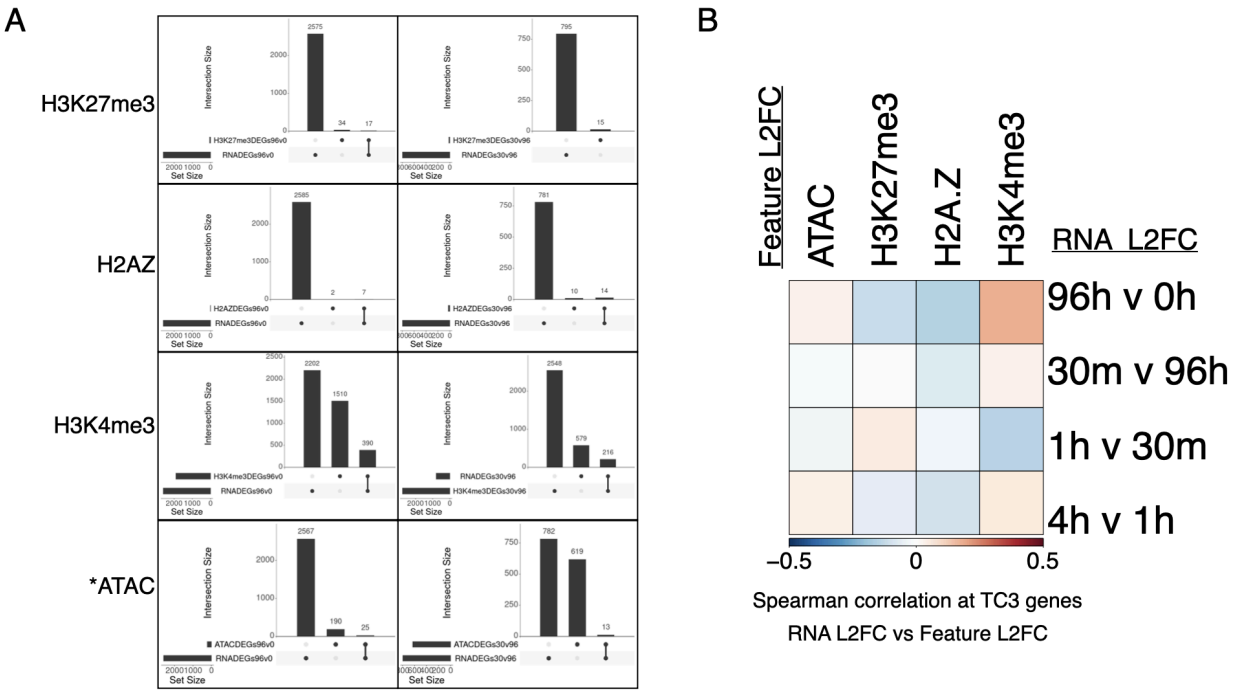

Supplemental Figure 2. Chromatin features across the time course.

(A) Upset plot of overlap between differentially enriched chromatin features (H3K4me3, H3K27me3, H2A.Z) and differentially expressed genes at 96h vs 0h and 30m vs 96h. *Differentially accessible promoters defined by ATAC were determined via p-value < 0.05 due to only one gene being significantly different when determined by the typical adjusted p-value. (**B**) L2FC Spearman correlation between RNA and each chromatin profile across the time course exclusively at TC3 genes. Each L2FC is measured relative to the previous time-point.

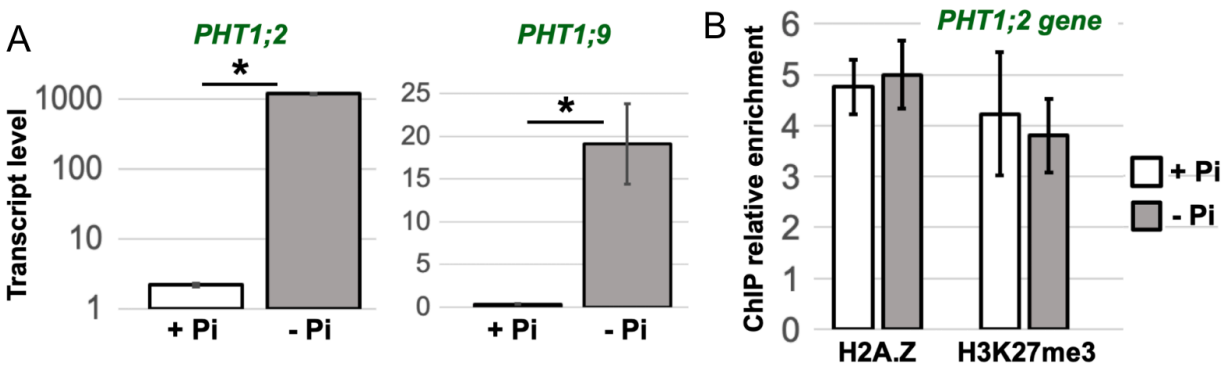

Supplemental Figure 3. Confirmation of transcript, H3K27me3, and H2A.Z levels at PSi genes in whole root.

(**A**) Quantitative RT-PCR analysis of RNA from whole roots grown on +P media and transferred to -P media for 48 hours. Error bars represent standard deviation from the mean for 3 replicates. (**B**) ChIP-qPCR analysis of H2A.Z, H3K27me3, and H2AUb enrichment at *PHT1;2* relative to ACT2 control site under + and -P conditions. Error bars represent standard deviation from the mean for 3 replicates.

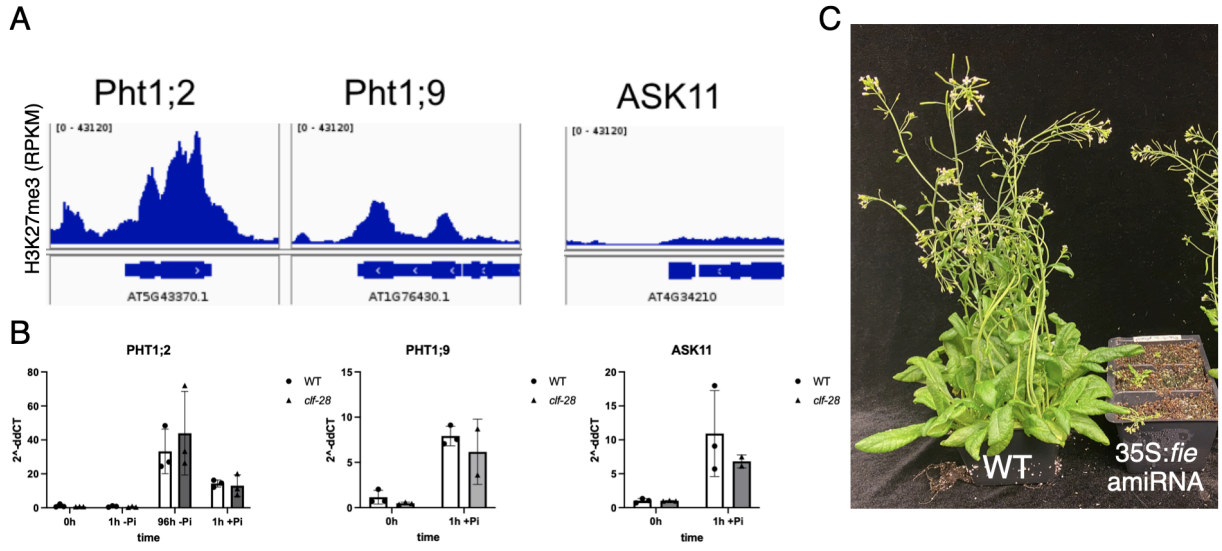

Supplemental Figure 4. Phenotypes of PRC2 knockdown plants.

(**A**) RPKM normalized H3K27me3 enrichment at three PSi genes. (**B**) Quantitative RT-PCR analysis of RNA from whole roots subject to P starvation and repletion gray bars represent clf-28 mutant plants. Error bars represent standard deviation from the mean for 3 replicates. Students t-test found no significant difference between WT and clf-28 at any gene. (**C**) WT vs 35S:fie amiRNA knockdown of PRC2 subunit FIE after 1 month growth on soil.

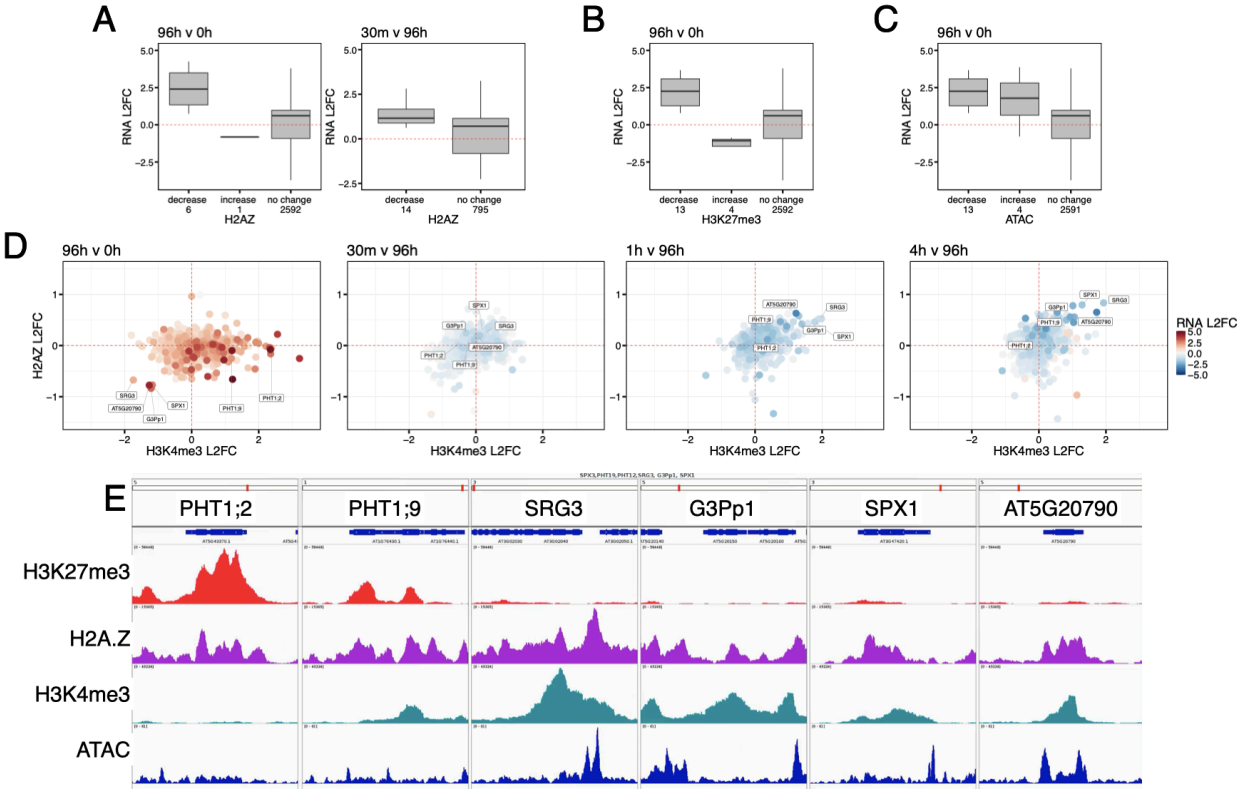

Supplemental Figure 5. Expression changes at genes with differential chromatin enrichment, chromatin dynamics of PSi genes across the starvation time course and 0h chromatin profiles at genes of interest.

(**A,B,C**) Boxplot of RNA L2FC of genes with increased, decreased and unchanged

H2A.Z, H3K27me3, and ATAC after 96h of Pi starvation and after 30m of resupply (no DE genes for H3K27me3 or ATAC after 30m). (**D**) L2FC of H3K4me3 after 96h of P starvation vs L2FC of H2A.Z relative to the most recent P change. Color represents L2FC of RNA. Points represent all TC3 genes. (**E**) RPKM normalized enrichment for PSi genes of interest from TC3.

References

1. Foroozani M, Holder DH, Deal RB. Histone Variants in the Specialization of Plant Chromatin. Annu Rev Plant Biol. 2022;73: 149–172.

2. Li B, Carey M, Workman JL. The Role of Chromatin during Transcription. Cell. 2007;128: 707–719.

3. Talbert PB, Meers MP, Henikoff S. Old cogs, new tricks: the evolution of gene expression in a chromatin context. Nat Rev Genet. 2019;20: 283–297.

4. Isbel L, Grand RS, Schübeler D. Generating specificity in genome regulation through transcription factor sensitivity to chromatin. Nat Rev Genet. 2022;23: 728–740.

5. Monteiro FL, Baptista T, Amado F, Vitorino R, Jerónimo C, Helguero LA. Expression and functionality of histone H2A variants in cancer. Oncotarget. 2014;5: 3428–3443.

6. Ávila-López PA, Guerrero G, Nuñez-Martínez HN, Peralta-Alvarez CA, Hernández-Montes G, Álvarez-Hilario LG, et al. H2A.Z overexpression suppresses senescence and chemosensitivity in pancreatic ductal adenocarcinoma. Oncogene. 2021;40: 2065–2080.

7. Clarkson MJ, Wells JR, Gibson F, Saint R, Tremethick DJ. Regions of variant histone His2AvD required for Drosophila development. Nature. 1999;399: 694–697.

8. Faast R, Thonglairoam V, Schulz TC, Beall J, Wells JR, Taylor H, et al. Histone variant H2A.Z is required for early mammalian development. Curr Biol. 2001;11: 1183–1187.

9. Noh Y-S, Amasino RM. PIE1, an ISWI family gene, is required for FLC activation and floral repression in Arabidopsis. Plant Cell. 2003;15: 1671–1682.

10. Deal RB, Topp CN, McKinney EC, Meagher RB. Repression of Flowering in Arabidopsis Requires Activation of FLOWERING LOCUS C Expression by the Histone Variant H2A.Z. the Plant Cell Online. 2007;19: 74–83.

11. Sura W, Kabza M, Karlowski WM, Bieluszewski T, Kus-Slowinska M, Pawełoszek Ł, et al. Dual Role of the Histone Variant H2A.Z in Transcriptional Regulation of Stress-Response Genes. Plant Cell. 2017;29. doi:10.1105/tpc.16.00573

12. Smith AP, Jain A, Deal RB, Nagarajan VK, Poling MD, Raghothama KG, et al. Histone H2A.Z Regulates the Expression of Several Classes of Phosphate Starvation Response Genes But Not as a Transcriptional Activator. Plant Physiol. 2010;152: 217–225.

13. Kumar SV, Wigge PA, Centre JI, Lane C, Nr N. H2A.Z-Containing Nucleosomes Mediate the Thermosensory Response in Arabidopsis. Cell. 2010;140: 136–147.

14. Cheng K, Xu Y, Yang C, Ouellette L, Niu L, Zhou X, et al. Histone tales: lysine methylation, a protagonist in Arabidopsis development. J Exp Bot. 2019;71: 793–807.

15. Zhang X, Clarenz O, Cokus S, Bernatavichute YV, Pellegrini M, Goodrich J, et al.

Whole-genome analysis of histone H3 lysine 27 trimethylation in Arabidopsis. PLoS Biol. 2007;5: e129.

16. Mizuguchi G, Shen X, Landry J, Wu W-H, Sen S, Wu C. ATP-driven exchange of histone H2AZ variant catalyzed by SWR1 chromatin remodeling complex. Science. 2004;303: 343–348.

17. Kobor MS, Venkatasubrahmanyam S, Meneghini MD, Gin JW, Jennings JL, Link AJ, et al. A protein complex containing the conserved Swi2/Snf2-related ATPase Swr1p deposits histone variant H2A.Z into euchromatin. PLoS Biol. 2004;2: E131.

18. Coleman-Derr D, Zilberman D. Deposition of Histone Variant H2A.Z within Gene Bodies Regulates Responsive Genes. PLoS Genet. 2012;8. doi:10.1371/journal.pgen.1002988

19. Bönisch C, Hake SB. Histone H2A variants in nucleosomes and chromatin: more or less stable? Nucleic Acids Res. 2012;40: 10719–10741.

20. Weber CM, Ramachandran S, Henikoff S. Nucleosomes are context-specific, H2A.Z-modulated barriers to RNA polymerase. Mol Cell. 2014;53: 819–830.

21. Boden SA, Kavanová M, Finnegan EJ, Wigge PA. Thermal stress effects on grain yield in Brachypodium distachyon occur via H2A.Z-nucleosomes. Genome Biol. 2013;14: R65.

22. Mao Z, Wei X, Li L, Xu P, Zhang J, Wang W, et al. Arabidopsis cryptochrome 1 controls photomorphogenesis through regulation of H2A.Z deposition. Plant Cell. 2021;33: 1961–1979.

23. Cortijo S, Charoensawan V, Brestovitsky A, Buning R, Ravarani C, Rhodes D, et al. Transcriptional Regulation of the Ambient Temperature Response by H2A.Z Nucleosomes and HSF1 Transcription Factors in Arabidopsis. Mol Plant. 2017;10: 1258–1273.

24. Nguyen NH, Cheong J-J. H2A.Z-containing nucleosomes are evicted to activate AtMYB44 transcription in response to salt stress. Biochem Biophys Res Commun. 2018;499: 1039–1043.

25. Lee TA, Bailey-Serres J. Integrative Analysis from the Epigenome to Translatome Uncovers Patterns of Dominant Nuclear Regulation during Transient Stress. Plant Cell. 2019;31: 2573–2595.

26. Förderer A, Zhou Y, Turck F. The age of multiplexity: recruitment and interactions of Polycomb complexes in plants. Curr Opin Plant Biol. 2016;29: 169–178.

27. Ku M, Jaffe JD, Koche RP, Rheinbay E, Endoh M, Koseki H, et al. H2A.Z landscapes and dual modifications in pluripotent and multipotent stem cells underlie complex genome regulatory functions. Genome Biol. 2012;13: R85.

28. Wang Q-F, Wang M, Zhuo B, Margueron R, Chang L, Yu J, et al. Histone variants H2A.Z and H3.3 coordinately regulate PRC2-dependent H3K27me3 deposition and gene expression regulation in mES cells. BMC Biol. 2018;16: 1–18.

29. Carter B, Bishop B, Ho KK, Huang R, Jia W, Zhang H, et al. The Chromatin Remodelers PKL and PIE1 Act in an Epigenetic Pathway that Determines H3K27me3 Homeostasis in Arabidopsis. 2018. doi:10.1105/tpc.17.00867

30. Yang S-Y, Lin W-Y, Hsiao Y-M, Chiou T-J. Milestones in understanding transport, sensing, and signaling of the plant nutrient phosphorus. Plant Cell. 2024;36: 1504–1523.

31. Thibaud M-C, Arrighi J-F, Bayle V, Chiarenza S, Creff A, Bustos R, et al. Dissection of local and systemic transcriptional responses to phosphate starvation in Arabidopsis. Plant J. 2010;64: 775–789.

32. Shukla D, Waigel S, Rouchka EC, Sandhu G, Trivedi PK, Sahi SV. Genome-wide expression analysis reveals contrasting regulation of phosphate starvation response (PSR) in root and shoot of Arabidopsis and its association with biotic stress. Environ Exp Bot. 2021;188: 104483.

33. Misson J, Raghothama KG, Jain A, Jouhet J, Block MA, Bligny R, et al. A genome-wide transcriptional analysis using Arabidopsis thaliana Affymetrix gene chips determined plant responses to phosphate deprivation. Proc Natl Acad Sci U S A. 2005;102: 11934–11939.

34. Kaya-Okur HS, Wu SJ, Codomo CA, Pledger ES, Bryson TD, Henikoff JG, et al. CUT&Tag for efficient epigenomic profiling of small samples and single cells. bioRxiv. 2019; 568915.

35. Deal RB, Henikoff S. A simple method for gene expression and chromatin profiling of individual cell types within a tissue. Dev Cell. 2010;18: 1030–1040.

36. Wang D, Deal RB. Epigenome profiling of specific plant cell types using a streamlined INTACT protocol and ChIP-seq. Methods Mol Biol. 2015;1284: 3–25.

37. Mengjun LG. TCseq: time course sequencing data analysis. 2019.

38. Bustos R, Castrillo G, Linhares F, Puga MI, Rubio V, Pérez-Pérez J, et al. A central regulatory system largely controls transcriptional activation and repression responses to phosphate starvation in Arabidopsis. PLoS Genet. 2010;6: e1001102.

39. Feng J, Liu T, Qin B, Zhang Y, Liu XS. Identifying ChIP-seq enrichment using MACS. Nat Protoc. 2012;7: 1728–1740.

40. Barragán-Rosillo AC, Peralta-Alvarez CA, Ojeda-Rivera JO, Arzate-Mejía RG, Recillas-Targa F, Herrera-Estrella L. Genome accessibility dynamics in response to phosphate limitation is controlled by the PHR1 family of transcription factors in *Arabidopsis*. Proceedings of the National Academy of Sciences. 2021;118: e2107558118.

41. Chanvivattana Y, Bishopp A, Schubert D, Stock C, Moon Y-H, Sung ZR, et al. Interaction of Polycomb-group proteins controlling flowering in Arabidopsis. Development. 2004;131: 5263–5276.

42. Bellegarde F, Herbert L, Séré D, Caillieux E, Boucherez J, Fizames C, et al. Polycomb Repressive Complex 2 attenuates the very high expression of the Arabidopsis gene NRT2.1. Sci Rep. 2018;8: 1–9.

43. Liu N, Ding Y, Fromm M, Avramova Z. Different gene-specific mechanisms determine the “revised-response” memory transcription patterns of a subset of A. thaliana dehydration stress responding genes. Nucleic Acids Res. 2014;42: 5556–5566.

44. Hani S, Cuyas L, David P, Secco D, Whelan J, Thibaud M-C, et al. Live single-cell transcriptional dynamics via RNA labelling during the phosphate response in plants. Nat Plants. 2021;7: 1050–1064.

45. Foley SW, Gosai SJ, Wang D, Selamoglu N, Sollitti AC, Köster T, et al. A Global View of RNA-Protein Interactions Identifies Post-transcriptional Regulators of Root Hair Cell Fate. Dev Cell. 2017;41: 204–220.e5.

46. Zander M, Willige BC, He Y, Nguyen TA, Langford AE, Nehring R, et al. Epigenetic silencing of a multifunctional plant stress regulator. Elife. 2019;8. doi:10.7554/eLife.47835

47. Krall EG, Deal RB. SWR1 is recruited to activated ABA response genes to maintain gene body H2A.Z in Arabidopsis thaliana. bioRxiv. 2024. p. 2024.07.14.603444. doi:10.1101/2024.07.14.603444

48. Willige BC, Zander M, Yoo CY, Phan A, Garza RM, Trigg SA, et al. PHYTOCHROME-INTERACTING FACTORs trigger environmentally responsive chromatin dynamics in plants. Nat Genet. 2021; 1–7.

49. Zhao F, Xue M, Zhang H, Li H, Zhao T, Jiang D. Coordinated histone variant H2A.Z eviction and H3.3 deposition control plant thermomorphogenesis. New Phytol. 2023;238: 750–764.

50. Xue M, Zhang H, Zhao F, Zhao T, Li H, Jiang D. The INO80 chromatin remodeling complex promotes thermomorphogenesis by connecting H2A.Z eviction and active transcription in Arabidopsis. Mol Plant. 2021;14: 1799–1813.

51. Gómez-Zambrano Á, Merini W, Calonje M. The repressive role of Arabidopsis H2A.Z in transcriptional regulation depends on AtBMI1 activity. Nat Commun. 2019;10: 2828.

52. Godwin J, Govindasamy M, Nedounsejian K, March E, Halton R, Bourbousse C, et al. The UBP5 histone H2A deubiquitinase counteracts PRCs-mediated repression to regulate Arabidopsis development. Nat Commun. 2024;15: 667.

53. Faivre L, Kinscher N-F, Kuhlmann AB, Xu X, Kaufmann K, Schubert D. Cold stress induces rapid gene-specific changes in the levels of H3K4me3 and H3K27me3 in Arabidopsis thaliana. Front Plant Sci. 2024;15: 1390144.

54. Clough SJ, Bent AF. Floral dip: a simplified method for Agrobacterium-mediated transformation of Arabidopsis thaliana. Plant J. 1998;16: 735–743.

55. Ron M, Kajala K, Pauluzzi G, Wang D, Reynoso MA, Zumstein K, et al. Hairy Root Transformation Using Agrobacterium rhizogenes as a Tool for Exploring Cell Type-Specific Gene Expression and Function Using Tomato as a Model. Plant Physiol. 2014;166: 455–469.

56. Schwab R, Ossowski S, Riester M, Warthmann N, Weigel D. Highly Specific Gene Silencing by Artificial MicroRNAs in Arabidopsis. Plant Cell. 2006;18: 1121–1133.

57. Earley KW, Haag JR, Pontes O, Opper K, Juehne T, Song K, et al. Gateway-compatible vectors for plant functional genomics and proteomics. Plant J. 2006;45: 616–629.

58. Curtis MD, Grossniklaus U. A gateway cloning vector set for high-throughput

functional analysis of genes in planta. Plant Physiol. 2003;133: 462–469.

59. Czechowski T, Stitt M, Altmann T, Udvardi MK, Scheible W-R. Genome-wide identification and testing of superior reference genes for transcript normalization in Arabidopsis. Plant Physiol. 2005;139: 5–17.

60. Bajic M, Maher KA, Deal RB. Identification of Open Chromatin Regions in Plant Genomes Using ATAC-Seq. Methods Mol Biol. 2018;1675: 183–201.

61. Dobin A, Davis CA, Schlesinger F, Drenkow J, Zaleski C, Jha S, et al. STAR: ultrafast universal RNA-seq aligner. Bioinformatics. 2013;29: 15–21.

62. Broad Institute. Picard Toolkit. Broad Institute, GitHub repository. 2019. Available: https://broadinstitute.github.io/picard/

63. Liao Y, Smyth GK, Shi W. featureCounts: an efficient general purpose program for assigning sequence reads to genomic features. Bioinformatics. 2013;30: 923–930.

64. Elizarraras JM, Liao Y, Shi Z, Zhu Q, Pico AR, Zhang B. WebGestalt 2024: faster gene set analysis and new support for metabolomics and multi-omics. Nucleic Acids Res. 2024; gkae456.

65. Bailey TL, Grant CE. SEA: Simple Enrichment Analysis of motifs. bioRxiv. 2021. p. 2021.08.23.457422. doi:10.1101/2021.08.23.457422

66. EpiCypher. EpiCypher® CUTANA™ Direct-to-PCR CUT&Tag Protocol. www.epicypher.com. 2022. Available: https://www.epicypher.com/resources/blog/epicyphers-optimized-cutana-cutrun-

protocol-for-transcription-factors-histone-ptms-and-more/

67. Zheng Y, Ahmad K, Henikoff S. CUT&Tag data processing and analysis tutorial v1. 2020. doi:10.17504/protocols.io.bjk2kkye

68. Hou X, Wang D, Cheng Z, Wang Y, Jiao Y. A near-complete assembly of an Arabidopsis thaliana genome. Mol Plant. 2022;15: 1247–1250.

69. Krueger F. Trim galore. The Babraham Institute, Github repository. Available: https://github.com/FelixKrueger/TrimGalore

70. Li H, Handsaker B, Wysoker A, Fennell T, Ruan J, Homer N, et al. The Sequence Alignment/Map format and SAMtools. Bioinformatics. 2009;25: 2078–2079.

71. Ramírez F, Dündar F, Diehl S, Grüning BA, Manke T. deepTools: a flexible platform for exploring deep-sequencing data. Nucleic Acids Res. 2014;42: W187–91.

72. Stempor P, Ahringer J. SeqPlots - Interactive software for exploratory data analyses, pattern discovery and visualization in genomics. Wellcome Open Res. 2016;1: 14.

73. Love MI, Huber W, Anders S. Moderated estimation of fold change and dispersion for RNA-seq data with DESeq2. Genome Biol. 2014;15: 550.

74. R Core Team. R: A Language and Environment for Statistical Computing. 2024. Available: https://www.R-project.org/

75. Zhao L, Xie L, Zhang Q, Ouyang W, Deng L, Guan P, et al. Integrative analysis of reference epigenomes in 20 rice varieties. Nat Commun. 2020;11: 1–16.

76. Zhou Y, Romero-Campero FJ, Gómez-Zambrano Á, Turck F, Calonje M. H2A monoubiquitination in Arabidopsis thaliana is generally independent of LHP1 and PRC2 activity. Genome Biol. 2017;18: 69.

77. Wollmann H, Stroud H, Yelagandula R, Tarutani Y, Jiang D, Jing L, et al. The histone H3 variant H3.3 regulates gene body DNA methylation in Arabidopsis thaliana. Genome Biol. 2017;18: 94.

Chapter 3:

Conclusion

H3K27me3 is not required for repression of Phosphate Starvation-induced genes

One of the most unexpected results of Chapter 2 was the lack of H3K27me3 dynamics in the face of extensive transcriptional reprogramming during phosphate starvation and resupply. Only 17 genes were differentially enriched for H3K27me3 after 96h of P starvation. While fewer than expected, these changes did track with changes in RNA, with all genes that lost H3K27me3 (n=13) after 96h of starvation also being induced across the same time. However, the fact remains that we observe an almost wholly unperturbed H3K27me3 environment despite several hundred induced genes being enriched for H3K27me3.

While there has not been a direct investigation into the role of H3K27me3 in the phosphate starvation response (PSR), the mark has been shown to be required for proper activation of select nitrogen response genes, an environmental response linked closely to phosphate starvation response [1]. *CURLY LEAF* (*CLF*) deficient plants had an aberrant increase in expression of *NRT1.2* during nitrogen starvation [2]. A similar phenomenon is observed in drought stress response genes, where H3K27me3 remained unchanged during drought stress at induced genes but *clf* plants displayed higher induction of drought responsive genes under stress [3]. Counter to these findings, we saw no such ablation of the rate of induction, absolute expression, or repression H3K27me3 enriched PSR genes *PHT1;2*, *PHT1;9,* and *ASK11* after Pi stress and resupply in *clf* or an estradiol-inducible knockdown of the PRC2 core subunit *FIE*. These results suggest that PSR genes do not require H3K27me3 despite significant enrichment for the mark in root hair cells at steady state. The question then arises as to why a root hair cell would maintain a supposed repressive chromatin mark at genes where the

mark is not required for repression. Perhaps H3K27me3 at these genes in root hair cells is a vestigial mark left by its progenitor cells where other components of the Polycomb silencing pathway are present to achieve the silencing we have come to expect from H3K27me3 enriched chromatin.

While H3K27me3 enrichment is synonymous with gene repression, there are several reported cases of gene expression and H3K27me3 being in disequilibrium, especially in mature tissue in response to stimulus. Senescence activated genes are enriched for H3K27me3 and hypersensitive to ABA treatment in PRC2-deficient plants [4]. Despite ABA hypersensitivity in PRC2 mutants, ABA induced genes show no change in H3K27me3 enrichment after 5h of ABA treatment and after 4 days only 13 induced genes display minor reductions in H3K27me3. This indicates that functional PRC2 may be required for repression of ABA induced genes, but that H3K27me3 present at these genes is not responsible for ABA mediated repression. This observation is not limited to plant biology, with the fungus *Verticillium dahliae* having no global changes to H3K27me3 despite robust transcriptional reprogramming of H3K27me3 enriched genes in response to different growth media [5].

A similar phenomenon was recently observed in the Arabidopsis cold stress response. H3K27me3 was largely unchanged despite genome-wide H3K4me3 changes and transcriptome changes during cold treatment [6]. Additionally, loss of H3K27me3 in *clf* null plants did not attenuate cold responsive gene induction or silencing, even at 2 of the genes previously shown to lose H3K27me3 after 3 days of cold stress [7]. The one gene that did in fact show aberrant activation in *clf* mutants was the developmental flowering time repressor *FLOWERING LOCUS C*. This highlights a divide between PRC2's role in regulation of developmental and environmentally responsive genes.

An in depth study of key anthocyanin biosynthetic genes found that loss of SWR1 complex subunit *ARP6* results in their overexpression and loss of H2A.Z and H3K27me3 [8]. However, their repression does not depend on H3K27me3. These authors proposed that H2A.Z mediated repression of these genes is achieved via exclusion of H3K4me3. These results likely represent a context specific mechanism because H2A.Z are H3K4me3 are not anticorrelated throughout the genome and H2A.Z has been shown to promote H3K4me3 in other eukaryotic systems such as mouse embryonic stem cells [9]. Based on the evidence above, it appears that H3K27me3 is generally dispensable to responsive gene repression.

H2A.Z eviction is a product of activation

Given our initial hypothesis that PSi genes would lose H2A.Z and H3K27me3 upon induction and re-establish H2A.Z and H3K27me3 to re-silence these genes following P resupply, we were surprised to observe minimal changes to H3K27me3 or H2A.Z after the initial induction period of 96h. While there are cases where induction of H3K27me3 enriched genes does not lead to loss of H3K27me3, as described above, H2A.Z is consistently lost following transcriptional induction across numerous distinct stimuli [10–15]. The two most likely scenarios to explain static H2A.Z in the face of transcriptional reprogramming are that the repression of PSi genes is indirectly controlled by H2A.Z/SWR1 or that the H2A.Z loss at induced genes observed in other experiments is a reflection of general nucleosome loss during the initial phases of gene activation.

In the case of light and heat stress, the INO80 chromatin remodeling complex is implicated in active H2A.Z removal to achieve gene activation during stress [16,17]. In

both cases, *ino80* plants fail to induce several response genes under stress conditions and the H2A.Z normally evicted during induction of WT plants remains on gene bodies. These results indicate a mechanism whereby activation of responsive genes is dependent on active removal of H2A.Z by INO80. However, how H2A.Z at these genes inhibits transcription or why INO80 dependent eviction is required for their activation remains unclear. We also found that two PSi genes did not require INO80 for induction, suggesting that there are likely multiple mechanisms for activating H2A.Z-silenced genes (unpublished results).

In fact, due to the vast distribution of H2A.Z across the genome and its involvement in several nuclear processes outside of transcription, it is difficult to conclude with certainty whether the observed H2A.Z loss at induced genes in H2A.Z deficient plants is directly responsible for their activation or merely a reflection of increased transcription brought about by the indirect effects of systemic INO80 deficiency during development. H2A.Z enrichment at the +1 nucleosome of genes in most organisms leads many to speculate that H2A.Z may help in the targeted recruitment of transcription initiation machinery. However, the presence of a second H2A.Z peak at the −1 nucleosome found in organisms with bidirectional initiation suggests that H2A.Z may serve as a mere mark of transcription as opposed to a targeting factor [18]. The suggestion that H2A.Z reflects transcription is supported by finding in human HCT116 cells, where H2A.Z increased at both the TSS and gene bodies following global inhibition of transcription [19].

We recognize that conclusions about transcribed genes made from total nuclear RNA after 96h can be confounded by post-transcriptional regulation of transcripts. The RNA and chromatin landscape at 96h represents a mix of active transcription and

previously produced transcripts. We initially included H3K4me3 to use in combination with RNA-seq to distinguish post-transcriptional changes in RNA abundance from active transcription. However, this relationship between RNA and H3K4me3 proved inconsistent across time. After 96h -P, genes gaining in H3K4me3 did increase in transcript and those losing H3K4me3 did decrease in transcript, but overall the correlation between RNA and H3K4me3 was weak. However, after 30m of P resupply, almost all induced genes lost H3K4me3 and H2A.Z coordinately, in direct contradiction with our understanding of H3K4me3 and transcription. Considering that transcripts produced after 30m have less time to be modified post-transcriptionally, genes induced after 30m of P resupply are more likely to be induced directly by increased transcription. Initial decreases in H2A.Z and H3K4me3 at 30m may represent nucleosome loss during the early phases of transcriptional induction, which might be compensated for after longer induction periods, such as 96 h.

In Chapter 2, we identified *SPX1*, *SRG3*, *G3pP1*, and *AT5G20790* as four outlier PSi genes due to their loss of H2A.Z and H3K4me3 at 96h. Intriguingly, these same genes were previously found to be the four highest expressed PSi genes after 30m of P starvation in whole root tissue [20]. These genes have the most pronounced loss of H2A.Z after 96h of starvation in our experiment. Given the transient loss of H2A.Z and H3K4me3 observed in induced genes after 30m of P resupply, the question arises; why do the four highest expressed PSi genes after 30m of P starvation stand out as the only four genes significantly depleted of H2AZ and H3K4me3 after 96h? Perhaps the mechanism of activation observed after 30m of Pi resupply is sustained in these four genes even after 96h of starvation. Interestingly, these four genes also stand out as having lower H3K27me3 enrichment, comparable to that of induced genes after 30m

(**Figure 5e**). This raises the notion that H3K27me3 may aid in retention of nucleosomal components during transcription.

The lack of a requirement for H2A.Z eviction during transcriptional induction is supported by recent findings in our lab profiling the dynamics of H2A.Z and the SWR1 complex at H3K27me3-enriched ABA response genes [21]. While many genes were induced following 4h of ABA treatment, H2A.Z levels and distribution at most of these genes was unperturbed. However, a subset of genes with the strongest induction did have measurable H2A.Z loss. Interestingly, these genes also had the strongest gain in SWR1 complex components PIE1 and MBD9. Based on these findings, we propose that SWR1 works to maintain the endogenous level of H2A.Z enrichment at a given gene in response to environmental stress-triggered induction. At most activated genes, rapid H2A.Z deposition by SWR1 compensates for H2A.Z lost by transcription and H2A.Z appears largely unchanged after four hours of induction. At the most highly induced genes, the rate of H2A.Z incorporation via SWR1 cannot match the rate of H2A.Z loss by elongating Pol II and a loss of H2A.Z is observed at 4h.

Given the transient loss of H2A.Z at induced genes after 30m of resupply, and the new finding that SWR1 enrichment increases at induced genes [21], we propose that loss of H2A.Z at 30m +P induced genes is quickly replenished by SWR1. Therefore, a sample of the transcriptome at a later time (4h+P) would only capture increased transcript levels but a chromatin sample taken at the same time would not capture the corresponding H2A.Z loss. At the four outlier PSi genes that lose H2A.Z after 96h, H2A.Z incorporation by SWR1 cannot occur fast enough to account for H2A.Z lost via transcription and a loss of H2A.Z is observed. Given our proposed model that H2A.Z loss is a feature of activation that is quickly replenished, it will be interesting to probe

the induction of PSi genes at a higher temporal resolution during the first moments of starvation.

This model can also be used to explain the loss of H2A.Z seen in other induced stress response genes as a result of activation as opposed to a cause. Only drought stress showed reduction of H2A.Z at activated genes beyond 4 days of stress imposition, with all other experiments measuring H2A.Z eviction earlier than the 4 days of -Pi stress measured in our experiment [11–15,22–24]. Additionally, in the case of heat stress, H2A.Z was actually seen to return to pre-stress levels after 4 hr of continuous stress [12]. After 30m of P resupply, we saw a prominent loss of H2A.Z but not a prominent gain of H2A.Z at repressed genes. This is similar to observations from hypoxic and drought stress responses, where the correlation between H2A.Z and transcript dynamics is driven largely by H2A.Z loss at induced genes as opposed to gain at repressed genes [14,15]. Future investigations using techniques designed to directly measure active transcription will help explain how drought response genes and certain PSi genes are still depleted of H2A.Z after 8 and 4 days of stress, respectively.

Future investigation is needed to understand whether H3K4me3 loss at transiently induced genes after 30m resupply is due to whole nucleosome loss or active H3K4 demethylation. Loss of H2A.Z occurs without loss of H3 in Arabidopsis temperature-responsive gene promoters and previous work in *Drosophila melanogaster* found that H2.Z occupancy is highest where H3-H4 turnover is lowest, suggesting H2A.Z loss occurs independently of whole nucleosome turnover [12,25]. This issue could be addressed using methods our lab has developed to probe the turnover of H3/H4 dimers in the nucleosome [26].

A call for temporally controlled knockout techniques when studying epigenetic modifiers

The theory that H2A.Z plays an active role in repression of responsive genes is often supported by evidence of aberrant responsive gene activation in mutants defective in the SWR1 complex, which deposits H2A.Z, including phosphate starvation-induced genes [27]. Similar to genetic H3K27me3 disruption experiments described above, these observations were made using stably integrated null mutants whose direct effects on transcription are confounded by a generation (or more) of defective chromatin organization in the mutant background. It is therefore difficult to distinguish between misexpression caused by loss of a given factor in that specific cell from misexpression caused by H2A.Z loss in the precursor cells or parent plants.

Indeed, mutants that impact chromatin composition are often developmentally deleterious and their phenotypes are observed across developmental time, where a daughter cell's epigenetic identity is inextricably linked to that of the parent cell. In Chapter 2, PRC2 disruption via estradiol-induced amiRNA knockdown of core subunit *FIE* was not sufficient to ablate expression of H3K27me3 enriched genes PHT1;2 and PHT1;9 during a phosphate starvation and recovery. These plants had no observable phenotypic deficiencies despite being germinated on induction media for continuous knockdown of *FIE* for two weeks. This is in stark contrast to the constitutively expressing 35S:amiRNA construct targeting *FIE* which phenocopies *fie* null plants. This suggests that the chromatin landscape established by PRC2 before germination is responsible for the developmental outcome of the plant, as continuous knockdown of PRC2 post germination is insufficient to elicit missexpression of responsive genes or phenotypic abnormalities. The lack of importance of the PRC2 complex in vegetative

growth and environmental response observed in Chapter 2 is supported by the findings described above that H3K27me3 is often unchanged in the face of responsive gene activation. In cases where PRC2 is found to be required for proper repression, PRC2 is disrupted by stably integrated null mutants that have gone through at least fertilization and embryogenesis with a deficient PRC2 complex. This observation highlights the need for temporally controlled knockouts to decouple the direct effects of a chromatin interacting protein from the effects inherited from previous generations or progenitor cells.

In summary, we have found that phosphate starvation can induce gene transcription without requiring removal of H2A.Z or PRC2 silencing marks. This finding is bolstered by other recent results and indicates a need to more closely evaluate the assumed causal connections between gene body enrichment of H2A.Z, H3K27me3, and transcriptional repression. Additionally, the fact that H2A.Z is maintained on newly activated responsive genes, likely due to SWR1 recruitment and continued H2A.Z deposition, suggests that H2A.Z is needed continuously to support transcription of these genes. The differences in the effects of H2A.Z on transcription (activation versus repression) likely come down to post-translational modifications to H2A.Z itself, and this will be an important area for future investigation.

References

1. Medici A, Szponarski W, Dangeville P, Safi A, Dissanayake IM, Saenchai C, et al. Identification of Molecular Integrators Shows that Nitrogen Actively Controls the Phosphate Starvation Response in Plants. Plant Cell. 2019;31: 1171–1184.

2. Bellegarde F, Herbert L, Séré D, Caillieux E, Boucherez J, Fizames C, et al. Polycomb Repressive Complex 2 attenuates the very high expression of the Arabidopsis gene NRT2.1. Sci Rep. 2018;8: 1–9.

3. Liu N, Fromm M, Avramova Z. H3K27me3 and H3K4me3 Chromatin Environment at Super-Induced Dehydration Stress Memory Genes of Arabidopsis thaliana. Mol Plant. 2014;7: 502–513.

4. Liu C, Cheng J, Zhuang Y, Ye L, Li Z, Wang Y, et al. Polycomb repressive complex 2 attenuates ABA-induced senescence in Arabidopsis. Plant J. 2019;97: 368–377.

5. Kramer HM, Seidl MF, Thomma BPHJ, Cook DE. Local Rather than Global H3K27me3 Dynamics Are Associated with Differential Gene Expression in Verticillium dahliae. MBio. 2021;13: e0356621.

6. Faivre L, Kinscher N-F, Kuhlmann AB, Xu X, Kaufmann K, Schubert D. Cold stress induces rapid gene-specific changes in the levels of H3K4me3 and H3K27me3 in Arabidopsis thaliana. Front Plant Sci. 2024;15: 1390144.

7. Kwon CS, Lee D, Choi G, Chung W-I. Histone occupancy-dependent and -independent removal of H3K27 trimethylation at cold-responsive genes in Arabidopsis. Plant J. 2009;60: 112–121.

8. Cai H, Zhang M, Chai M, He Q, Huang X, Zhao L, et al. Epigenetic regulation of anthocyanin biosynthesis by an antagonistic interaction between H2A . Z and H3K4me3. 2019;1: 295–308.

9. Hu G, Cui K, Northrup D, Liu C, Wang C, Tang Q, et al. H2A.Z facilitates access of active and repressive complexes to chromatin in embryonic stem cell self-renewal and differentiation. Cell Stem Cell. 2013;12: 180–192.

10. Boden SA, Kavanová M, Finnegan EJ, Wigge PA. Thermal stress effects on grain yield in Brachypodium distachyon occur via H2A.Z-nucleosomes. Genome Biol. 2013;14: R65.

11. Mao Z, Wei X, Li L, Xu P, Zhang J, Wang W, et al. Arabidopsis cryptochrome 1 controls photomorphogenesis through regulation of H2A.Z deposition. Plant Cell. 2021;33: 1961–1979.

12. Cortijo S, Charoensawan V, Brestovitsky A, Buning R, Ravarani C, Rhodes D, et al. Transcriptional Regulation of the Ambient Temperature Response by H2A.Z Nucleosomes and HSF1 Transcription Factors in Arabidopsis. Mol Plant. 2017;10: 1258–1273.

13. Nguyen NH, Cheong J-J. H2A.Z-containing nucleosomes are evicted to activate AtMYB44 transcription in response to salt stress. Biochem Biophys Res Commun. 2018;499: 1039–1043.

14. Sura W, Kabza M, Karlowski WM, Bieluszewski T, Kus-Slowinska M, Pawełoszek Ł, et al. Dual Role of the Histone Variant H2A.Z in Transcriptional Regulation of

Stress-Response Genes. Plant Cell. 2017;29. doi:10.1105/tpc.16.00573

15. Lee TA, Bailey-Serres J. Integrative Analysis from the Epigenome to Translatome Uncovers Patterns of Dominant Nuclear Regulation during Transient Stress. Plant Cell. 2019;31: 2573–2595.

16. Xue M, Zhang H, Zhao F, Zhao T, Li H, Jiang D. The INO80 chromatin remodeling complex promotes thermomorphogenesis by connecting H2A.Z eviction and active transcription in Arabidopsis. Mol Plant. 2021;14: 1799–1813.

17. Yang C, Yin L, Xie F, Ma M, Huang S, Zeng Y, et al. AtINO80 represses photomorphogenesis by modulating nucleosome density and H2A.Z incorporation in light-related genes. Proceedings of the National Academy of Sciences. 2020;117: 33679–33688.

18. Silver BD, Willett CG, Maher KA, Wang D, Deal RB. Differences in transcription initiation directionality underlie distinctions between plants and animals in chromatin modification patterns at genes and cis-regulatory elements. G3 . 2024;14. doi:10.1093/g3journal/jkae016

19. Lashgari A, Millau J-F, Jacques P-É, Gaudreau L. Global inhibition of transcription causes an increase in histone H2A.Z incorporation within gene bodies. Nucleic Acids Res. 2017;45: 12715–12722.

20. Hani S, Cuyas L, David P, Secco D, Whelan J, Thibaud M-C, et al. Live single-cell transcriptional dynamics via RNA labelling during the phosphate response in plants. Nat Plants. 2021;7: 1050–1064.

21. Krall EG, Deal RB. SWR1 is recruited to activated ABA response genes to maintain gene body H2A.Z in Arabidopsis thaliana. bioRxiv. 2024. p. 2024.07.14.603444. doi:10.1101/2024.07.14.603444

22. Kumar SV, Wigge PA, Centre JI, Lane C, Nr N. H2A.Z-Containing Nucleosomes Mediate the Thermosensory Response in Arabidopsis. Cell. 2010;140: 136–147.

23. Zander M, Willige BC, He Y, Nguyen TA, Langford AE, Nehring R, et al. Epigenetic silencing of a multifunctional plant stress regulator. Elife. 2019;8. doi:10.7554/eLife.47835

24. Willige BC, Zander M, Yoo CY, Phan A, Garza RM, Trigg SA, et al. PHYTOCHROME-INTERACTING FACTORs trigger environmentally responsive chromatin dynamics in plants. Nat Genet. 2021; 1–7.

25. Weber CM, Ramachandran S, Henikoff S. Nucleosomes Are Context-Specific, H2A.Z-Modulated Barriers to RNA Polymerase. Mol Cell. 2014;53: 819–830.

26. Willett C. Investigating the dyanamics of transcription initiation and nucleosome turnover in Arabidopsis thaliana. Deal RB, editor. Phd, Emory University. 2024.

27. Smith AP, Jain A, Deal RB, Nagarajan VK, Poling MD, Raghothama KG, et al. Histone H2A.Z Regulates the Expression of Several Classes of Phosphate Starvation Response Genes But Not as a Transcriptional Activator. Plant Physiol. 2010;152: 217–225.